DOCTORAL (PhD) DISSERTATION

The Role of Geology Formation and Anthropogenic Activities in Radionuclide Distribution in Selected Regions in Ghana

Written by:

Esther Osei Akuo-ko

Doctoral School of Chemical Engineering and Material Sciences

DOI:10.18136/PE.2025.937

Supervisors:

Dr. Tibor Kovács (PhD)

Dr. Anita Csordás (PhD)

University of Pannonia

Department of Radiochemistry and Radioecology, Research Centre for Biochemical, Environmental and Chemical Engineering

Veszprem

2025

The Role of Geology Formation and Anthropogenic Activities in Radionuclide Distribution in Selected Regions in Ghana

Thesis for obtaining a PhD degree in the Doctoral School of Chemical Engineering and Material Sciences of the University of Pannonia, Department of Radiochemistry and Radioecology, Research Centre for Biochemical, Environmental and Chemical Engineering

Written by:

Esther Osei Akuo-ko

Supervisors:

Dr. Tibor Kovács (PhD)

Dr. Anita Csordás (PhD)

Propose acceptance (yes/no) ….…….....

Dr. Tibor Kovács (PhD)

Propose acceptance (yes/no) ...…….....

Dr. Anita Csordás (PhD)

As a reviewer, I propose acceptance of the thesis:

Name of reviewer: …….. yes/no ….……..

(reviewer)

Name of reviewer: …… yes/no ….……..

(reviewer)

The PhD candidate has achieved …… % at the public discussion.

Vesprem, ……..

(Chairman of the committee)

The grade of the PhD diploma ……. (……..%)

Vesprem, …….

(Chairman of the UDHC)

Abstract

The exposure of humans to ionizing radiation through the natural enviroment and anthropogenic activities constitute significant sources of radiation dose estimated annually. In this work, activity concentrations of Ra-226, Ra-228, Th-232, K-40, Po-210 and Cs-137 were determined in different enviromnetal media. The mean radioactivity levels measured in some coastal sediments were above worldwide averages. Consequently, the radiological hazards determined for such areas were high. Indoor radon levels were measured in dwellings within the Greater Accra region, with the annual mean concentration of 50.8 ± 3.4 Bq/m^3. Po-210 activity concentrations determined in commonly smoked cigarettes in Ghana were relatively low. The research evaluated that indoor radon and Po-210 concentrations in cigarettes contribute to the annually lung cancer cases recorded in Ghana.

Activity concentrations of natural radionuclides were measured in soils and sediments from artisanal mining areas. Th-232 activity concentrations were higher than Ra-226 concentrations for the investigated locations. Farms and undisturbed lands close to mining sites recorded high activity concentrations. Rn-222 activity concentrations determined in soils from mining areas were between 390.6 ± 38 and 907.5 ± 93 Bq/m^3, with an average of 560.0 ± 54 Bq/m^3. High Rn-222 exhalation rates were observed in some farming and undisturbed areas. The activity concentrations of Ra-226 and Ra-228 in surface and groundwater resources were observed to be above world average concentrations of 1.0 Bq/L and 0.1 Bq/L, respectively. Activity concentrations of Ra-228 were consistent with Th-232 concentrations measured in soils from the study area.

The research helped to identify the distribution pattern of radionuclides in some parts of the country. Thus, geological formations significantly affect the radionuclide's distribution observed in the study areas. The measured activity concentrations were used to evaluate the associated radiological risks. Spatial distribution maps helped to visualize the distribution of the radionuclides in different locations. The results from this work can serve as baseline data for future reference and monitoring activities.

Kivonat

Az embereknek a természetes környezeten és az antropogén tevékenységeken keresztül történő ionizáló sugárzásnak való kitettsége az évente becsült sugárzási dózis jelentős forrását jelenti. Ebben a munkában a Ra-226, Ra-228, Th-232, K-40, Po-210 és Cs-137 aktivitáskoncentrációja került meghatározásra különböző környezeti közegekben Ghánában. Az egyes part menti üledékekben mért átlagos radioaktivitási szintek meghaladták a világátlagokat. Következésképpen az ilyen területeken megállapított radiológiai veszélyek magasak voltak. A beltéri radonszinteket a Greater Accra régióban lévő lakásokban mérték, az éves átlagos koncentráció 50,8 ± 3,4 Bq/m^3 volt. A Ghánában általánosan elszívott cigarettákban meghatározott Po-210 aktivitáskoncentrációk viszonylag alacsonyak voltak. A kutatás értékelése szerint a beltéri radon és a cigarettákban lévő Po-210 koncentráció hozzájárul a Ghánában évente regisztrált tüdőrákos esetekhez.

A természetes radionuklidok aktivitáskoncentrációját a bányászati területekről származó talajban és üledékben mérték. A vizsgált helyszíneken a Th-232 aktivitáskoncentráció magasabb volt, mint a Ra-226 koncentrációja. A bányatelepekhez közeli gazdaságokban és érintetlen területeken magas aktivitáskoncentrációkat mértek. A bányászati területekről származó talajokban meghatározott Rn-222 aktivitáskoncentrációk 390,6 ± 38 és 907,5 ± 93 Bq/m^3 között voltak, az átlag 560,0 ± 54 Bq/m^3 volt. Néhány mezőgazdasági és háborítatlan területen magas Rn-222 kilégzési arányt figyeltek meg. A Ra-226 és Ra-228 aktivitáskoncentrációja a felszíni és felszín alatti vízkészletekben a világátlagot meghaladó, 1,0 Bq/l, illetve 0,1 Bq/l koncentrációt mutatott. A Ra-228 aktivitáskoncentrációi összhangban voltak a vizsgált terület talajában mért Th-232 koncentrációkkal.

A kutatás segített azonosítani a radionuklidok eloszlási mintázatát az ország egyes részein. Így a geológiai képződmények jelentősen befolyásolják a vizsgált területeken megfigyelt radionuklidok eloszlását. A mért aktivitáskoncentrációkat a kapcsolódó radiológiai kockázatok értékelésére használták. A térbeli eloszlási térképek segítettek a radionuklidok különböző helyeken való eloszlásának szemléltetésében. A munka eredményei alapadatként szolgálhatnak a jövőbeni referencia- és megfigyelési tevékenységekhez.

Résumé

L'exposition de l'homme aux rayonnements ionisants par le biais de l'environnement naturel et des activités anthropogéniques constitue une source importante de dose de rayonnement estimée annuellement. Dans ce travail, les concentrations d'activité de Ra-226, Ra-228, Th-232, K-40, Po-210 et Cs-137 ont été déterminées dans différents milieux environnementaux. Les niveaux moyens de radioactivité mesurés dans certains sédiments côtiers étaient supérieurs aux moyennes mondiales. Par conséquent, les risques radiologiques déterminés pour ces zones étaient élevés. Les niveaux de radon à l'intérieur des habitations ont été mesurés dans la région du Grand Accra, avec une concentration moyenne annuelle de 50,8 ± 3,4 Bq/m^3. Les concentrations d'activité du Po-210 déterminées dans les cigarettes couramment fumées au Ghana étaient relativement faibles. La recherche a évalué que les concentrations de radon intérieur et de Po-210 dans les cigarettes contribuent aux cas de cancer du poumon enregistrés chaque année au Ghana.

Les concentrations d'activité des radionucléides naturels ont été mesurées dans les sols et les sédiments des zones d'exploitation minière artisanale. Les concentrations d'activité du Th-232 étaient plus élevées que celles du Ra-226 pour les sites étudiés. Les fermes et les terres non perturbées proches des sites miniers ont enregistré des concentrations d'activité élevées. Les concentrations d'activité Rn-222 déterminées dans les sols des zones minières étaient comprises entre 390,6 ± 38 et 907,5 ± 93 Bq/m^3, avec une moyenne de 560,0 ± 54 Bq/m^3. Des taux d'exhalation élevés de Rn-222 ont été observés dans certaines zones agricoles et non perturbées. Les concentrations d'activité de Ra-226 et de Ra-228 dans les eaux de surface et les eaux souterraines étaient supérieures aux concentrations moyennes mondiales de 1,0 Bq/L et 0,1 Bq/L, respectivement. Les concentrations d'activité de Ra-228 étaient cohérentes avec les concentrations de Th-232 mesurées dans les sols de la zone d'étude.

La recherche a permis d'identifier le schéma de distribution des radionucléides dans certaines parties du pays. Ainsi, les formations géologiques affectent de manière significative la distribution des radionucléides observée dans les zones étudiées. Les concentrations d'activité mesurées ont été utilisées pour évaluer les risques radiologiques associés. Des cartes de distribution spatiale ont permis de visualiser la distribution des radionucléides en différents endroits. Les résultats de ce travail peuvent servir de données de base pour les futures activités de référence et de surveillance.

Table of Contents

List of Tables

List of Figures

List of Abbreviations and Acronyms

NORM	Naturally Occurring Radioactive Material
UNSCEAR	United Nations Scientific Committee on the Effects of Atomic Radiation
WHO	World Health Organization
IAEA	International Atomic Energy Agency
ICRP	International Commission on Radiological Protection
SSNTD	Solid State Nuclear Track Detector
IDW	Inverse Distance Weighting
OK	Ordinary Kriging
EBK	Empirical Bayesian Kriging
MDL	Minimum Detectable Limit
ELCR	Excess Lifetime Cancer Risk
CED	Committed Effective Dose
AED	Annual Effective Dose
AGDE	Annual Gonadal Dose Equivalent
Ra_{eq}	Radium equivalent
LCC	Lung Cancer Cases
PCA	Principal Component Analysis
MOFEP	Ministry of Finance and Economic Planning
IUCN	International Union for Conservation of Nature
NDPC	National Development Planning Commission
Globacon	Global Cancer Observatory

Acknowledgement

I am grateful to God for life, strength, and health to complete my PhD training successfully. My sincere appreciation goes to my excellent supervisors, Dr. Tibor Kovács and Dr. Anita Csordás of the Department of Radiochemistry and Radioecology of the University of Pannonia, for their guidance, indispensable support, professional advice, and encouragement throughout the years of my PhD training. I would not have completed my training without your constant guidance and corrections. A very special thanks to Dr. Tibor Kovács for his constructive criticisms, invaluable advice, and the opportunity to research diverse fields while in touch with my family.

I would genuinely appreciate Dr. Edit Tóth-Bodrogi, Dr. Amin Shahrokhi, and Mohammemad Adelikhah (PhD) for helping me navigate certain challenging aspects of the training. I thank Dr. Francis Otoo and Dr. Miklos Hegedűs for their great contribution, support, and kindness. I am also thankful to my colleagues for the knowledge-sharing, help, motivation, and support that contributed to my success story.

I am grateful to my family and loved ones, especially my husband and beautiful children. I cannot thank you enough for the sacrifices, love, and encouragement you have given me throughout the journey. I could not have made it without you being my unwavering pillar of support. We cried, laughed, and overcame the challenges together, and now I have completed the PhD training. I love you so much, and you will always remain my precious gems in this world.

CHAPTER ONE

INTRODUCTION

1.1 Background

Natural radioactive elements have been part of the Earth since its beginning (Sivakumar et al., 2014). Their long existence on the earth is due to their long half-lives and isotopic abundance (Oliveira de Souza et al., 2015). Three natural radioelements predominantly occur in the Earth's crust; these are U-238, Th-232, and K-40 (Pintilie-Nicolov et al., 2021; Khandaker et al., 2016). These long-lived radionuclides have some progenies that are also long-lived; an example is Ra-226 from the U-238 series, which represents 98% of the total external gamma dose induced by U-238 (Leuangtakoun et al., 2018; Olise et al., 2010). U-238, Ra-226, Th-232, and K-40 have long half-lives equivalent to the age of the Earth, making them the focus of several radioactivity measurement studies (Öge et al., 2021; Ramadhany et al., 2022). They can be found in environmental media such as soil, rocks, water, air, sediment, plants, and food, as well as in building materials and dwellings (Wang et al., 2015). The distribution of natural radionuclides in the lithosphere depends on the mineral composition, geological formation, and geographical conditions, resulting in varying concentrations of radionuclides in the media. Hence, environmental radionuclides are not evenly distributed (Suresh et al., 2020; Olise et al., 2016; 2010).

The human environment is radioactive, exposing the human body to radiation sources from the environment. Natural radioactivity is associated with exposure to gamma radiation (Suresh et al., 2020). Radiation sources can be natural and artificial, leading to internal and external exposures (Giri et al., 2013). Internal exposure of the human body to ionizing radiation occurs through inhalation of air and ingestion of food and water. In contrast, external exposure is due to the emission of gamma rays by radionuclides in soil, sediment, and rocks (Pintilie-Nicolov et al., 2021).

The decay of radionuclides produces ionizing radiation, which is detrimental to human health and causes biological damage to organs of the human body (Atibu et al., 2022). Thus, radioactive materials are characterized by ionizing natural radiation and exposing humans to natural radiation at every minute of life (Zubair & Shafiqullah, 2020). This is because

radionuclides are part of the chemical activity of soil, water, air, and plants, and therefore, inducing ionizing radiation results in radiological dose for living organisms (Galhardi et al., 2017). Epidemiological research and empirical observations have proven that ionizing radiation has carcinogenic characteristics above a certain threshold (Atibu et al., 2022). The radiological consequence of natural radionuclides in the environment above background levels is the exposure of the human body to gamma rays, which irradiate the organs and tissues due to the inhalation and ingestion of radionuclides and their progenies (Suresh et al., 2020; Giri et al., 2013). This suggests that natural radiation is the main contributor to the public's external radiation dose. Since nature is the largest source of radiation exposure, the measurement of natural background radiation levels has gained significant recognition recently (Giri et al., 2013).

1.2 Research problem

Investigations of natural and artificial radionuclides distribution in the environment are of interest to the public, governments, and international organizations due to the associated health risks. Research on the radioactivity levels in the environment by individuals and organizations has been on the rise worldwide due to the health hazards associated with their existence in the environment and anthropogenic activities (Joel et al., 2019). This is because radiations from natural radionuclides U-238/ Ra-226, Th-232, and K-40 make significant contributions to the dose induced in humans, and thus evaluating the radiation levels of natural radionuclides is an important part of radiation monitoring (Yordanova et al., 2015). Natural radioactivity is present in environmental media, while artificial radioactivity, such as Cs-137, occurs through radioactive contamination. Natural and artificial radionuclides contribute to the total radiation dose estimated for the human population (Öge et al., 2021).

Human activities in the environment result in the accumulation of radioactive elements, thereby modifying original concentrations. Determining the activity concentration and natural background levels of radionuclides is important for long-term environmental and human protection (Yordanova et al., 2015). Human activities in the environment, such as mining and oil and gas extraction, continually change the biochemical balance and geochemical cycles of radionuclide elements in the environment. Studies have shown that anthropogenic activities result in increased radioactivity concentrations from elements that

contain natural radionuclides; as such, it becomes significant to undertake regulatory control (Focus et al., 2012). Natural radioactivity is extensively distributed in the Earth's environment (Abdulkarim et al., 2018). However, there is an unequal distribution of radionuclides in the Earth's environment (Akpanowo et al., 2019). Due to the lack of uniform distribution of radionuclides, information on their distribution in the rocks and soil is imperative for radiation protection and measurement (Innocent et al., 2013). The differences in geological formation in the earth's crust ascertain the need to determine radioactive concentrations in such formations' soil, rock, or water samples. These kinds of studies cannot be underestimated in assessing the likely radiological hazards to the inhabitants who live within that geological location (Joel et al., 2019). Knowledge of the radioactivity distribution pattern in a geological location is necessary for controlling radiation exposure levels and provides some information on variations in the background radiation levels (Zaini et al., 2011). The presence of radionuclides in the environment in different concentrations depends on the parent rock type. They emit gamma radiation into the environment, changing the background radiation levels (Yachiso et al., 2022). Exposure to gamma rays in both indoor and outdoor environments is due to the radiation emitted by Ra-226, Th-232, and K-40, which are present in nature (Zubair & Shafiqullah, 2020).

Human activities concentrate natural and artificial radionuclides in the environment (Hamideen & Sharaf, 2012; Ladan et al., 2022; Galhardi et al., 2017). The radionuclides can adhere to and accumulate in aerosols, contaminate soil, water, and food, and enter the human system. Radionuclides bioaccumulate in different body organs once they enter the body, causing human health risks (Focus et al., 2021). Several serious health effects have been identified as the cause of long-term exposure to radioactivity and ingestion and inhalation of radionuclides. These include lung diseases, hemorrhage, anemia, acute leucopenia, necrosis of the mouth, etc. (Qureshi et al., 2014; Focus et al., 2021). As a result, it is necessary to continuously monitor and assess the concentrations of natural and artificial radionuclides in the environment and to regulate human activities that lead to the elevation of radioactivity levels in the environment.

1.3 Research objectives

General objective

The primary objective of the study is to investigate the radioactivity concentration of natural and artificial radionuclides in soil, sediment, water, indoor air, and consumed products such as cigarettes in selected regions of Ghana and to evaluate the consequential radiological effects associated with the radioactivity concentrations in the environmental samples.

Specific objectives

The specific objectives of the research are:

a. To determine the activity concentrations of:
   - Ra-226, Th-232, K-40, and Cs-137 in sediment along coastal areas of Ghana and in soils from selected mining areas.
   - Ra-226, Ra-228, and K-40 in surface water and groundwater resources in selected mining areas.
   - Rn-222 in soil gas and radon exhalation rates of soils from selected mining areas.
   - Indoor Rn-222 concentrations in residences within selected country regions.
   - Po-210 concentrations in commonly smoked cigarette brands in Ghana.

b. To determine the radiological suitability of:
   - Soils and sediment as building materials in the study regions.
   - Surface water and groundwater resources as potable sources of drinking water.

c. To evaluate the consequential radiological hazards associated with the radionuclides' activity concentration in the environment.

d. To evaluate the excess lifetime cancer risk and lung cancer cases associated with Rn-222 in dwellings and Po-210 in cigarettes, and their subsequent contribution to lung cancer cases in Ghana from a radiological perspective.

e. To determine the primary source of radiation exposure among the Ghanaian population.

1.4 Justification

Radionuclides provide significant information regarding the exposure to ionizing radiation levels in anthropogenic and naturally occurring radioactive materials (NORM) samples. Hence, environmental samples undergo many regulations to assess their possible radiological risks (Barba-Lobo et al., 2022). Several studies on radioactivity levels in different environmental media have been conducted in Ghana. However, some areas need background study, while others need further investigations to understand the risks associated with radiation exposure.

Natural radioactivity in building materials like sediment or beach sand, and soil is mainly from the uranium and thorium series and potassium, which are internal and external sources of radiation exposure. The inhalation of indoor or outdoor air contaminated with radioactive elements can expose an individual to radon gas and Po-210, leading to internal radiation exposure and associated health problems (Chandrasekaran et al., 2015). Research shows that most populations spend about 80% of their time indoors. Therefore, it is essential to resolve the health risks associated with indoor radon and the use of sediment and soil as construction materials (Zubair & Shafiqullah, 2020).

In Ghana, coastal sediment and soils are particularly used as building materials by coastal dwellers and inland dwellers. This necessitates the need to evaluate the radioactivity levels in such materials. The coastline of Ghana is known for ecological and economic values (fishing, oil exploitation, energy production, tourism, imports, and exports) as well as a fast-growing population, infrastructure expansion, and sand-winning activities, which are likely to cause elevated radioactivity levels (Nyarko et al., 2011). Previous studies on the radionuclide activity concentrations in coastal sediments did not cover the entire coastline of the country (Botwe et al., 2017; Nyarko et al., 2011; Amekudzie et al., 2011). Evaluating the radioactivity levels in the entire coastal stretch is important for protecting human health from the harmful effects of ionizing radiation, particularly for beachgoers and coastal dwellers who use beach sediment for building construction.

Using beach sediment and soil as building materials has been known to be a potential source of indoor radon activity concentration (Akuo-ko et al., 2023a; 2023b). They release radon gas and its daughter isotopes in closed environments like residences and offices (Otoo et al.,

2020). This is a health concern because inhalation of indoor radon (Rn-222) is a major cause of lung cancer (WHO, 2011). Measurement of indoor radon levels in dwellings is important for radiation protection, as well as the continuous use of soil and sediment for building constructions, and the radiological safety of indoor environments. Previous indoor radon studies in the country did not focus on specific health risks associated with indoor radon levels, and no indoor radon map was created (Nsiah-Akoto et al., 2011; Otoo et al., 2018; Kpodzro, 2018). Therefore, there is a need for such investigations.

Another cause of lung cancer is the smoking of cigarettes. Smoking is the leading cause of lung cancer, which leads to the death of smokers (Zagà et al., 2011; Kovács et al., 2007). In Ghana, the prevalence of smoking is below 10% of the total population (Nketiah-Amponsah et al., 2018); however, each year, more than 5000 people die as a result of smoking-related illnesses, including lung cancer (Singh et al., 2020). As the country seeks to introduce preventive measures to control the number of smoking-related illnesses and deaths since the number of smokers increases year by year (Doku et al., 2012), it is very important to also determine the radioactive constituents and concentrations of cigarette products available on the Ghanaian market and their induced radiation doses. This will help educate the public on their health effects.

Human activities give rise to radioactive materials being released into the environment, and an example of such activity is mining (Ladan et al., 2022). Mining activities lead to the dispersion of naturally occurring radioactive materials, polluting the environment and causing radiation exposure to mine workers and the public (UNSCEAR, 2000). Studies indicate that artisanal and small-scale mining causes more environmental harm than good, particularly in developing countries like Ghana. The situation of mines, unregulated extraction procedures, and the lack of enforcement of mining regulations make mining an environmental catastrophe (Souffit et al., 2022). This makes it crucial to investigate and develop comprehensive scientific proof to evaluate the exposure levels of radioactivity to populations within mining locations. Although some studies on radioactivity levels in mining areas have been conducted across the country (Anyimah-Ackah et al., 2021; Adukpo et al., 2015; Faanu et al., 2016, 2014; 2013; 2011; Doyi et al., 2013), the mining industry in Ghana has not been subjected to radiological regulatory control. As a result, there is little

information and cognizance of the detrimental effects of radioactivity concentration exposure in mining areas (Faanu et al., 2011). Mining activities and their waste increase the background radioactivity levels in soil, water (surface and groundwater), air, and vegetation in mining regions (Galhardi et al., 2017). It also increases the soil exhalation rates in those areas (Liza et al., 2023). Hence, determining radioactivity levels in mining areas is significant for radiological impact assessment and as excellent geochemical and biochemical tracers in the environment (Chandrasekaran et al., 2015).

1.5 Scope of research

The research investigated the radioactivity levels of environmental media that act as sources of ionizing radiation to the human body and organs. The radioactive materials studied in this research include soil, sediment, tobacco leaves in cigarettes, indoor air, surface water, and groundwater samples. These were examined because of their availability and frequency of use among the Ghanaian population. They have a common characteristic of being carcinogenic if activity concentrations exceed world average values. In addition, the general population, stakeholders, and policymakers have very little information and, to a large extent, are unaware of their radiological hazards. Therefore, the study sought to determine activity concentrations of natural and artificial radionuclides in soil, sediment, indoor air, cigarettes, surface water, and groundwater resources in selected areas in Ghana. The radiological risks associated with the concentrations were estimated and reported, and finally, recommendations were made.

1.6 Limitation of research

The research focused on the activity concentrations of radionuclides and the health risks associated with their concentrations. The research was based on natural radionuclide levels in the environmental media; however, in the case of sediment, the concentrations of the anthropogenic radionuclide Cs-137 were also determined. Sampling activities were carried out in different locations and regions of the country, and they were expensive and time-consuming. Consequently, limited samples were collected in each investigation, affecting the sample size. The sampling periods were also restricted. Thus, increasing sampling sites and locations could increase the samples collected to obtain more representative data on the distribution of radionuclides in the country. Again, the research received partial funding,

limiting sampling days, collection volumes, and quantity, and the laboratory analyses performed on the samples. Another limiting factor was instrumentation analyses. Apart from the spectrometric techniques used in the investigations, other measurement techniques could have been employed to determine the concentration of other radionuclides in samples.

CHAPTER TWO

LITERATURE REVIEW

2.1 Introduction

This chapter reviews literature on environmental radioactivity and its effects on environmental resources and human health. It reviews some of the studies done so far on radioactivity concentrations in soils, sediment, water, etc., in different geographical locations and the impact of human activities on radioactivity levels in the environment.

2.2 Sources of radiations

The component of the Earth's crust is the main source of natural background radiation. This is the level of ionizing natural radiation present in a geographical location without contribution from human activities (Jha et al., 2024; Najam & Younis, 2015; Akpanowo et al., 2019). However, the human population is vulnerable to environmental radiation from natural sources and artificial sources. Natural radioactivity in the environment results from elemental radionuclides such as uranium, thorium, and potassium, which occur in different concentrations due to their isotopic abundances (Hamideen & Sharaf, 2012; Taqi et al., 2018; Khandaker et al., 2016). Natural radioactivity emanates from emitted rays from the decomposition of natural radionuclides in environmental media (Öge et al., 2021). Natural radiation sources are the most significant contributor to the world population's external dose (UNSCEAR, 2000).

Artificial radionuclides, such as Cs-137, Sr-90, and I-131, are also present in the environment in significant amounts due to nuclear weapon testing in the atmosphere, nuclear power plant accidents, the continuous discharge of radionuclides from nuclear installations and medical applications (Abate, 2022; Shahrokhi et al., 2021; Zhao et al., 2018; Ademola et al., 2014; Agbalagba et al., 2012). After the 1950s nuclear weapon tests in the Northern and Southern hemispheres and the 1986 Chernobyl nuclear power plant accident, which led to the dispersion of Cs-137 into the atmosphere in huge quantities, there were concerns about studying the behavior of artificial radionuclides in the atmosphere and the environment (Shahrokhi et al., 2021; Nyarko et al., 2011; Dizman et al., 2019). Again, the Fukushima nuclear power plant accident in 2011 also led to the dispersion of Cs-137 in the atmosphere

(Zhao et al., 2018; Mouri et al., 2014; Kitamura et al., 2014). The radionuclides can be accumulated and concentrated in certain parts of the environment due to natural and artificial processes. The existence of natural and artificial radionuclides in the environment finds its way into the human body via the food chain and the uptake by plants and animals as illustrated in Figure 1. Similarly, due to radionuclides' physical and chemical properties, radioactive pollution can be long-standing with minimal changes over time (Agbalagba et al., 2012).

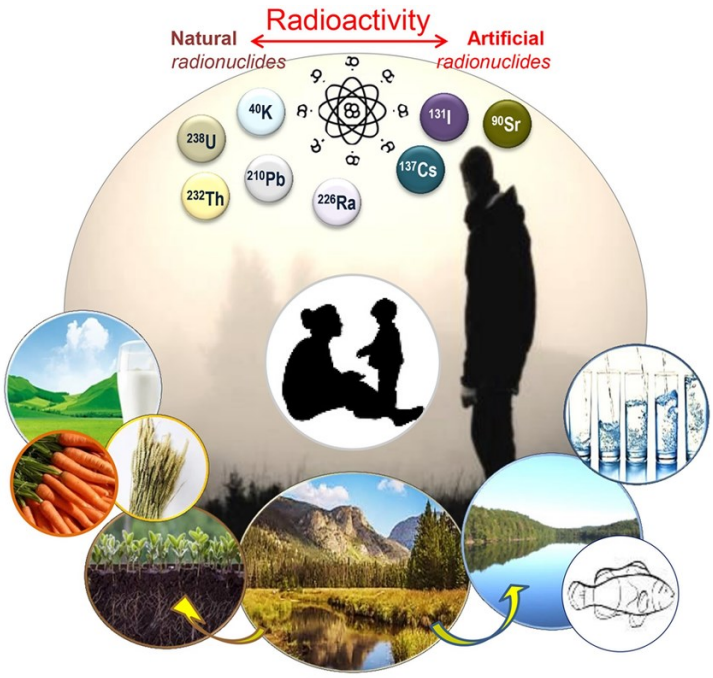

Figure 1. Exposure of humans to natural and artificial radioactivity (Cuculovic et al., 2024).

It has been estimated that natural radionuclides in the environment contribute 80% of the total radiation dose received by the world's population, while artificial sources contribute the remaining 20% of the dose (Ademola et al., 2014; Isinkaye & Emelue, 2015; UNSCEAR, 2000). Estimating radiation dose due to natural and artificial radionuclides is important in assessing human health risks and documenting environmental changes due to human activities (Jwanbot et al., 2013). In recent years, research into the evaluation of radioactivity concentrations in environmental media have been carried out all over the world as a result of the human health risks associated with radionuclides (Yachiso et al., 2022; Botwe et al., 2017;

Shahrokhi et al., 2021; Imani et al., 2021; Gezera et al., 2019; Coletti et al., 2020; Erőss et al., 2018; Csordás et al., 2021; Baltrenas et al., 2020; Nyhan et al., 2018; Öge et al., 2021; Mathuthu et al., 2021).

2.3 Exposure pathways

The decay of radionuclides produces ionizing radiation, which causes biological damage to human organs and tissues (Liu et al., 2021). Forms of ionizing radiation include gamma rays, X-rays, and alpha and beta particles. When present at sufficient levels, these can harm human and animal health (Souffit et al., 2022; Ladan et al., 2022). The radiation exposure can be internal or external, emanating from different environmental sources. Internal exposure to radiation originates from the inhalation of Rn-222, Rn-220, Po-210, Pb-210, and other short-lived radionuclides emitted from building materials, smoking cigarettes, or the radionuclides attached to aerosols in the atmosphere. Internal exposure can also be due to ingesting radionuclides in water, plants, and animals. Ingestion of radionuclides via consumption of water or food has been recognized as the most significant pathway of internal exposure to radiation as compared to the level of internal exposure to soils and sediment by inhalation and ingestion (Giri et al., 2013; Suresh et al., 2020; Kaur et al., 2017). External exposure to radiation is caused by the emission of gamma rays by radionuclides in environmental materials. They contain gamma-emitting radionuclides such as Ra-226, Th-232, and K-40, among which Ra-226 is the most radiologically important due to its abundance and radiological effects (Chandrasekaran et al., 2015).

2.3.1 Radioactivity of sediment

Beach sediments are significant sources of ionizing radiation and are essential for evaluating human health hazards related to gamma radiation exposure (Zakaly et al., 2021; Huang et al., 2015; Shuaibu et al., 2017). Sediments contain radionuclides such as U-238, Th-232, Ra-226, Ra-228, Th-228, Po-210, and K-40, and thus, a means of evaluating radioactivity levels and the impact of radiation in the environment since they are widely distributed in the earth (Isinkaye & Emelue, 2015; Botwe et al., 2017; Imani et al., 2021; Shahrokhi et al., 2021). Consequently, it is considered a medium for obtaining valuable geochemical and environmental information regarding the contamination of radionuclides (Zakaly et al., 2021). Sediments are used as ecological indicators and tracers for contamination of

radionuclides and monitoring (Amekudzie et al., 2011). Through measured activity concentrations of sediment, necessary information concerning the radiological hazards due to exposure to gamma radiation is derived. This helps develop a reference database to monitor potential radiological change over time (Shuaibu et al., 2017). They act as reservoirs of materials derived from natural and artificial weathering processes (Chaparro et al., 2017; Nyarko et al., 2011) and a medium of migration of radionuclide transfer in the aquatic environment (Isinkaye & Emelue, 2015).

Beach sediments contain natural radionuclides and, more importantly, artificial radionuclides. (Nyarko et al., 2011). Studies show that the marine environment aids in the transfer of radionuclides from one location to another through ocean and atmospheric distribution (Botwe et al., 2017; Zhao et al., 2018; Kubo et al., 2018), and as such, it is imperative to study the possible level of Cs-137 contamination along the shores of Ghana, although there is not yet a nuclear power plant at the Ghanaian coastline (Botwe et al., 2017). The coastline of Ghana is known for several ecological and economic activities, including tourism, fishing, sand winning, import and export activities, etc. (Nyarko et al., 2011). These activities attract indigenes and foreigners to the beaches year-round for various purposes. Hence, investigating the radioactivity concentrations in sediment along the Ghanaian coast is important for human and environmental assessments. In addition, coastal dwellers use beach sediment as a building material. Thus, it is important to measure their radioactivity levels and estimate the resulting radiological effects due to their usage. Studies have been conducted in previous years to evaluate the radioactivity levels in sediment in some coastal zones in Ghana (Botwe et al., 2017; Amekudzie et al., 2011; Nyarko et al., 2011). These studies determined activity concentrations to be generally within world average values.

Figure 2. Images of various activities along the coast of Ghana (OHG, 2025; Daily Guide News, 2021; West Africa, 2024).

2.3.2 Radon measurements

Radon (Rn-222) is a radioactive gas produced from the natural radioactive decay of uranium in soil and rocks. Radon is a decay product of the U-238 series from the alpha decay of Ra-226, with the progenies Po-218, Pb-214, Bi-214, Po-214, Pb-210, Bi-210, Po-210 and Pb-206. Due to the free movement of radon in the air, its progenies adhere to dust particles and are inhaled into the human respiratory system (Akuo-ko et al., 2023). Radon gas emanates from soils and rocks, with building materials being sources of indoor radon pollution (Gezera et al., 2019; Coletti et al., 2020; Martins da Silva et al., 2022). Radon emanation is the escape of radon atom from a radium bearing grain into pore spaces (Sakoda et al., 2011). Radon can be exhaled into the air or soil surface after emanation from grain pores. Thus, radon exhalation describes the escape of radon from soil and rock surfaces into the air as illustrated in Figure 3. Radon exhalation is the emission of Rn-222 per unit area per unit of time (Mazur & Kozak, 2014; Bala et al., 2017; Saad et al., 2013; Sakoda et al., 2011). With a half-life of 3.8 days, it can accumulate in the air after exhalation and later be inhaled, leading to radiological effects. The radiological effects result from inhaling radon daughter isotopes Po-214, Po-218, Pb-214, and Bi-214 (Martins da Silva et al., 2022; Munoz et al., 2017).

The exhalation of radon is dependent on some factors, including physical and chemical characteristics of soil, Ra-226 concentration, soil structure, emanation coefficient, and variations in meteorological factors (Mazur & Kozak, 2014; Mullerova et al., 2017; Vaupotic et al., 2010). Soil is the ultimate source of Ra-226 and Rn-222 (Kumar & Narang, 2014). Rn-222 is produced from the disintegration of Ra-226 in soil; hence, the concentration of Ra-226 in soil affects the concentration of Rn-222 in the atmosphere (Abate & Amtatie, 2020). Radon exhalation in soils is an essential parameter for evaluating the Rn-222 and related radiological impacts in a geographical area (Bala et al., 2017; Singh et al., 2010).

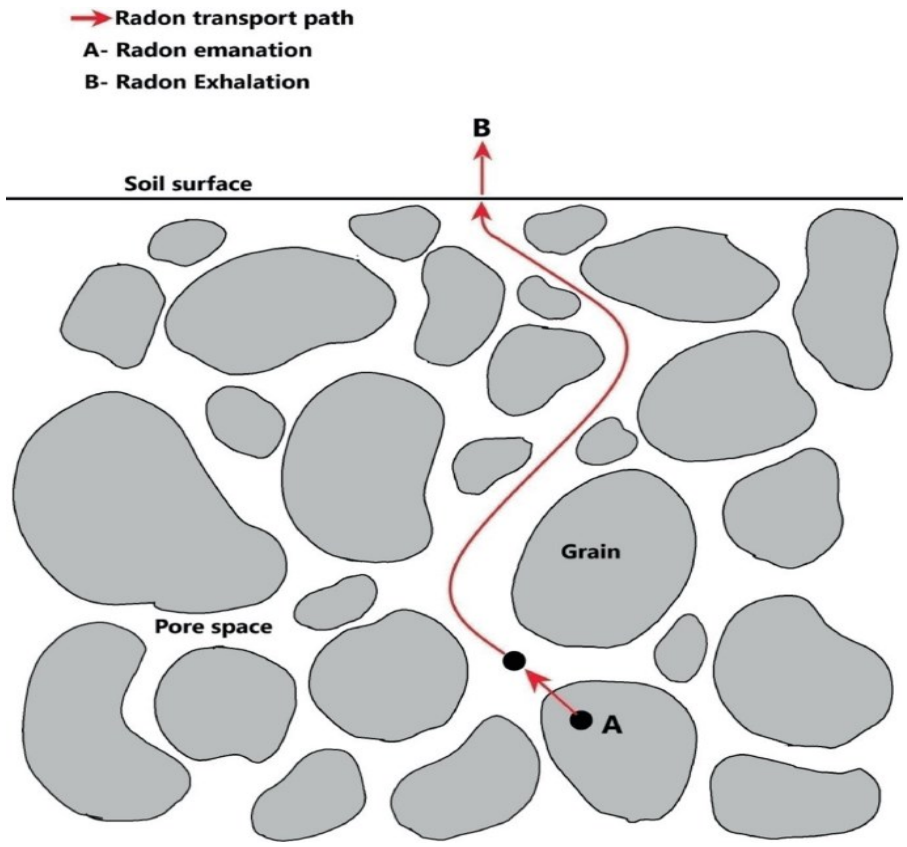

Figure 3. Diagram of Rn-222 escaping from soil pores (Joseph, 2023).

Radon exhaled from soil can accumulate in high concentrations in closed environments. The level of radon concentrations in homes and workplaces depends on several factors, including soil composition, ventilation, the age of the building, and the type of building materials used in construction. Radon gas can also accumulate in buildings by its seepage through fractures in connecting parts of buildings, drainage pipes, concrete floors and walls, ventilation, and heating and air conditioning ducts as shown in Figure 4 (IAEA, 2019; Csordás et al., 2021;

Mihci et al., 2010; Baltrenas et al., 2020; Nyhan et al., 2018; Kocsis et al., 2021; Shahrokhi et al., 2021; 2020; Adelikhah et al., 2022; 2021).

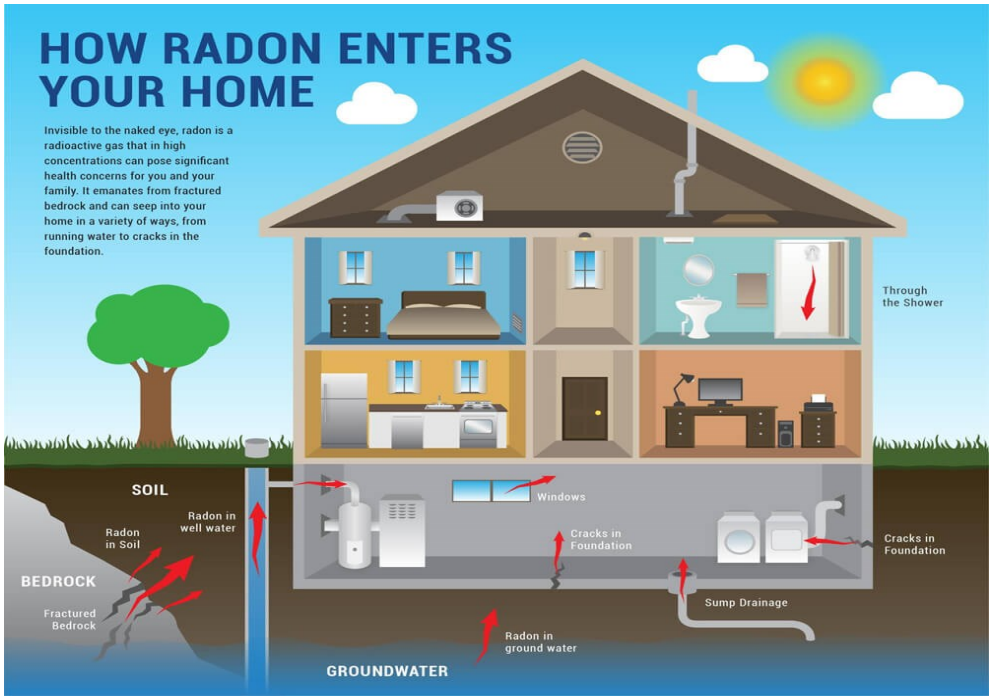

Figure 4. Diagram depicting radon entry routes into buildings (Radon Solutions, 2022).

Rn-222 is known to cause significant health problems, as studies have shown evidence of a relationship between Rn-222 and health hazards (Sahoo et al., 2011; WHO, 2009). The World Health Organization (WHO) states that exposure to radon over a prolonged period increases lung cancer risk. The risk is estimated at a radon concentration of 100 Bq/m^3 and increases by 16% for every 100 Bq/m^3 radon concentration (Ramadhany et al., 2022; Modibo et al., 2021; Soniya et al., 2021). Radon accounts for 3-14% of the lung cancer cases recorded in the world (WHO, 2009). It also leads to toxicity in the bone marrow and blood and changes in respiratory functions (Abo-Elmagd, 2014; Mann et al., 2014; El-Mageed et al., 2014). The radiological effect of radon and its daughter isotopes is estimated to account for 1.15 mSv (50%) of the total 2.4 mSv radiation dose received by humans per year from natural and artificial sources (Lee et al., 2021; Martins da Silva et al., 2022; Pantelić et al., 2018; IAEA, 2019; Misdaq et al., 2015; Mazur & Kozak, 2014). Consequently, the European Union Basic Safety Standards recommends the protection against exposure to radon in residences and workplaces and the associated health implications (EU-BSS, 2013). International bodies have

recommended reference levels for indoor radon concentrations to control exposure levels in dwellings and work environments and decrease lung cancer risk. The European Union's Basic Safety Standards Directive sets the reference level for indoor radon concentration at 300 Bq/m^3 (EU-BSS Directive, 2013), the Basic Safety Standards of the International Atomic Energy Agency has it at 200 Bq/m^3 for homes and 1000 Bq/m^3 for workplaces (IAEA, 1996), the International Commission on Radiological Protection has it at 300 Bq/m^3 (ICRP, 2010) and the World Health Organization has set it at 100 Bq/m^3 (WHO, 2009).

To assess the risk of lung cancer by radon concentrations in dwellings and workplaces, several indoor radon measurements have been carried out in several parts of Ghana, especially in the Greater Accra Region. These include indoor radon levels in Dome using Solid State Nuclear Track Detectors (SSNTD) with LR-115 type II detectors by Nsiah-Akoto et al. (2011). Kpozdro (2018) investigated factors influencing indoor radon concentrations in residences of Dome and surrounding areas and soil gas radon levels using LR-115 type II detectors. Otoo et al. (2018) measured seasonal indoor radon levels in homes and offices in the Accra metropolis using the CR-39 SSNTD. Loffredo et al. (2022) assessed indoor radon concentrations in Kpong using the Kodak-Pathe LR-115 type II detectors (Loffredo et al., 2022; Otoo et al., 2018; Kpodzro, 2018; Nsiah-Akoto et al., 2011). However, with these and other studies conducted, no radon map has been developed for the country or any part of the country. Indoor radon measurements and a radon map for a geographical location offer important information to experts and authorities for construction works and policies to reduce the public's exposure to radon gas. This will enhance the area's general well-being and quality of life. Therefore, measuring indoor radon levels in homes across the Greater Accra region and creating a radon map for this area is crucial, as it is one of Ghana's most developed regions with many infrastructural advancements.

Again, investigations to determine the radon exhalation rate in soils in an area help to evaluate correctly the potential radiological hazards of radon in air to individuals within the area. Generally, radon exhalation rate has been studied extensively in soils, rocks, and building materials, and the results are communicated in publications. Nevertheless, in Ghana, only a few of such studies have been conducted, and these studies have been limited to specific geographical areas (Otoo et al., 2022; 2020; 2018; Nsiah-Akoto et al., 2019).

Insufficient data is available on radon exhalation rate in soils and building materials in the country and thus, the need to perform such investigations.

2.3.3 Radioactivity in tobacco leaves and cigarettes

Radionuclides are found in plants through their uptake from soils to the various parts of the plants including the leaves. Hence, tobacco leaves are a natural source of radiation in the environment. One main radionuclide of radiological concern in tobacco leaves and cigarettes is Po-210 (Zagà et al., 2021; Desideri et al., 2007). The concentration of Po-210 in tobacco leaves is traced from its absorption from soils through the roots of the tobacco plant and the absorption of aerosols' polonium content via the tobacco leaves' surfaces, as illustrated in Figure 5a. Phosphate fertilizers are rich in uranium and a primary source of Po-210 in soils when used to fertilize tobacco plantations. The phosphate fertilizers contain radium (due to uranium decay) and its progenies Po-210 and Pb-210. The tobacco leaves accumulate Po-210 and Pb-210 through the trichomes, and over time, the Pb-210 isotope decays to Po-210, increasing the Po-210 concentration in the tobacco leaves (Zagà et al., 2011; Kovács et al., 2007; Schayer et al., 2009).

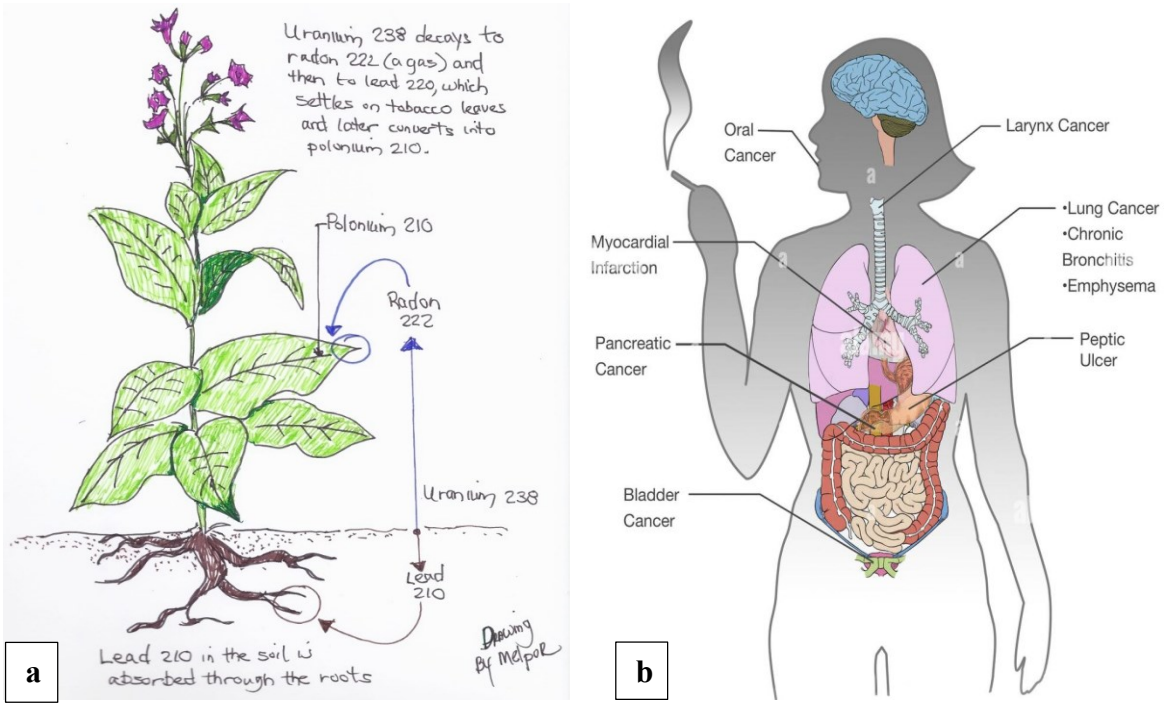

Figure 5. Diagram illustrating a) how Po-210 enters tobacco leaves and b) the effect of smoking cigarettes (Hub Pages, 2017; Alamy, 2024).

The burning of tobacco leaves in cigarettes releases Po-210 which when inhaled can be detrimental to human health. Po-210 ($T_{1/2}$ = 138 days) is one of the major carcinogenic agents in cigarette smoke causing lung cancer (Figure 5b). The burning of cigarettes releases about 50% of its radioactive substances into the lungs, as well as sending almost 32% of Po-210 to the lungs through inhaled smoke (Zagà et al., 2021; Desideri et al., 2007). Volatile polonium compounds mixed with cigarette smoke are released into the human body at the burning temperatures of cigarettes of 500-800 °C, causing severe harm to the body in the long term (Iwaoko et al., 2019). Therefore, natural radionuclides contribute largely to the mean radiation dosage in the human body, of which alpha emitters such as Po-210 significantly contribute to their probable radiation exposure (Desideri et al., 2007).

Smoking is known to be the primary cause of lung cancer disease and is responsible for approximately 85-90% of all lung cancer cases (Kovacs et al., 2007; Zagà et al., 2011). According to the World Health Organization (WHO), 8 million people will lose their lives annually by 2030 due to the gradual increase in smoking, especially in developing countries (Doku et al., 2012). Smoke from cigarettes has cancerous constituents in significant quantities. These are mainly poisonous chemical compounds and several natural radionuclides (Kovacs et al., 2007). Recent reports state that the tobacco industry is expanding in middle and low-income countries in Eastern Europe, Asia, and Africa, including Ghana, due to a decrease in patronage of tobacco and cigarette products in high-income countries (Singh et al., 2020). Though the smoking rate in Ghana is low compared to other countries, there is public concern about the increase in cigarette smoking among the youth (Doku et al., 2012). One of the concerns is the rise in smoking-related diseases and deaths, with over 5000 deaths recorded annually (Singh et al., 2020). For this reason, there is a need to initiate pragmatic measures to curb the surge in smoking-related diseases and deaths.

Determining the activity concentration of radioactive substances in cigarettes specifically, Po-210 and estimating the radiological risks is significant as it provides information on the level of risks associated with the health of the public due to smoking cigarettes. Studies on the radiological risks associated with cigarette smoking have not yet been conducted in Ghana. The only available data found during this investigation was a study on the elemental profile of local tobacco products using Instrumental Neutron Activation Analysis (INAA)

(Addo et al., 2008). Due to the lack of data in this area of study, this investigation aimed to evaluate Po-210 activity concentrations in Ghanaian cigarettes and assess the related health hazards due to the inhalation of Po-210 during smoking.

2.3.4 Radioactivity of soil

Most natural and anthropogenic radionuclides in the environment remain generally in soils (Yordanova et al., 2015; Ademola & Obed, 2012). The occurrence of natural radionuclides in soils in different concentrations is dependent on the nature of the parent rock during the beginning of formation (Yachiso et al., 2022). The radioactivity of soil and sediment depends on their formation, transport processes, and chemical and biochemical interactions. These also affect the patterns of distribution of U-238 and Th-232 and their daughter isotopes (Agbalagba et al., 2012). The radioactivity and related radiation exposure depend on the type of soil at the location and its geological formation, and these significantly impact the radiation dose distribution (Laith et al., 2015; Yordanova et al., 2015). Hence, the knowledge of radionuclides distribution in soils is important for radiation monitoring and protection (Innocent et al., 2013).

Radionuclides in soil emit gamma radiation into the environment and the atmosphere, changing background radiation levels (Yachiso et al., 2022; Shayeb & Baloch, 2020). Thus, the radioactivity of soils contributes to the terrestrial constituent of the natural background (Inayatullah & Madihah, 2016). Humans are exposed to terrestrial radiations that are emitted primarily from the upper 30 cm of the surface of soils (Jwanbot et al., 2013). Soil acts as a means of migration for the transport of radionuclides to the environment, and as such, it is regarded as the primary indicator for radiological pollution in the environment (Akpanowo et al., 2019; Agbalagba et al., 2012; Hamideen & Sharaf, 2012). Radioactivity in soil can be transported to humans via plant root uptake or deposition on vegetation, and finally be inhaled or ingested. These radiation exposure pathways from soil are potentially important for radiation risk assessment (Ademola & Obed, 2012).

Radioactivity levels in soils are generally significant in establishing baseline data for future assessment of radiation impact. The chemical and physical properties of radionuclides cause radioactive pollution to be long-lasting, with little change in concentration over time. This explains why radiation exposure due to human environmental activities harms human health.

They increase background radiation levels where the increased radioactivity concentration in the soils may become substantial enough to authorize regulatory control (Hamideen & Sharaf, 2012; Focus et al., 2012; Inayatullah & Madihah, 2016). Recently, studies on radionuclide concentrations in soils have been on a global rise due to the health hazards they pose to the population within a geographical location (Joel et al., 2019). The estimated worldwide average concentrations of Ra-226, Th-232, and K-40 in soils and sediment are 35 Bq/kg, 30 Bq/kg, and 400 Bq/kg, respectively. Nonetheless, in some countries like China, Iran, and Brazil, these values can be higher due to the high concentrations of uranium, radium, and thorium in their soils (UNSCEAR, 2000; 2008; Akuo-ko et al., 2023a).

2.4 Mining and natural radiation levels

Mining is a human activity that has the potential to redistribute and enhance the radionuclides activity concentration in the environment by altering levels of natural concentrations (Ramadhany et al., 2022; Ladan et al., 2022; Yordanova et al., 2015). This has resulted in the global assessment of radionuclides in soil and water in mining regions and their surroundings (Yachiso et al., 2022; Souffit et al., 2022; Joel et al., 2019). Radionuclides are in equilibrium when undisturbed, but this becomes the opposite in mining and mineral processing (Ladan et al., 2022). As a result, natural radioactivity levels in mining areas are usually higher than in neighbouring non-mining regions. It also increases the background radiation levels (Leuangtakoun et al., 2020).

During mining, the mine workers and the public are exposed to external gamma radiation emanating from the mineral ores, the ingestion and inhalation of water and dust containing daughter isotopes of uranium and thorium, and the inhalation of radon gas and its progenies. Mining processes like drilling, digging, leaching, storage, handling, transportation, use of contaminated equipment or waste media, and the discharge of tailings and seepage waters without control measures increase radioactivity levels in mining areas (Bansah et al., 2018; Ademola et al., 2014; Galhardi et al., 2017; Yachiso et al., 2022; Innocent et al., 2013; UNSCEAR, 2000). Continuous discharge of tailings and mine waste into the environment can cause the concentration of radionuclides in soil, water, and air, and then irradiation in humans (Aliyu et al., 2015). Inhabitants living near mining sites get exposed through the food chain, drinking water, and using mine waste as building materials (Bello et al., 2020; Odumo

et al., 2011; Idriss et al., 2016). Since mine tailings are more concentrated with natural radionuclides than surrounding soils, mining activities must be appropriately monitored; otherwise, it could lead to significant exposure to radioactivity in workers at mining sites and residents in neighbouring areas (Focus et al., 2021; Ladan et al., 2022; Barba-Lobo et al., 2022; Galhardi et al., 2017; Nguelem et al., 2016; Innocent et al., 2013).

2.4.1 Radioactivity levels of soils and surface water resources in mining areas

One problem facing the human environment these days is soil and water pollution with radionuclides, because they serve as a route for ingestion and inhalation of radiation in humans. Consequently, investigations of soil and water to evaluate the level of pollution are necessary, as well as continuous monitoring of the human environment (Akpanowo et al., 2019; Taqi et al., 2018; Chandrasekaran et al., 2015; Öge et al., 2021; Yordanova et al., 2015). The transfer of radionuclides into the environment occurs through various pathways, including the atmosphere, water resources, and soil sub-compartments (Liu et al., 2021; Asaduzzaman et al., 2014). The public is also exposed to natural radionuclides via secondary transmission modes like ingesting polluted water resources and food cultivated on contaminated lands and animals (Mathuthu et al., 2021). The ingestion of radionuclides through food and water is extensively regarded as the most significant route of internal radiation exposure (Giri et al., 2013). Again, natural radionuclides are transferred from soil to water or from soil to plants. This is essential in evaluating the internal radiation from plant or water consumption since these environmental components have a linear relationship (Asaduzzaman et al., 2014).

Water is undeniably essential for life on Earth. Water resources can contain different amounts of radioactive substances, which can cause radiological hazards. Radionuclides are released from rocks and minerals through erosion and dissolution, which transport the radionuclides from the rocks into water. Drinking water may contain radionuclides from parent and daughter isotopes of uranium, thorium, radium, and radon (Suresh et al., 2020; Giri et al., 2013; Nuccetelli et al., 2012). The concentration of radionuclides in water depends on the type of rock, variation of minerals occurring in the rock, presence of cracks, porosity-permeability, physicochemical characteristics, and characteristics of geological aquifers (Suresh et al., 2020). U-238, Ra-226, Ra-228, and Rn-222 are considered the most critical

contaminants due to their relatively high radiotoxicity and solubility in water (Nuccetelli et al., 2012; Avwiri et al., 2013). These can cause severe health threats. Their ingestion or respiration may produce high radiation doses to delicate cells in digestive organs, respiratory tracts, and other human body organs (Suresh et al., 2020; UNSCEAR, 2000). Since water is vital for human existence, it is also a medium of exposure to cancerous diseases, as it has been recognized that cancers caused by chemical carcinogens are primarily found in drinking water (Orosun et al., 2020).

Artisanal and small-scale predominantly cause severe environmental damage than good in developing countries, even though they are a means of income and wealth creation (Souffit et al., 2022). Mine locations, unusual extraction procedures, and the lack of implementation of mining regulations have made mining in Ghana a disaster (Figure 6). Therefore, investigations to provide comprehensive scientific evidence will help assess human exposure to radioactivity in mining areas. Although various studies on radioactivity levels within mining areas in Ghana have been carried out (Faanu et al., 2011; 2013; 2014; 2016; Doyi et al., 2013; Adukpo et al., 2015; Anyimah-Ackah et al., 2021), the country is yet to subject mining activities to radiological regulatory control. Because of the lack of such regulation, there is little or no knowledge and cognisance of the radiological risks associated with radioactivity exposures in mining locations.

Figure 6. Damage caused by artisanal mining in the selected study areas (by author).

2.4.2 Groundwater quality in mining areas

The global population growth has led to a significant rise in demand for water as it is a vital resource in sustaining life and community (Sherif & Sturchio, 2018; Fang, 2019; Baeza et al., 2017). As a geological agent, groundwater interacts with its environment as illustrated in Figure 7, by mobilising, transporting, and accumulating matter, including radioactive substances (Alomari et al., 2020; Csondor et al., 2020; Erőss et al., 2018). A continuous water-rock interaction underneath the earth results in appreciable radionuclides dissolving in groundwater resources. Due to this phenomenon, groundwater may contain levels of radionuclides which cause radiation dose to users and consequently a risk to human health (Shabana & Kinsara, 2014; Turhan et al., 2013). Thus, natural radioactivity concentration is a limiting factor to groundwater quality. This has called for examining radioactivity levels in groundwater as an important parameter for assessing the quality of groundwater resources in many countries (Sherif & Sturchio, 2018; Alomari et al., 2020).

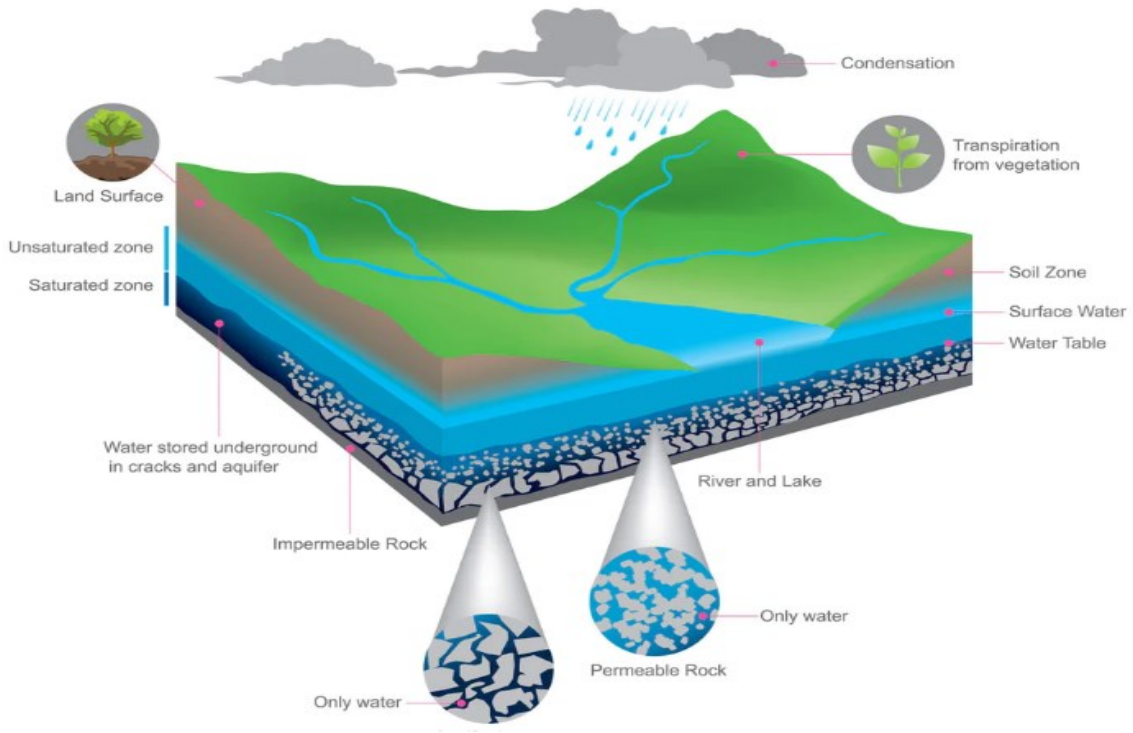

Figure 7. Interaction of groundwater with bedrock and soil (Fresh Water Systems, 2021).

Natural radionuclides of the decay series of U-238 and Th-232 and K-40 in bedrocks and soil cause radioactivity levels in groundwater. They are primary sources of external gamma radiation, and their presence in rocks and water influences background radiation levels, leading to human exposure to radiation. Radionuclides in drinking water such as groundwater can accumulate in different organs of the body when ingested (Baeza et al., 2017; Turhan et al., 2013; O¨rgu¨n et al., 2005; Mathuthu et al., 2021; Akweetelela et al., 2020; UNSCEAR, 2000). The relatively high radiotoxicity of some natural radionuclides necessitates the radiological characterisation of groundwater as a monitoring activity for drinking water and to study the cumulative radiation hazards on the health of humans (Zhong et al., 2020).

Groundwater has widely been recognized as an indispensable resource for consumption and irrigation (Gordon et al., 2013). In Ghana, groundwater serves both domestic and irrigation uses, especially in rural areas with limited access to potable water (Gampson et al., 2017). People rely on groundwater and surface water resources for their water supplies. However, the use of these sources of water has not been evaluated for their radionuclide contents, especially in areas where there are several illegal mining activities taking place, which have

polluted many water resources that inhabitants depend on (Gordon et al., 2013; Yidana et al., 2012; Bansah et al., 2018; Snapir et al., 2017).

Mining activities have led to the contamination of drinking water resources with mine wastes due to the increasing mining activities, particularly in the Atiwa West district of Ghana. Mining in the area is primarily done with artisanal techniques, and they are mostly unregulated (Bansah et al., 2018; Snapir et al., 2017; Yankson & Gough, 2019; Patel et al., 2016; Klubi et al., 2020). The pollution of surface water resources in the area has led to the population relying on groundwater as an alternate water source for drinking, domestic, and irrigation purposes. Studies have indicated that groundwater resources can contain significant levels of radionuclides. This is caused by the leaching of radionuclides from soils into groundwater during mining, resulting in further contamination of groundwater resources with radionuclides as several cracks are created in bedrocks due to mining activities (Baeza et al., 2017; Csondor et al., 2020; Shabana & Kinsara, 2014; O¨rgu¨n et al., 2005; Giri et al., 2011). However, groundwater in mining areas has not been investigated for radionuclide contamination and thus, a lack of information on likely radiological hazards among the population. Since groundwater can contain appreciable levels of radionuclides, the study sought to determine the concentrations of natural radionuclides in groundwater resources in mining areas and evaluate their potability for drinking and domestic purposes.

2.5 Radiological effects of ionizing radiation on humans

Naturally occurring radionuclides in some environmental media can induce hazardous radiological amounts, as the concentrations of such radioactive materials in the environment differ according to geological formation. This is attributed to the Earth's irregular distribution pattern of radionuclides (Akpanowo et al., 2019). The annual effective dose estimated for natural background radiation is 2.4 mSv/y, which forms almost 80% of the total radiation dose for an individual. Radon gas contributes approximately 50% of the total radiation dose from natural exposures (Oliveira de Souza et al., 2015; Ademola et al., 2014; Ademola & Obed, 2012; UNSCEAR 2000).

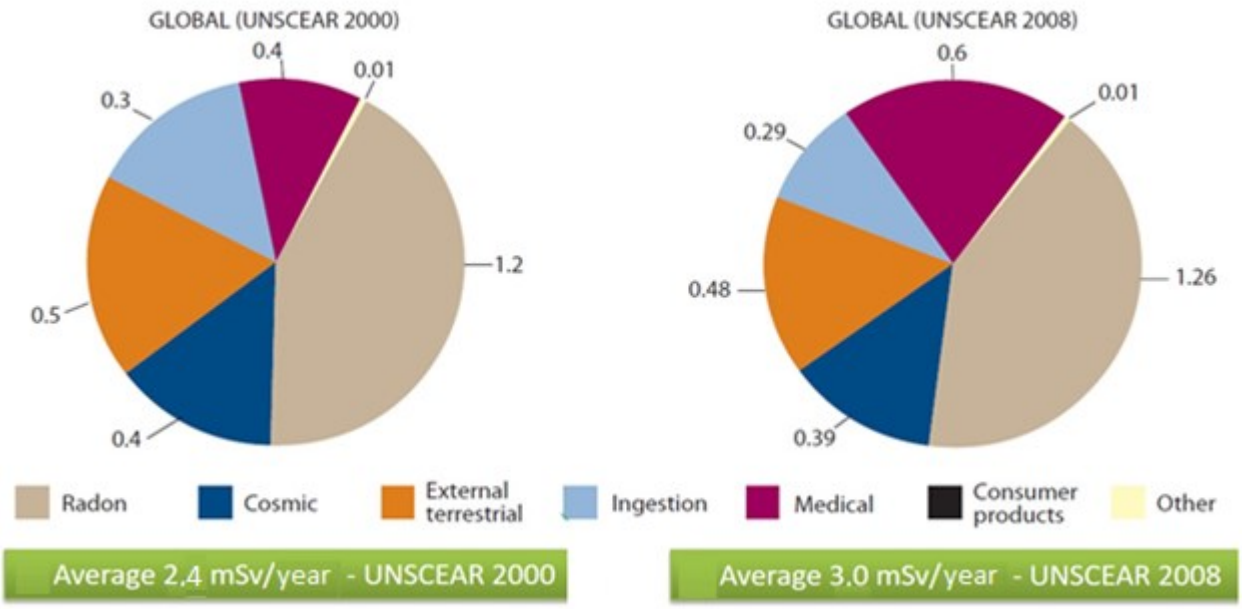

Figure 8. Estimation of annual effective dose from various radiation sources (Taroni, 2017).

The exposure of the human population to radionuclides via ingestion and inhalation results in internal and external exposures (Ladan et al., 2022). Such exposures in the long term cause detrimental health implications, including lung disease, chronic haemorrhage, cardiovascular complications, anaemia, premature ageing, necrosis of the mouth, and acute leucopenia. Concerning specific radionuclide health problems, radium accumulation in the human body can lead to tooth fractures, cataracts, and several types of cancers. Thorium exposure can cause leukaemia, lung, bone, kidney, and pancreas cancers (Zubair & Shafiqullah, 2020; Focus et al., 2021; Qureshi et al., 2014). Radioactive contaminants can reach the human body by ingesting polluted food, water, and soil, inhaling particulate pollutants, and exposure to external radiation, causing illnesses including lung and bone cancers and cell damage (Ramadhany et al., 2022). Hence, determining the radioactivity levels and radiation doses from sources and assessing the correlated health effects is important in every environmental radiation measurement study (Öge et al., 2021).

CHAPTER THREE

MATERIALS AND METHODS

3.1 Introduction

This chapter details the various methods and instruments used to conduct the investigations. The outline used in this chapter describes study areas, sampling methods and procedures, sample preparations, instruments of analysis and their minimum detection limit, description of radiological parameters assessed, and the statistical tools employed to analyze the acquired data.

3.2 Study areas

The study areas were described according to the geographical areas within which samples were collected for radionuclide measurement and assessments. Figure 9 illustrates a map of the study areas. The sampling process states detailed information on sampling points, types of samples, and the number of samples collected from each geographic study area.

3.2.1 Coastline of Ghana

The coastline of Ghana covered in the study lies between the latitudes 5°0'44.64"N 2°42'44.38"W and 6°6'21.88"N 1°11'4.02"E. The entire Ghanaian coastline covers a distance of 550 km from Aflao to Axim. The coastline is endowed with fishery resources, and about 25% of the Ghanaian population lives in that part of the country. The livelihoods of the population living along the coast are fishing and sand winning (Quansah, 2014; Alabi-Doku et al., 2018). The shores of Ghana are popular locations for tourists and holidaymakers all year round. For this reason, it is crucial to evaluate the radionuclide concentrations and the extent of any irregularity in radioactivity along the shores of Ghana.

3.2.2 Greater Accra region

The Greater Accra region of Ghana is bounded by the Central, Volta, and Eastern regions on the west, east, and north. The region is positioned between longitudes 0° 20' 0" W and 0° 5' 0" W and latitudes 5° 40' 0" N and 5° 45' 0" N. It is the country's capital, and the second most populated region. It is also the most developed region, with about 87.4% of the population dwelling in city centres. The region has the smallest land area, occupying a size of 3.245 km^2,

representing 1.4% of the country's total land area. The topography of the region is made up of several categories of soils and rocks. The soil categories include residual clays and gravels, laterite sandy clay soils, and the alluvial and marine motted clay soils. The main categorization of rocks in the region consists of gneiss, quartzites, granites, the Precambrian Togo series, and the Dahomeyan schists (Otoo et al., 2018).

3.2.3 Atiwa West

The Atiwa West of the Eastern region of Ghana is between latitude 6°18'50.4"N and longitude 0°35'34"W. The Atiwa West district has a population of approximately 62,000 people. The populace is predominantly involved in mining, agriculture, and agro-based industrial activities. The area has an elevation of 240-750 m above sea level. The area is located within a semi-deciduous forest with 12- 20% of the land covered by commercial trees such as Triplochiton scleroxylon, Milicia regia, Mahogany, Terminalia, bamboo, etc. The landscape is gentle and undulating, with diverse rock formations resulting in the area's diverse relief features, extending from flat-bottom basins to steep-sided highlands. The soils are mainly reddish-brown with uplands categorised by well-drained, deep, gravel-free silty loams and silty clay loams, whereas poorly drained alluvial silty clays characterise the plains. The area is known for mineral deposits, especially gold, hence the reason for numerous artisanal and small-scale gold mining activities in the area. The mining activities are mainly located near water resources, farmlands, and inhabited areas. Atiwa West district is adjoining to one of the largest national forest reserves in the country, the Atiwa Forest (Gordon et al., 2013; MOFEP, 2019; Amponsah et al., 2022; NDPC, 2019; IUCN, 2020).

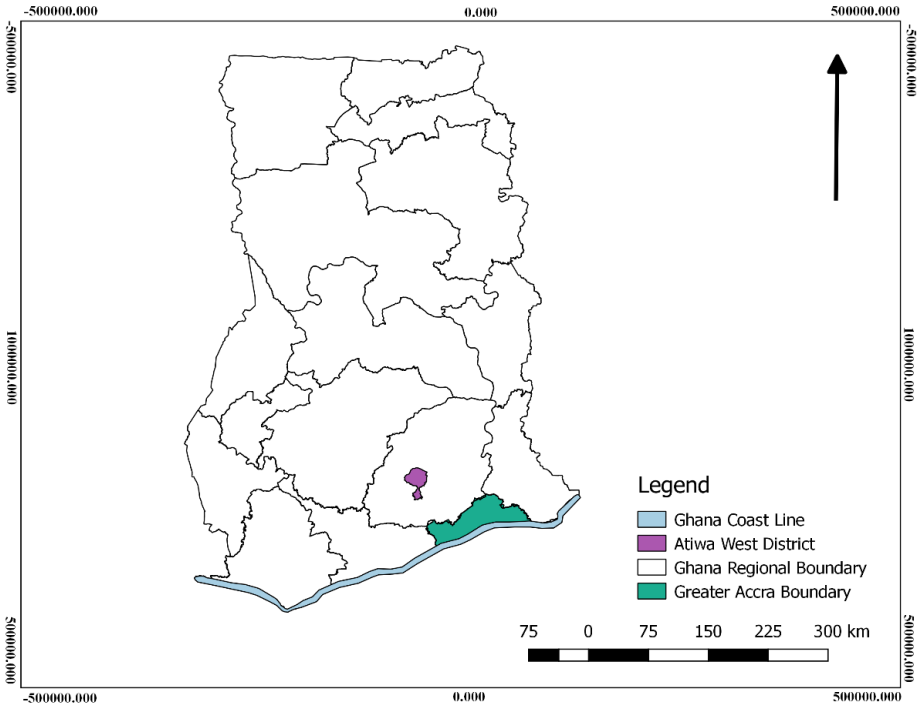

Figure 9. Map of areas in Ghana investigated in the study (by author).

3.3 Sampling methods

3.3.1 Sediment

Sampling at coastal areas was selected based on the ongoing activities in the area which are likely to expose the public to radiological hazards. Sediment samples were collected with a plastic core tube (diameter: 7 cm). At each coastal sampling location, two sites were marked 100-200 m apart as subsampling points. Four samples were collected from a 1 m^2 marked depth of 25-50 cm. Samples were collected 100- 150 m away from the seawater. A total of 152 samples were collected from 19 sampling locations along the coast of Ghana as shown in Figure 10. Sediment samples were stored in Ziploc bags, well-labelled, and transported to the laboratory for analysis.

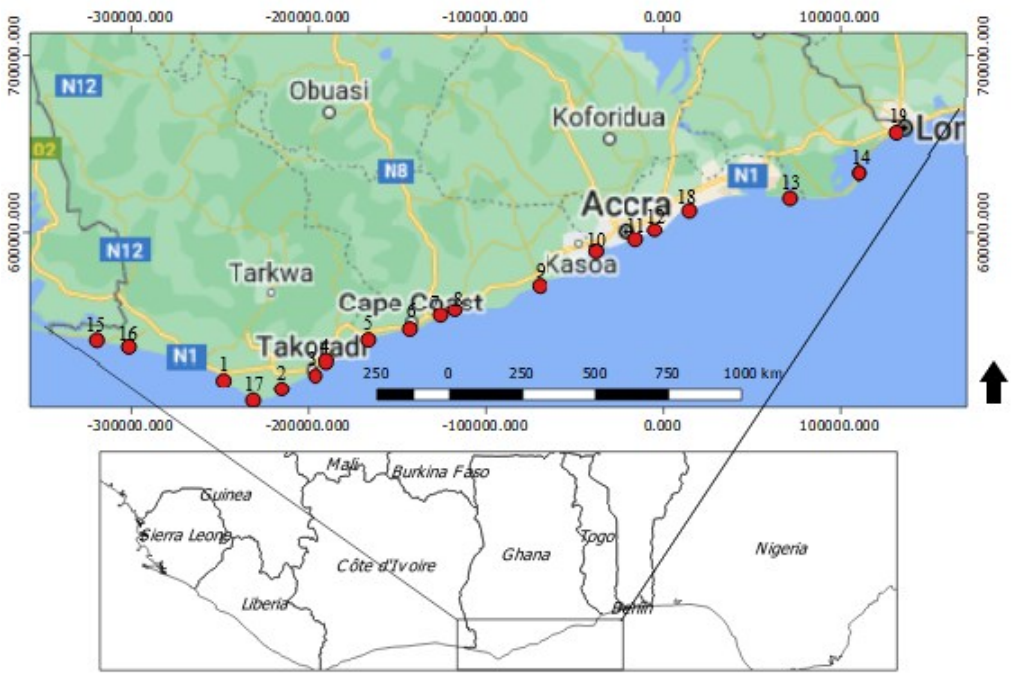

Figure 10. Map of sediments sampling locations along the coast of Ghana (by author).

3.3.2 Indoor radon

This investigation surveyed the ground floors of residences such as houses, villas, and apartments. The participating homes were constructed with concrete, clay bricks, gravel, cement, sandstone, and tiles. Residences involved in this investigation were selected randomly and also based on the willingness of occupants to keep the detectors in their homes for the entire duration of exposure. A total of 95 residences were surveyed in the study (Figure 11). Detectors were positioned at a 1.0- 1.5 m height above the ground in the dwellings. They were placed at a distance greater than 0.5 m from walls and 15 cm away from objects. The detection of indoor radon gas in residences was conducted using NRPB dosimeters with CR-39 detectors (Figure 12). The detectors were placed in the living rooms and bedrooms, depending on where residents spent most of their time. The majority of residences surveyed were between 7 and 80 years old. They were constructed with cement and sand bricks along with tiled floors. The detectors were exposed to indoor radon for 3 months, and afterwards, they were covered with aluminium foil and transported to the laboratory for analysis.

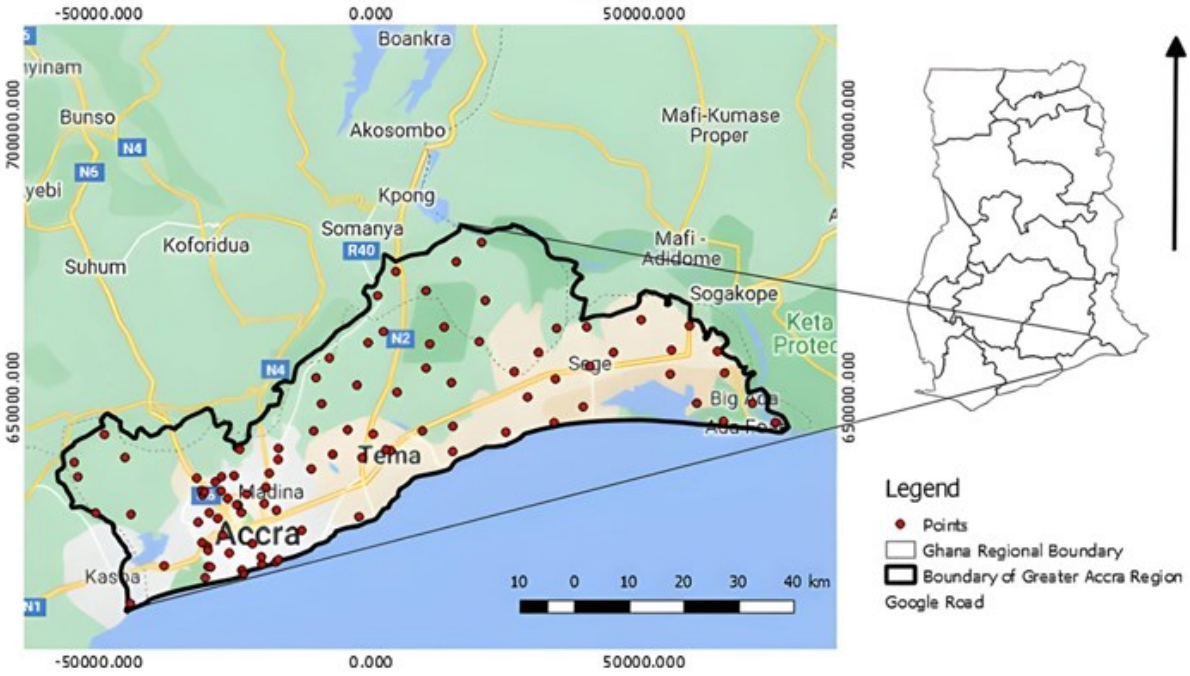

Figure 11. Map of indoor radon measurement locations (by author).

Figure 12. NRPB dosimeter with a CR-39 detector (by author).

3.3.3 Cigarettes

Determining the activity concentration of Po-210 in cigarettes was performed by sampling commonly smoked cigarette brands on the Ghanaian market. Both foreign and local cigarette brands were sampled for analysis. In all, 15 different cigarette brands were sampled. These were Pall Mall red, Pall Mall green, Oris red, Oris green, Rothmans white, Rothmans black, State Express, London king size, Gold seal, Fisher virginia blend, Malboro, Camel blue,

Benson and Hedges, Kent, and Esse change. For each cigarette brand, three samples were purchased from retail outlets, including shops, supermarkets, and pubs.

3.3.4 Soil

Soil samples were collected from a surface area of 2 m × 2 m at each sampling location from a depth of 10-30 cm below the surface. Four sampling points were marked and sampled at each location. Forty-six locations within the mining areas of Atiwa West were selected and sampled. Soils and sediment from mining sites, farms, and undisturbed lands were collected in the study area. Samples were stored in Ziploc bags, well-labelled, and transported to the laboratory for analysis.

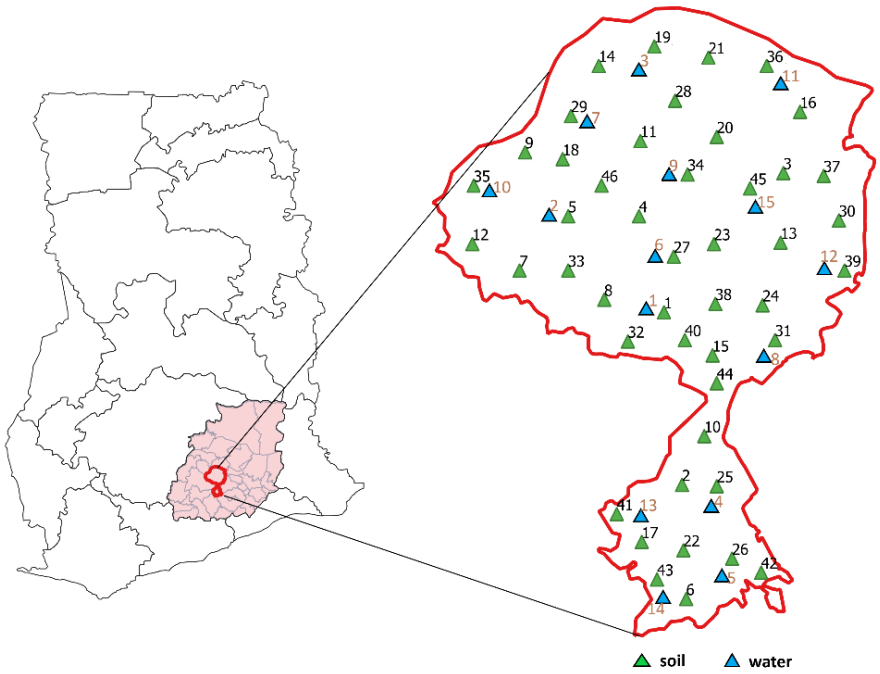

Figure 13. Map of soil and water sampling locations within Atiwa West mining areas (by author).

3.3.5 Surface water and groundwater

Surface water samples were collected from 15 locations (Figure 13) identified within mining sites and communities of Atiwa West. The surface water samples were collected from streams and rivers within the mining communities. Groundwater samples were collected based on the proximity of the groundwater resource to mining sites and within mining communities. They

were sampled from 16 locations within Atiwa West (Figure 14). Surface and groundwater samples for each area were composite samples of triplicate samples. Samples were collected directly from the source into pre-conditioned polyethylene bottles by immersing an entire bottle into water and closing it up tightly before bringing it out. Afterwards, water samples were acidified with hydrochloric acid to prevent radionuclide precipitation and adherence on the walls of the bottles, thereby preserving the integrity of radionuclide composition within the water matrix. Samples were then labelled and transported to the laboratory.

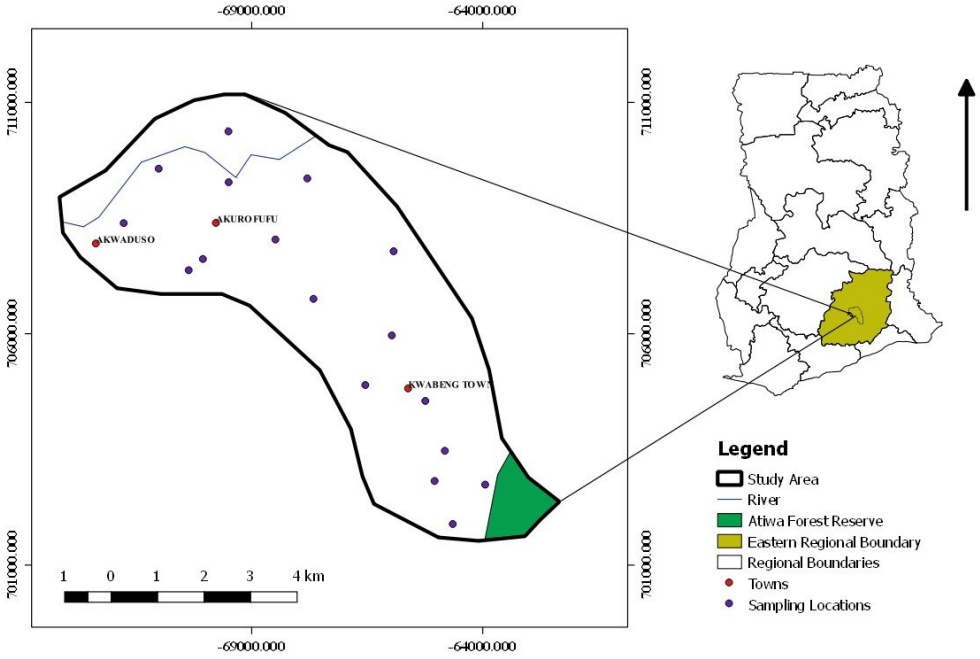

Figure 14. Map of groundwater sampling locations (by author).

Figure 15. Soil and water sampling activities (by author).

3.4 Sample preparations

3.4.1 Sediment and soil

In the laboratory, samples were air-dried for 7 days, oven dried at 105 °C for 24 hours, pulverized, and sieved with a 2 mm mesh sieve. Samples were homogenized for each location, transferred into Marinelli beakers, sealed, and labelled accordingly. The prepared samples were kept for 28 days to allow for secular equilibrium between parent and daughter nuclides (i.e. where the activity of the daughter isotopes equals the activity of the parent radiouclide). After the waiting period, the samples were analyzed by gamma spectrometry to determine the major gamma-emitting radionuclides (Ra-226, Th-232, K-40, and Cs-137).

Figure 16. Preparation of soil and sediment samples for gamma measurement (by author).

3.4.2 Radon measurements

(i) Indoor radon

The exposed CR-39 detectors were washed with deionized water and then air-dried. Next, they were chemically etched in an etching device. The chemical conditions employed in the etching process were a 6.25 M NaOH solution, a temperature of 90 °C, and an etching duration of 8 hours. After etching, the detectors were kept in deionized water for 24 hours and rinsed again with deionized water. Finally, they were air-dried, and later the track densities were counted.

(ii) Radon exhalation

Soil samples were air-dried for 7 days and later dried in the oven at 60 ℃ for 24 hours. The radon exhalation rate in soil samples was measured using a CR-39 Solid State Nuclear Track Detector (SSNTD). The CR-39 detectors were obtained from Radosys, Hungary, which is traceable to the Radon calibration laboratory of the Federal Office for Radiation Protection, Germany. Soil samples were measured (300 g) and placed at the bottom of the vessel, which has a 25 cm height and a 10 cm diameter. A CR-39 detector was placed at the top of a cylindrical vessel from the surface of the soil sample to detect only radon and prevent thoron from evading the soil surface, as shown in Figure 17. The measurement of radon exhalation was done for 90 days (Otoo et al., 2018; Faheem & Matiullah, 2008). After 90 days, the detectors were etched in a 6.25 N NaOH solution at 90 °C for 5 hours and neutralized for 15 minutes in 36 ml of 96% diluted acetic acid. They were then rinsed in deionized water for 15 minutes to remove excess chemicals and dried for 4 days.

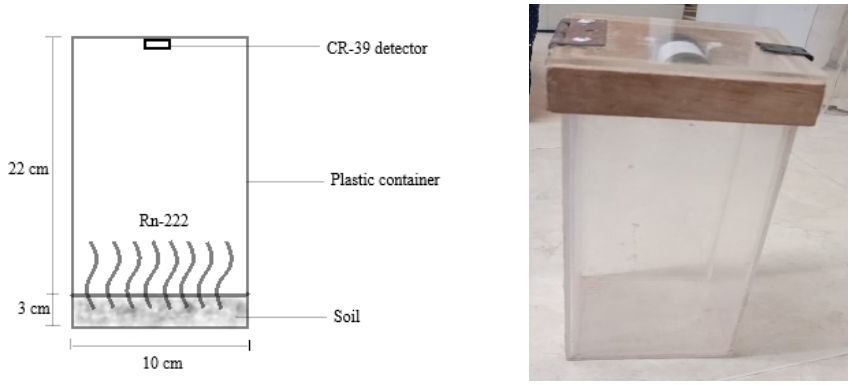

Figure 17. Radon exhalation setup (by author).

3.4.3 Cigarette

The tobacco leaves in the cigarettes were air-dried for a day. A known activity of 43.8 mBq/g of Po-209 was added as a tracer to 2g of tobacco samples in a beaker for the dissolution process. The addition of Po-209 was to help trace the radiochemical yield of Po-210 and to act as a reference for the alpha spectrometry measurement. 3 portions of 25 ml HNO_3 were added to dissolve the samples. It was dissolved on a hot plate at 80 °C to evaporate to near dryness. Few drops of H_2O_2 were added cautiously to digest the organic matter. Three portions of concentrated 25 ml HCl were added and evaporated to dryness. The samples were then dissolved in 10 ml 6M HCl to make a 100 ml stock solution and filtered. A nickel-content stainless steel disc (KO 33 MSZ 9-11%) acid-resistant was used for the spontaneous deposition of polonium. A Dlab MS-H380-Pro device and 50 ml stock solution were used for the deposition. The deposition was done at 85 °C for 3 hours in the presence of $C_6H_8O_6$ to minimize the F^{3+} ions in the solution. Afterwards, the discs were left before counting with the alpha spectrometer (Kovács et al., 2007).

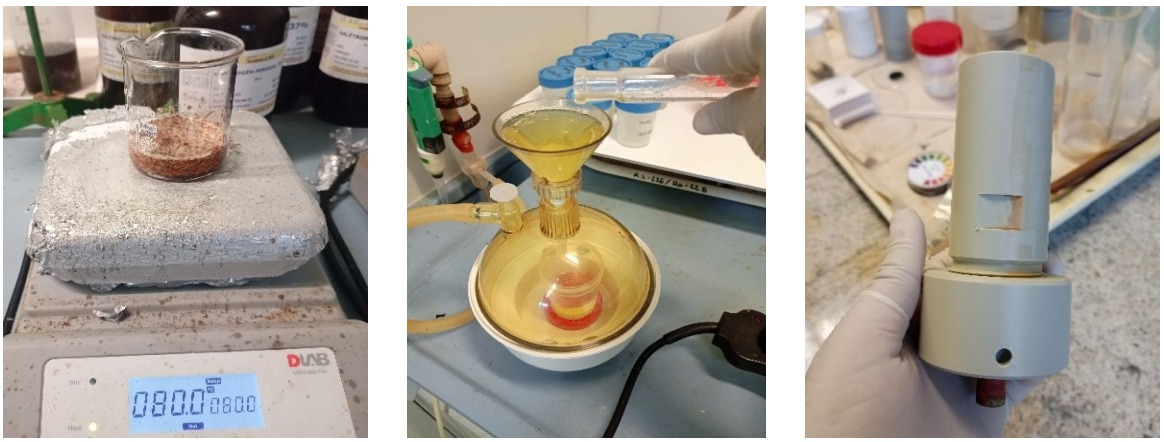

Figure 18. Dissolution and deposition process of Po-210 in cigarette samples (by author).

3.4.4 Surface and groundwater

In the laboratory, water samples were transferred into pre-cleaned Marinelli beakers without pre-treatment. The beakers were sealed and kept for 28 days to establish secular equilibrium between parent and daughter radionuclides prior to counting with a gamma ray spectrometer.

Figure 19. Sample preparation activities (by author).

3.5 Instrumentation and measurement

Different analytical techniques were employed to measure radionuclide activity in samples collected for the research. Gamma ray spectrometry was used to measure radionuclide activities in soil, sediment, and water samples. Alpha spectrometry was used to determine the activities of Po-210 in cigarette samples. The CR-39 detectors, radon exhalation chamber, and the etching device were used to determine radon concentrations. The analytical methods employed and the description of the analytical process have been given below.

3.5.1 Gamma ray spectrometry

The measurement of radionuclide activities in samples was performed with a semiconductor High Purity Germanium (HPGe) detector (ORTEC GMX40-76). The detector has 40% relative efficiency. The detector is coupled with a Multi-Channel Analyzer software (MCA) from APTEC to analyze the generated gamma spectra. The detector was calibrated with three closed sources: Am-241 at a peak energy of 59 keV, Cs-137 at 662 keV, and Co-60 at two peak energies of 1173 and 1332 keV. The detector was cooled, and the temperature was maintained at -196 °C using liquid nitrogen. The detection efficiency of each peak was calculated using the known activity of radionuclides of the IAEA-375 reference material with a similar sample geometry. The background measurement was done with an empty Marinelli beaker with the same geometry as the standard and samples at a count time of 200,000 s. The

background measurements were performed to establish the detector's environmental background distribution. To minimize counting errors and to achieve better statistics in the gamma spectra, sample measurements were done at 80,000 s (Akuo-ko et al., 2023a; Faanu et al., 2024).

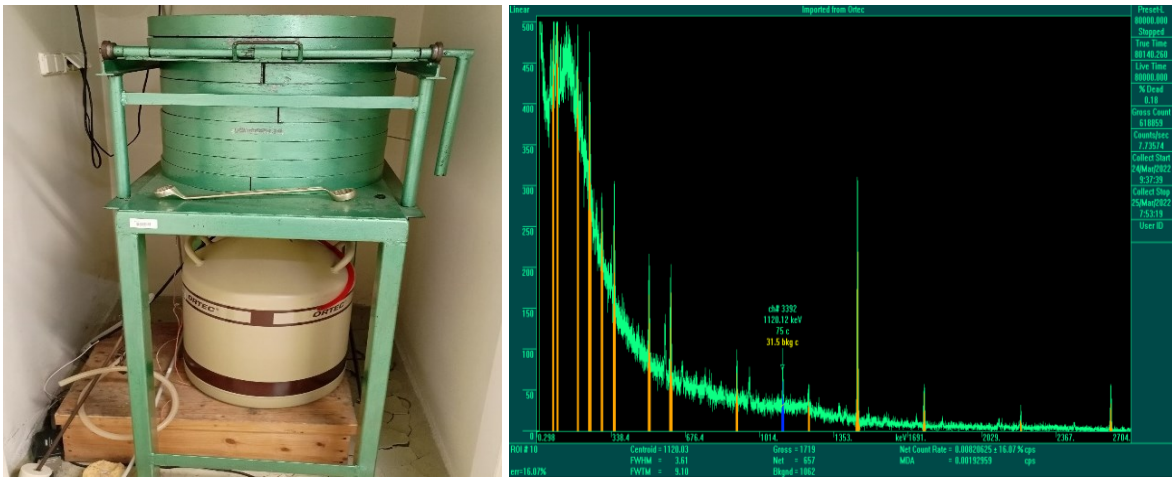

Figure 20. Gamma ray spectrometer and the spectra generated after measurement (by author).

The Minimum Detectable Limit (MDL) and uncertainty of the measurements were determined using the data provided by the APTEC analyzer software. The MDL calculation was done by the equation:

$$MDL = \frac{(\sigma 2 + 2\sigma(\sqrt{2B}))}{t} \quad (1)$$

Where *MDL* is the minimum detectable for photo-peak, σ is the uncertainty, *B* is the background rate under the photo-peak region of interest in cps, and *t* is the live counting time in s.

The corresponding uncertainties were evaluated using the statistical uncertainties of the peak areas given by the APTEC analyzer software. The following equation was used:

$$\sigma = \frac{2\sqrt{(C + B)}}{C} \quad (2)$$

Where σ is the uncertainty, *C* is the net sample count rate under the photo-peak region of interest in cps, and *B* is the net background rate under photo-peak region of interest in cps.

The MDL determined for the measured radionuclides are presented in the table below.

Table 1. Minimum detectable limits of the radionuclides.

Soil/ sediment		**Water**	
Radionuclide	MDL (Bq/kg)	Radionuclide	MDL (Bq/L)
Ra-226	0.5	Ra-226	0.4, 0.12*
Th-232	0.7	Ra-228	0.6, 0.26*
K-40	23	K-40	10.5, 1.03*
Cs-137	0.3		

* MDL for groundwater measurements

3.5.2 Alpha spectrometry

The deposition discs were measured for Po-209 ($T_{1/2}$ = 102.5 years) and Po-210 ($T_{1/2}$ = 138.4 days) at alpha energies of 4883 keV and 5304 keV, respectively. The measurement was performed with an ORTEC Alpha Duo two-chamber spectrometer of a semiconductor base detector (Passive Implanted Planar Silicon- PIPS). The PIPS detector in the alpha spectrometer has an energy resolution of less than 20 keV. The spectrometer system was calibrated with three sources: Am-241 at 5486 keV, Cm-244 at 5805 keV, and Pu-239 at 5156 keV. Prior to measurements, the background counts of the spectrometer system were determined. The background measurement was counted for 200,000 s while the sample measurements were counted for 80,000 s.

The minimum detectable limits (MDL) determined for the two chambers were calculated using the equation:

$$MDL = \frac{2.71 + 4.65\ x\ \sqrt{I}}{\varepsilon\ x\ t\ x\ m} \quad (3)$$

Where *MDL* is the minimum detectable limit in mBq/g, *I* is the background in the energy range to be investigated (impulse), $\mathcal{E}$ is the detector efficiency, *t* is the measurement time in s, and m is the mass of the sample in g.

The MDL of Po-210 estimated for the two chambers were 0.196 mBq/g and 0.382 mBq/g.

3.5.3 Etching and scanning devices for CR-39 detectors

(i) Indoor radon

The exposure to indoor radon was measured with the NRPB radon dosimeter with a CR-39 detector of the Baryotrak type. The detector is 1 cm × 1 cm × 0.1 cm and has a background of 0.5 tracks/mm^2. It has a lower limit of detection value of 44.5 kBqh/m^3 and a minimum measurable radon activity concentration of 20.6 Bq/m^3 for a 90-day exposure. The detector also has a sensitivity between 1.5 and 1.7 (track/cm^2) (Bqd/m^3), depending on the storage duration before measurement. The calibration factor of the detectors is 0.00003346 track/mm^2/(Bqh/m^3). The etching system used has a bulk etch rate of 7 µm/h at 90 °C (Csordás et al., 2021; 2020). The radon track densities on the CR-39 detectors were counted with a high-resolution image scanner and analysis software.

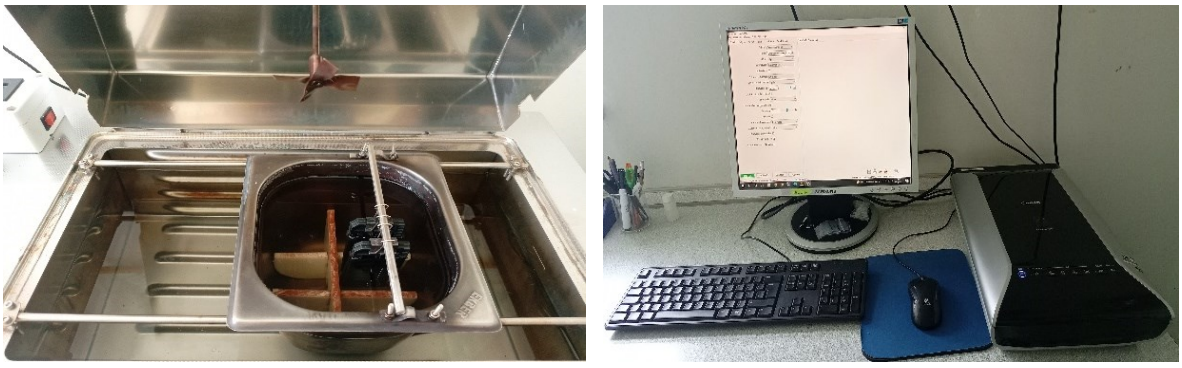

Figure 21. Etching device and high-resolution image scanner for indoor radon (by author).

(ii) Radon exhalation

CR-39 detectors were etched in a Radobath (etching system) with a solution volume of 5 L and dimensions 400 mm × 400 mm × 600 mm. An optical microscope with a 40x magnification objective lens was used to scan (with a RadoMeter) the latent tracks generated on the detectors and tallied in 144 fields. The track density on the track films was used to calculate the radon concentrations (Otoo et al., 2018).

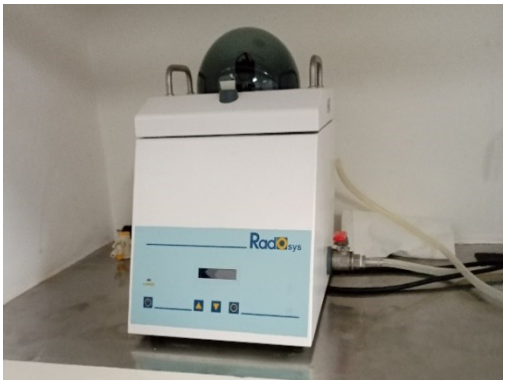


Figure 22. Radobath and Radometer devices for radon exhalation measurements (by author).

3.6 Radionuclide activity concentrations

3.6.1 Ra-226, Ra-228, Th-232, K-40 and Cs-137 in soil and water samples

The activity concentration of radionuclides was evaluated with specific gamma peaks in some cases using the decay products of the parent radionuclide. For Ra-226, using the maximum energies of Bi-214 (609.3 keV), Pb-214 (351.9 keV), Th-232 and Ra-228 from the maximum energies of Tl-208 (583.2 keV and 2614.5 keV) and Ac-228 (911.2 keV), K-40 at 1460.8 keV and Cs-137 at 661.6 keV. The activity concentrations were calculated with the equation:

$$A = \frac{N}{\varepsilon \, x \, P \, x \, m \, x \, t} \tag{4}$$

Where A is the activity concentration in Bq/kg for soil and sediment and in Bq/L for water, N is the net area beneath the related full energy peak, $\mathcal{E}$ is the gamma detection efficiency at energy E, P is the gamma yield in a radionuclide, m is the mass in kg or volume in l of a sample and t is counting time in s.

3.6.2 Indoor radon concentrations

The concentration of indoor radon measured in residences was evaluated by the expression:

$$C_{Rn} = (N_t\text{-}N_b) \times E/(T \times A) \tag{5}$$

Where C_{Rn} is the average indoor radon level in Bq/m^3, N_t is the total number of tracks, N_b is the number of background tracks, E is the calibration factor in Bq/m^{3}h/tracks mm^2, T is the

time of exposure in hours and A is the reading area of the tracks in mm^2 (Adelikhah et al., 2022; 2021).

3.6.4 Radon exhalation

To determine the exhalation rates, the radon concentrations detected in the soil samples were initially calculated by the expression:

$$C_{Rn} = \frac{\varrho}{\varepsilon \, x \, t} \tag{6}$$

Where C_{Rn} is the activity concentration of radon in Bq/m^3, $\boldsymbol{\varrho}$ is the measured track surface density in $track/cm^2$, $\boldsymbol{\varepsilon}$ is the calibration factor of the detector in $track/cm^2d/(Bq/m^3)$, and t is the time of exposure in s.

The radon exhalation rates in terms of mass (E_M) and area or surface (E_A) were determined by the following expressions:

$$E_M = \frac{CV\lambda}{M[(T+1/\lambda(e\text{^}(-\lambda T)-1)]} \tag{7}$$

$$E_A = \frac{CV\lambda}{A[(T+1/\lambda(e\text{^}(-\lambda T)-1)]} \tag{8}$$

Where E_M is the mass radon exhalation rate in mBq/kg/h, E_A is the area radon exhalation rate in $mBq/m^{2/}h$, C is the radon activity at equilibrium in Bq/m^3, V is the volume of the exhalation vessel in m^3, A is the area of the exhalation vessel in m^2, M is the mass of soil sample in kg, T is the time of exposure in hours and $\boldsymbol{\lambda}$ is the decay constant in hours (Saad et al., 2014; Zubair et al., 2012; Gusian et al., 2009; Akuo-ko et al., 2024b).

3.6.3 Po-210 activity concentration

The activity concentration of Po-210 in cigarette samples was calculated with the expression:

$$C_A = \frac{(r_g - r_o).A_T}{(r_{gT} - r_{oT}).m} \tag{9}$$

Where C_A is the activity concentration of Po-210 in cigarette samples in Bq/cig, r_g is the counts per second in the Po-210 range, r_o is the background counts per second in the Po-210 range, r_{gT} is the counts per second in the Po-209 range, r_{oT} is the background counts per

second in the Po-209 range, A_T is the Po-209 activity in the sample in Bq/g and m is the sample mass in kg.

3.7 Determination of radiation dose and radiological hazards

3.7.1 Annual effective dose and other radiological indices due to radionuclides in soil and sediment

(i) Absorbed gamma dose rate (D)

It is the amount of gamma radiation energy released by radionuclides per unit of time and mass of the material exposed. The gamma dose rate at 1 m above the ground, assuming the radionuclides are homogenously distributed in soil or sediment, is evaluated by the equation:

$$D = 0.462A_{Ra} + 0.604A_{Th} + 0.0417A_K + 0.03A_{Cs} \quad (10)$$

Where D is the gamma dose rate in nGy/h, A_{Ra}, A_{Th}, A_K, and A_{Cs} are the activity concentrations of Ra-226, Th-232, K-40, and Cs in Bq/kg, respectively. The world mean absorbed gamma dose rate level is 60.0 nGy/h (UNSCEAR, 2000; Beogo et al., 2022; Atibu et al., 2022).

(ii) Annual effective dose (AED)

It is the effect of gamma radiation emitted by radionuclides on various human body organs. To evaluate the effective dose to the human body, the total hours in a year of 8760, an outdoor occupancy factor of 0.2, and a dose conversion factor of 0.7 Sv/Gy were used for the evaluation in the expression:

$$AED = D\ (Gy/h) \times 8760\ (h/y) \times 0.2 \times 0.7\ (SvGy^{-1}) \quad (11)$$

Where AED is the annual effective dose in mSv/y and D is the gamma dose rate in nGy/h. The world mean annual effective dose is 0.07 mSv/y (UNSCEAR, 2000; Akuo-ko et al., 2023a; Atibu et al., 2022).

(iii) Annual gonadal dose equivalent (AGDE)

The AGDE is the effect of radiation on living cells, which can cause mutation of cells of organisms or death. Radiation can also affect the active bone marrow and bone surface cells. The AGDE was evaluated with the equation:

$$AGDE = 3.09A_{Ra} + 4.18A_{Th} + 0.314A_K \quad (12)$$

Where $AGDE$ is the annual gonadal dose equivalent in μSv/y, A_{Ra}, A_{Th}, and A_K are the activity concentrations of Ra-226, Th-232, and K-40, respectively, in Bq/kg. The world average AGDE value is 300 μSv/y (UNSCEAR, 2000).

(iv) Radium equivalent activity (Ra_{eq})

Since radionuclides are not uniformly distributed, radium equivalent activity assesses the specific activity of materials containing varying levels of radionuclides and characterizes radiation exposure. Radium equivalent activity assumes that 370 Bq/kg of Ra-226, 259 Bq/kg of Th-232, and 4810 Bq/kg of K-40 will produce the same gamma dose rates (Orosun et al., 2019; Akuo-ko et al., 2023a). This is determined by the expression:

$$Ra_{eq} = A_{Ra} + 1.43A_{Th} + 0.077A_K \quad (13)$$

Where Ra_{eq} is the radium equivalent activity in Bq/kg, A_{Ra}, A_{Th}, and A_K represent the activity concentrations of Ra-226, Th-232, and K-40, respectively, in Bq/kg. The maximum allowable Ra_{eq} activity is 370 Bq/kg, corresponding to an effective dose of 1 mSv/y (UNSCEAR, 2000).

(v) Internal and external hazard indices

Radionuclides in sediment and soil generate external gamma radiation, which exposes a population to radiation hazards. For the radiation hazard to be negligible, the internal (H_{in}) and external (H_{ex}) must be less than 1. The internal hazard index (H_{in}) assesses the risk of exposure of the respiratory organs to radon and its daughter isotopes. External hazard index (H_{ex}) equal to 1 translates to the upper limit of radium equivalent dose of 370 Bq/kg, which agrees with the ICRP suggested value of 1 mSv/y (ICRP, 1990; Orosun et al., 2019). The H_{in} and H_{ex} were evaluated using the equations:

$$H_{in} = (A_{Ra}/ 185) + (A_{Th}/ 259) + (A_K/ 4810) \quad (14)$$

$$H_{ex} = (A_{Ra}/ 370) + (A_{Th}/ 259) + (A_K/ 4810) \quad (15)$$

Where A_{Ra}, A_{Th}, and A_K are the activity concentrations of Ra-226, Th-232, and K-40, respectively, in Bq/kg.

3.7.2 Estimation of annual effective dose, ELCR, and LLC due to indoor radon

The annual effective dose due to indoor radon concentrations was evaluated by the expression:

$$E_{Rn} = C_{Rn} \times F_{Rn} \times t \times K_{Rn} \quad (16)$$

Where E_{Rn} is the radon annual effective dose in mSv/y, C_{Rn} is the annual average radon concentration in residences in Bq/m^3, F_{Rn} is the indoor equilibrium factor for radon and its progenies (0.40), t is the number of hours spent indoors per year (7,000 hours), and K_{Rn} is the dose conversion factor in Bqh/m^3 (9 nSv per unit of integrated radon concentrations) (WHO, 2009; UNSCEAR, 2000).

Excess Lifetime Cancer Risk (ELCR), which represents the excess risk of cancer for radon exposure per 100,000 population and the Lung Cancer Cases (LLC) per 1,000,000 population, were estimated by the expression:

$$ELCR = E_{Rn} \times DL \times RF \quad (17)$$

$$LCC = E_{Rn} \times 18 \times 10^{-6} \quad (18)$$

Where $ELCR$ is the excess lifetime cancer risk, LCC is the lung cancer cases, E_{Rn} is the annual effective dose, DL is the mean lifetime duration (70 years), RF is terminal cancer risk (0.055 per Sv), and the lung cancer induction value of 18×10^{-6} /mSv (Akuo-ko et al., 2023b).

3.7.3 Radiation dose due to Po-210

The annual effective dose due to the inhalation of Po-210 in cigarette smoke was determined by:

$$E = F_1 \times F_2 \times K \times G \times C \times t \tag{19}$$

Where E is the annual committed effective of Po-210 in cigarettes in Sv/y, F_1 is the average transfer factor from cigarette to smoke (0.7), F_2 is the inhaled smoke per total smoke ratio (0.5), K is the Po-210 inhalation dose conversion factor (3.3) in μSv/Bq, G is the quantity of cigarettes smoked a day (6 cigarettes), C is the activity concentration of Po-210 in Bq/cig and t is the smoking duration of 365 days (Nketiah-Amponsah et al., 2018; Kovács et al., 2007; UNSCEAR, 2000).

The ELCR per 100,000 people was determined:

$$ELCR = E \times DL \times RF \tag{20}$$

Where E is the annual effective dose Sv/y, DL is the mean life expectancy projected to be 70 years, and RF is the fatal cancer risk factor per Sv, it is stochastically given as 0.055 for the public (Boumala et al., 2019; Stabile et al., 2017; ICRP, 1990).

3.7.4 Annual effective dose due to radionuclides in water

The annual effective dose associated with the ingestion of surface water and groundwater was evaluated by the expression:

$$E_{ing}(w) = I_w \sum_{j=1}^{3} DCF_{ing}(^{226,228}Ra, ^{40}K) A_{sp}(w) \tag{21}$$

Where $E_{ing(W)}$ is the effective dose due to ingestion of water in mSv/y, I_w is the water intake per year (adults: 730 L, children: 350 L, infants: 250 L), DCF is the ingestion dose coefficient in Sv/Bq (Ra-226: 2.3 x 10^{-4} mSv/Bq, Ra-228: 6.9 x 10^{-4} mSv/Bq and K-40: 6.2 x 10^{-6} mSv/Bq), $A_{sp(W)}$ is the activity concentration of radionuclides in water samples in Bq/L (UNSCEAR, 2000).

3.7.5 ELCR due to radionuclides in water, soil, and sediment

The cancer-causing consequences of gamma radiation through ingestion, inhalation, and external exposure to radioactivity are defined by an estimation of the probability of cancer occurring during a specific lifetime (Beogo et al., 2022; Atibu et al., 2022). The assessment of ELCR determines this likelihood in a human population, and it is calculated by the expression:

$$ELCR = AED \times DL \times RF \quad (22)$$

Where *AED* is the annual effective dose in mSv/y, *DL* is the average period of life of 70 years, and *RF* is the risk factor (i.e., fatal cancer risk) in per Sv. The ICRP 60 recommends an RF value of 0.055 for members of the public when dealing with stochastic impacts. The world recommended value for ELCR is 0.00029 (UNSCEAR, 2000; ICRP, 1990).

3.8 Statistical analysis of data

The statistical analysis of the data obtained was mainly performed with IBM SPSS Statistics version 26 and Microsoft Excel. Tests for normal distribution of data were done using log-normal distribution, Kolmogorov-Smirnov, and Shapiro-Wilk tests. The mean, median, standard deviation, geometric mean, and geometric standard deviation were evaluated from the obtained data. Regression analysis, Pearson correlation, principal component analysis, and cluster analysis were also performed to understand the relationship between radionuclides and radiological parameters.

3.9 Spatial distributions

Interpolation maps were created to visualize the appropriate spatial distribution of a variable at its position. The maps were created with ArcGIS software version 10.4.1. To clearly understand the distribution pattern of radionuclides in an area. Different interpolation techniques were employed to develop the maps. These included the Inverse Distance Weighting (IDW), Ordinary Kriging (OK), and Empirical Bayesian Kriging (EBK).

CHAPTER FOUR

RESULTS AND DISCUSSION

4.1 Introduction

This chapter presents data from measuring radioactivity concentrations in the investigated environmental media. The data were analyzed, interpreted, and compared with world reference levels. Radiological hazards due to radioactivity levels were determined, and the impact on the human population was examined. Relationships between radionuclide concentrations and radiological hazards were evaluated to understand the strength of the relationship between the variables in an environment.

4.2 Radioactivity in sediment along the coastline of Ghana

4.2.1 Radionuclide activity concentrations in sediment

Table 2 presents Ra-226, Th-232, K-40, and Cs-137 radioactivity concentrations in sediment along Ghana's coast.

Table 2. Mean activity concentration of radionuclides in Bq/kg in sediment along the shores of Ghana.

Locations	Ra-226	Th-232	K-40	Cs-137
1. Axim	18 ± 5	12 ± 2	285 ± 77	1.6 ± 0.5
2. Dixcove	17 ± 4	12 ± 1	282 ± 75	109.8 ± 0.3
3. Takoradi	23 ± 5	9 ± 1	322 ± 74	1.7 ± 0.7
4. Sekondi	30 ± 6	12 ± 1	1270 ± 69	2.3 ± 0.3
5. Komenda	48 ± 6	10 ± 1	337 ± 73	2.3 ± 0.7
6. Cape Coast	38 ± 5	17 ± 1	253 ± 74	3.6 ± 0.4
7. Anomabo	75 ± 6	25 ± 1	380 ± 73	4.2 ± 0.5
8. Saltpond	22 ± 6	13 ± 1	378 ± 73	1.2 ± 0.6
9. Winneba	35 ± 6	13 ± 1	277 ± 75	3.0 ± 0.7
10. Bortianor	130 ± 5	59 ± 1	307 ± 74	2.6 ± 0.2
11. Labadi	27 ± 6	15 ± 1	546 ± 72	2.2 ± 0.6
12. Tema	66 ± 5	34 ± 1	211 ± 75	2.2 ± 0.5

13. Ada Foah	23 ± 7	9 ± 1	313 ± 75	2.8 ± 0.7
14. Keta	133 ± 7	76 ± 1	355 ± 73	2.8 ± 0.5
15. Half Assin	22 ± 6	25 ± 2	428 ± 77	2.3 ± 0.5
16. Jomoro	31 ± 7	27 ± 2	298 ± 77	2.4 ± 0.6
17. Cape 3 Points	16 ± 4	13 ± 1	564 ± 76	7.5 ± 0.6
18. Prampram	47 ± 6	31 ± 2	357 ± 76	3.9 ± 0.5
19. Aflao	15 ± 4	9 ± 2	304 ± 76	1.8 ± 0.6
Study mean	**43 ± 6**	**22 ± 1**	**393 ± 74**	**8.4 ± 0.5**
World mean*	**35**	**30**	**400**	**18.2**
Geometric mean	34	18	358	3.1
Median	30	13	322	2.4
Minimum	15	9	211	1.2
Maximum	133	76	1270	109.8
Standard deviation	35	18	230	24.6
Skewness	2	2	3	4.3
Kurtosis	3	4	13	18.9

*World mean average values by UNSCEAR, 2000.

From Table 2, activity concentrations of Ra-226 ranged from 15 ± 4 to 133 ± 7 Bq/kg, 9 ± 1 to 76 ± 1 Bq/kg for Th-232, 211 ± 75 to 1270 ± 69 Bq/kg for K-40 and 1.2 ± 0.6 to 109.8 ± 0.3 Bq/kg for Cs-137. The average activity concentrations were 43 ± 6 Bq/kg, 22 ± 1 Bq/kg, 393 ± 74 Bq/kg, and 8.4 ± 0.5 Bq/kg for Ra-226, Th-232, K-40, and Cs-137, respectively. The determined geometric means were less than the arithmetic means of the measured radionuclides except for Ra-226. The Ra-226 concentrations in the sediment samples exceeded all Th-232 concentrations measured at the different coastal locations. Ra-226 activity concentrations for Cape Coast, Tema, Komenda, Anomabo, Keta, Bortianor, and Prampram were notably higher than the world mean of 35 Bq/kg, whereas Th-232 mean concentrations were below the world mean of 30 Bq/kg except for Bortianor, Tema, Prampram, and Keta (UNSCEAR, 2000). In the case of K-40, Sekondi, Cape 3 Points, Half Assin, and Labadi recorded activity levels above the world mean of 400 Bq/kg. Beach sediments are mineral deposits from the weathering and erosion of igneous and metamorphic rocks. Such rocks are enriched with uranium and thorium, hence primary sources of Ra-226

and Th-232 in sediment. Also, the decay of uranium and thorium in oceans contaminates sediment with Ra-226 and Th-232, which are then deposited at the shores by tides and wave actions (Nyarko et al., 2011). High K-40 in soils and sediments is attributed to potassium in fertilizers applied to crop plantations, which leach into soils and sediments, raising the K-40 activity concentrations (Huang et al., 2015).

The anthropogenic radionuclide Cs-137 recorded the highest activity concentration of 109.8 ± 0.3 Bq/kg at Dixcove. This affected the overall mean of Cs-137 for the study to be 8.4 ± 0.5 Bq/kg, though it was below the world mean of 18.2 Bq/kg (UNSCEAR, 2008). If the Cs-137 concentration for Dixcove is considered an outlier, then the mean value for the entire coastline would have been 2.7 ± 0.5 Bq/kg. The activity levels of Cs-137 in the environment are mainly due to nuclear power plant accidents, bombs, and nuclear weapon tests (Shahrokhi et al., 2021; Nyarko et al., 2011; Dizman et al., 2019). The Chernobyl and Fukushima accidents released huge quantities of Cs-137, 85 PBq, and 12 PBq, respectively, into the global atmosphere. This led to a significant fraction of the released radionuclide being deposited into oceans and sediments (Kubo et al., 2018; Zhao et al., 2018). Nuclear bomb tests also released large amounts of Cs-137 into the stratosphere and later fell to the Earth's surface mainly by rainfall (FAO/IAEA, 2017; Zhao et al., 2018). Research shows that Cs-137 has a high retention ability on the surface of soils and sediments because of the existence of clay minerals and organic matter in the soils and sediments. The retention property of Cs-137 causes the radionuclide to be trapped in sediments, restricting its movement (Yasumiishi et al., 2017; Nguyen et al., 2020; Yamada et al., 2015). Again, fine-grain particles of sediment increase Cs-137 concentrations with decreasing particle sizes (Kubo et al., 2018; Mouri et al., 2014; Kitamura et al., 2014).

4.2.2 Normality of radionuclides distribution

The skewness and kurtosis values were used to test the normality of the data. The skewness and kurtosis coefficients in Table 2 indicated an asymmetric distribution of the determined radionuclides. The absence of a normal distribution can be attributed to the different sources and types of rocks and sediment found at the various sampling locations and the mineral complexity in the sediment samples (Shahrokhi et al., 2021; Nyarko et al., 2011). However, the Kolmogorov-Smirnov normality test showed that Ra-226 and Th-232 had a normal distribution, having *p*-values of 0.06 and 0.05, respectively, while K-40 and Cs-137 did not

show normal distributions (p-values < 0.05). The radionuclide data were normalized for a lognormal distribution. The lognormal distribution of the radionuclide concentration of Ra-226, Th-232, K-40, and Cs-137 is presented in Figure 23.

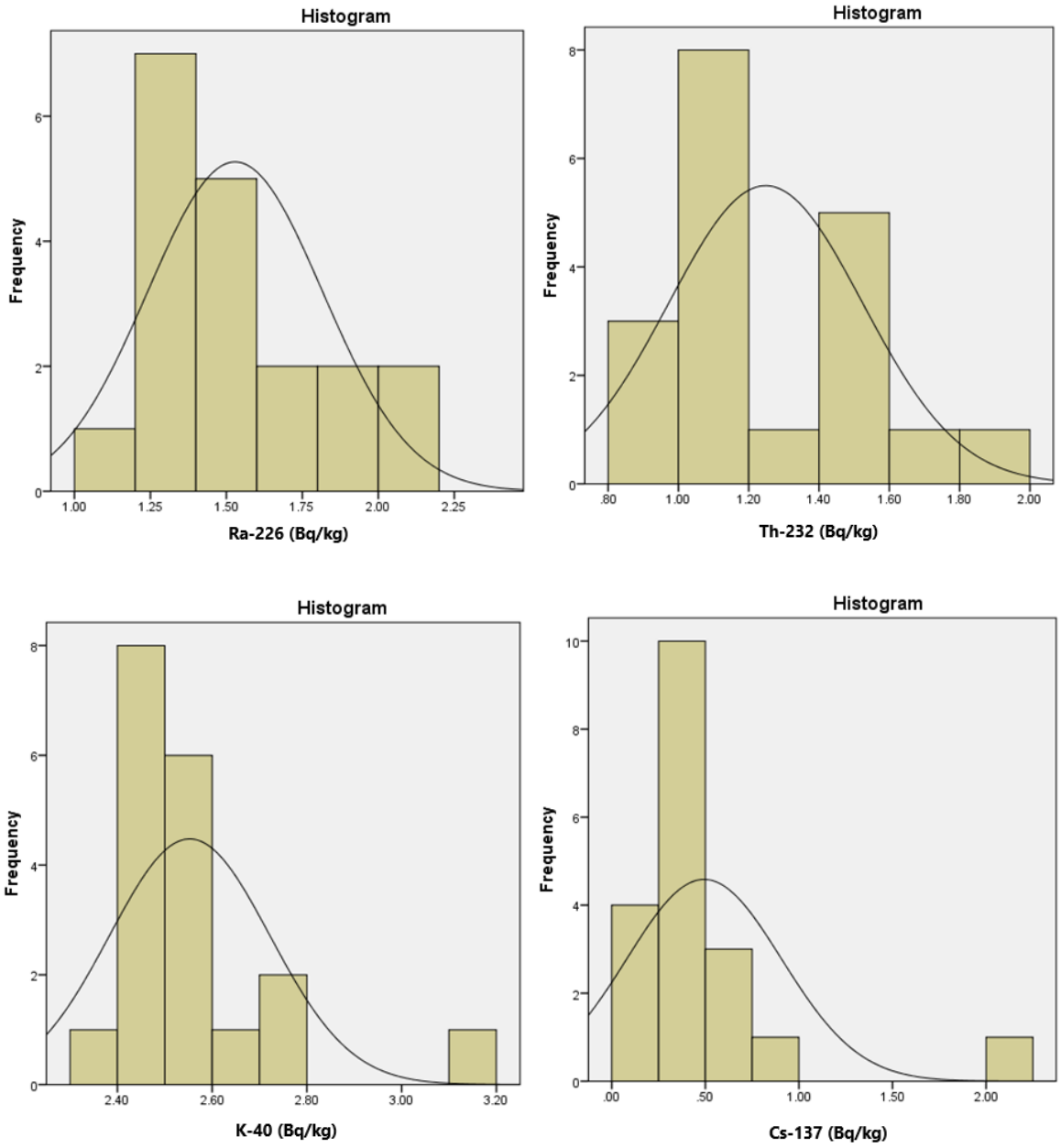

Figure 23. Lognormal distribution of Ra-226, Th-232, K-40 and Cs-137 (by author).

4.2.3 Radiological risk assessment

The radiological effects of gamma radiations from sediments are presented in Table 3.

Table 3. Radiological risk indices evaluated in sediment samples.

Locations	Ra_{eq} (Bq/kg)	H_{ex}	H_{in}	I_γ	D (nGy/h)	AED (µSv/y)	AGDE (µSv/y)
1. Axim	57.1	0.2	0.2	0.2	27.7	34.0	195.2
2. Dixcove	54.7	0.1	0.2	0.2	29.8	36.6	187.7
3. Takoradi	59.7	0.2	0.2	0.2	29.3	35.9	207.0
4. Sekondi	145.3	0.4	0.5	0.6	74.5	91.4	542.7
5. Komenda	88.3	0.2	0.4	0.3	42.5	52.2	296.1
6. Cape Coast	81.1	0.2	0.3	0.3	38.5	47.2	265.8
7. Anomabo	140.4	0.4	0.6	0.5	66.3	81.3	456.7
8. Saltpond	69.2	0.2	0.2	0.3	33.8	41.5	239.5
9. Winneba	74.6	0.2	0.3	0.3	35.8	43.8	248.6
10. Bortianor	238.2	0.6	1.0	0.8	109.6	134.5	745.1
11. Labadi	89.6	0.2	0.3	0.3	44.2	54.2	315.0
12. Tema	129.8	0.4	0.5	0.5	60.0	73.6	409.1
13. Ada Foah	59.8	0.2	0.2	0.2	29.3	35.9	206.5
14. Keta	268.9	0.7	1.1	0.9	123.5	151.5	839.9
15. Half Assin	90.7	0.2	0.3	0.3	43.6	53.4	306.6
16. Jomoro	93.1	0.3	0.3	0.3	43.8	53.8	303.9
17. Cape 3 Points	78.1	0.2	0.3	0.3	39.2	48.1	281.1
18. Prampram	118.6	0.3	0.4	0.4	55.9	68.5	386.2
19. Aflao	52.0	0.1	0.2	0.2	25.6	31.4	181.6
Study average	**104.7**	**0.3**	**0.4**	**0.4**	**50.1**	**61.5**	**348.1**
World average	**370**[a]	**≤1**[a]	**≤1**[b]	**≤1**[b]	**60**[a]	**70**[a]	**300**[b]

a= UNSCEAR, 2008; b= UNSCEAR, 2000

The Ra_{eq} values were from 52.0- 268.9 Bq/kg, less than the world average of 370 Bq/kg. Since coastal dwellers use sediment as building materials, the Ra_{eq} is recommended not to exceed 370 Bq/kg to reduce the effect of radon and its progenies (Amekuzie et al., 2011; UNSCEAR,2000; Otoo et al., 2021;2018). H_{ex} and H_{in} indices assess the hazard of radiation to the respiratory organs, specifically the lungs. The mean H_{ex} and H_{in} estimated in the

sediment samples were less than unity (0.4). This demonstrates the suitability of sediment for building construction purposes, and less radiation dose is conveyed to occupants of such houses (UNSCEAR, 2000). The gamma index (I_γ) assesses the collective radiation effect of natural radionuclides. In this study, the I_γ values observed between 0.2 and 0.9, with an average of 0.4, were less than the world average of 1. Hence, there is a minimal collective effect from the radionuclides (Botwe et al., 2017). The gamma dose rate (D) ranged from 25.6 to 123.5 nGy/h. Though the mean D value of 50.1 nGy/h was below the world mean value of 60.0 nGy/h, the high values recorded at Keta, Bortianor, Sekondi, and Anomabo indicate a radiation hazard associated with the use of such sediments. The high D values result from high Ra-226 levels measured in the sediments of those coastal areas. The AED to the population corresponding to the natural and anthropogenic radioactivity in the sediments ranged between 31.4 μSv/y and 151.5 μSv/y. The average AED (61.5 μSv/y) was less than the reference level of 70 μSv/y (UNSCEAR, 2008). Apart from locations with high AED, Ghanaian beaches can be considered safe, having normal background radiation, making the induced radiation to the public low. The AGDE, which assesses the effect of radiation on living cells (UNSCEAR, 2008), was estimated to vary between 181.6 μSv/y and 839.9 μSv/y with a mean of 348.1 μSv/y. Coastal locations with AGDE values higher than the reference mean of 300 μSv/y indicate that their sediment can induce radiation dose rates that pose a health risk to humans.

4.2.4 Statistical analysis of data

(i) Pearson correlation

Pearson correlation estimates the degree of relationship and strength of association among variables, particularly between radionuclide distribution and radiological factors. The results of the Pearson correlation analysis, as presented in Table 4, showed a good correlation coefficient of $R^2 = 0.92$ between Ra-226 and Th-232, signifying a strong relationship between the radionuclides and their progenies, whose decay occurs together in nature (Shahrokhi et al., 2021; Sureshghandhi et al., 2014).

Table 4. Pearson correlation analysis between radionuclides and radiological hazards.

Parameters	Ra	Th	K	Cs	Ra_{eq}	H_{ex}	H_{in}	I_{γ}	D	AED	AGDE
Ra	1										
Th	0.92	1									
K	-0.14	-0.15	1								
Cs	-0.18	-0.14	-0.11	1							
Ra_{eq}	0.94	0.92	0.15	-0.20	1						
H_{ex}	0.94	0.92	0.15	-0.20	1	1					
H_{in}	0.98	0.94	0.04	-0.19	0.99	0.99	1				
I_{γ}	0.92	0.91	0.23	-0.20	0.99	0.99	0.98	1			
D	0.93	0.91	0.20	-0.18	0.99	0.99	0.98	0.99	1		
AED	0.93	0.91	0.20	-0.18	0.99	0.99	0.98	0.99	1	1	
AGDE	0.91	0.89	0.25	-0.21	0.99	0.99	0.98	0.99	0.99	0.99	1

Again, strong associations were observed between the radiological parameters (Ra_{eq}, H_{ex}, H_{in}, I_{γ}, D, AED, and AGDE) and Ra-226 and Th-232 since the determination of the parameters is based on the radionuclides. Thus, the radionuclides significantly contributed to the radiological hazards estimated in the sediment samples. Conversely, negative correlations were observed between K-40, Ra-226, and Th-232 due to their different decay series. K-40 had low correlation coefficient values with the radiological parameter, and Cs-137 negatively correlated with them. Therefore, Ra-226 and Th-232 present gamma radiation hazards in the coastline sediments, while K-40 had a minimal contribution to the radiological risks associated with such sediments. Cs-137 did not influence the radiological parameters evaluated in the coastline sediments.

(ii) Cluster analysis

The cluster analysis graphically described the level of relationship between variables. The cluster analysis used the single linkage method with the correlation coefficient distance between variables. The single linkage method assumes that the likeness of 2 clusters is the likeness of their most members. The cluster analysis results in Figure 24 show the

categorization of the variables into 3 distinct clusters. Cluster 1 presented the correlation distance of similarity between the radiological parameters Ra_{eq}, H_{ex}, H_{in}, D, I_{γ}, AED, AGDE, and Ra-226 and Th-232. These variables are combined at a lower rescaled distance because they are quite similar, as their estimation mainly depends on the activity concentrations of Ra-226 and Th-232. Thus, the radionuclides are in one cluster with the radiological parameters because they largely influenced them. Between the two radionuclides, Ra-226 had a greater influence on the radiological parameters than Th-232 because it recorded higher activity concentrations in all the samples. Hence, Ra-226 contributed more radiation dose than Th-232. Cluster 2 is composed of K-40, while the last cluster represents Cs-137. K-40 and Cs-137 are in different clusters owing to their different decay series and sources. The rescaled distances of K-40 and Cs-137 show that K-40 slightly influenced the radiological parameters compared to Cs-137, which had no influence. The outcome of the cluster analysis is comparable to the Pearson correlation analysis.

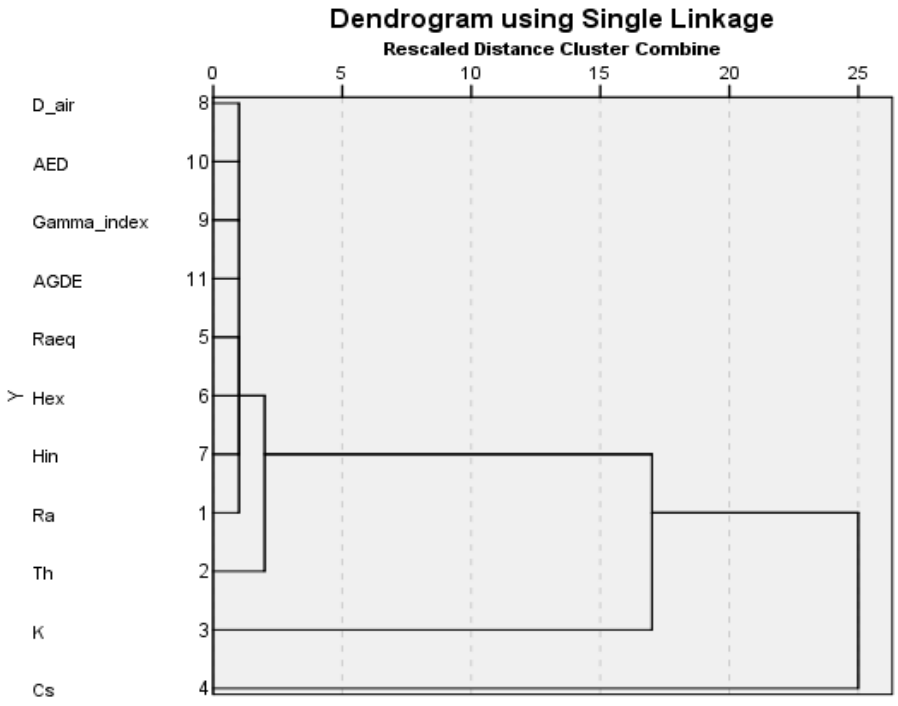

Figure 24. Dendrogram of the cluster analysis between radionuclides and radiological factors (by author).

(iii) Principal Component Analysis (PCA)

PCA describes patterns in variables and presents the data in a way that emphasizes similarities and differences. The PCA was performed using the Kaiser normalization method with varimax rotation, as shown in Figure 25. The criterion used for the analysis was eigenvalues greater than 1. A correlation matrix was generated, and eigenvalues and eigenvectors were determined, suggesting the significant factors and the explained variance as presented in Table 5. The outcome of the PCA revealed that two factors had eigenvalues greater than 1, and they explained 90.63% of the overall variance. Component 1, with a variance of 79.88%, loaded heavily on Ra-226, Th-232, and the radiological parameters. This explains that Ra-226 and Th-232 are the main sources of radioactivity and the radionuclides contributing to the radiation dose evaluated in the sediment samples. Component 2, with a variance of 10.75%, loaded heavily on K-40 and less on the radiological parameters. This is because the contribution of K-40 to radiation dose is minimal, though it is from a natural origin and present in high concentrations in the sediment samples. Cs-137 had almost no radiological effect on humans since its contribution to the estimated parameters was very low. Again, Figure 25 showed that Ra-226, Th-232, and the radiological parameters are grouped because they are positively correlated, while Cs-137, which is negatively correlated, is positioned at the opposite side of the origin with less impact on the varimax rotation. K-40 is positively correlated with clustered variables. However, its influence is minimal.

Table 5. Varimax of rotated component matrix

Variables	**Component**	
	1	**2**
^{226}Ra	0.982	--
^{232}Th	0.964	--
^{40}K	--	0.971
^{137}Cs	-0.167	-0.346
Ra_{eq}	0.978	0.204
H_{ex}	0.978	0.205
H_{in}	0.993	--
D_air	0.965	0.252
I_index	0.960	0.274
AED	0.965	0.252
AGDE	0.952	0.299
Variance explained (%)	**79.88**	**10.75**

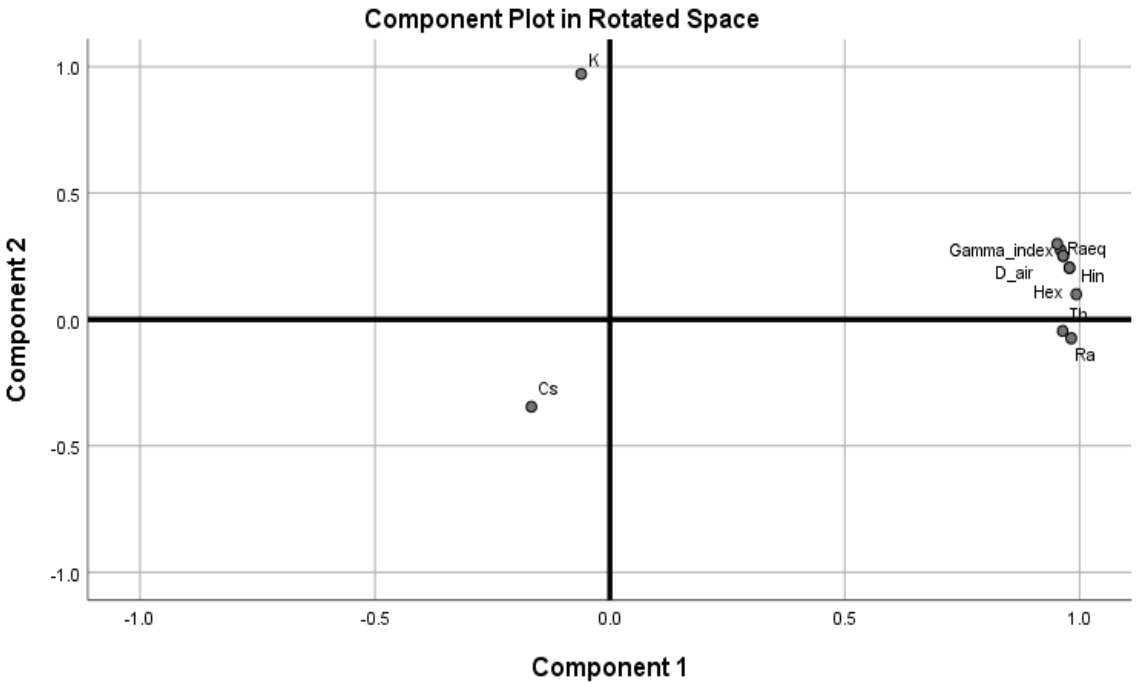

Figure 25. The rotated factor loadings of the measured radionuclides and radiological hazards (by author).

4.2.5 Spatial distribution of radionuclides

The Ordinary Kriging (OK) technique was applied for the spatial distribution. It generates visually interpolated maps identifying trends from unequally spaced data (Kucukomeroglu et al., 2016). The spatial distribution maps created with the OK method enabled the pictorial view of the radionuclides and radiological hazard distribution along the shores of Ghana. The interpolation was done with 2.5 km from the beach to the sea and 2.5 km inland to determine the distribution of radionuclides from the sea and the impact on sediment by dust and particles from natural phenomena (Kucukomeroglu et al., 2016).

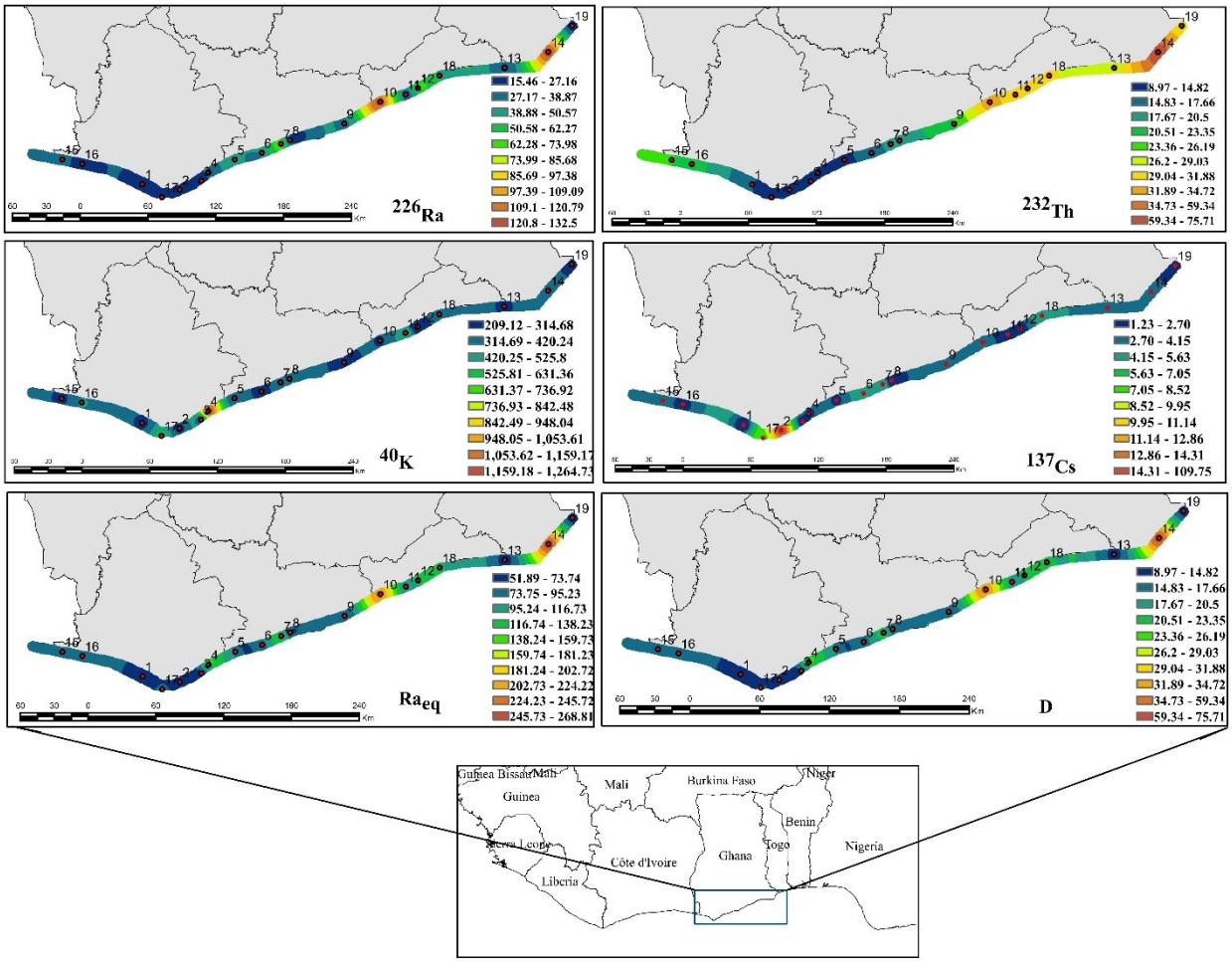

Figure 26. The distribution of Ra-226, Th-232, K-40, Cs-137, Ra_{eq} and D along the coastline of Ghana (by author).

From Figure 26, it was observed that radionuclide concentrations varied between locations. This explains that radioactivity concentrations depend on the geological properties of rocks, soils, and sediments along Ghana's coast, which differ according to the area. The distribution map helped realize a high radionuclide concentration with Ra-226 and Th-232 activity at the eastern and central parts of the Ghanaian coast. In contrast, the western part has low activity concentrations, showing their level of abundance in the geographical areas. However, K-40 and Cs-137 displayed an uneven distribution along the coastline. The distribution of Ra_{eq} and D were comparable to that of Ra-226 and Th-232.

4.2.6 Further investigation of Cs-137 concentration at Dixcove

The transport of Cs-137 from anthropogenic sources through the ocean could pollute sediments along coastal regions, including Dixcove. Earlier investigations along the coast of Dixcove indicated Cs-137 activity concentration to be 109.8 Bq/kg. This raised concerns about the possible radiological hazards and the need for further investigations, as this will provide valuable insights into the factors influencing Cs-137 distribution in the coastal area. The investigation was conducted in three coastline zones, i.e., on-shore, near-shore, and off-shore. The approach was used to understand the influence of hydrodynamic and geochemical processes on radionuclide distribution. Therefore, the activity concentration of Cs-137 was measured in sediment samples collected from the three coastline zones, and the results are presented in Table 6.

Table 6. Activity concentrations of Cs-137 (in Bq/kg) distribution at the Dixcove shore.

	Off-shore	**Near-shore**	**On-shore (coastline)**
Minimum (Bq/kg)	0.3 ± 0.1	0.2 ± 0.1	0.5 ± 0.1
Maximum (Bq/kg)	0.6 ± 0.1	0.9 ± 0.1	1.3 ± 0.2
Average (Bq/kg)	0.4 ± 0.1	0.2 ± 0.1	0.8 ± 0.1

The near-shore recorded the lowest concentration of 0.2 Bq/kg while the highest concentration of 1.3 Bq/kg was recorded at the off-shore. The variability of Cs-137 activity concentration in sediment samples could be influenced by the chemical and physical characteristics, mineralogy, and surface areas of sediment particles. Cs-137 is known to firmly adhere to fine particles, including clay minerals, and thus high Cs-137 radioactivity is sometimes observed in such sediments. It also concentrates less on sandy sediments compared to muddy sediments (Łokas et al., 2017; Jagercikova et al., 2015; Takata et al., 2017; Tabaris et al., 2012; Thorton et al., 2013; Bakar et al., 2017).

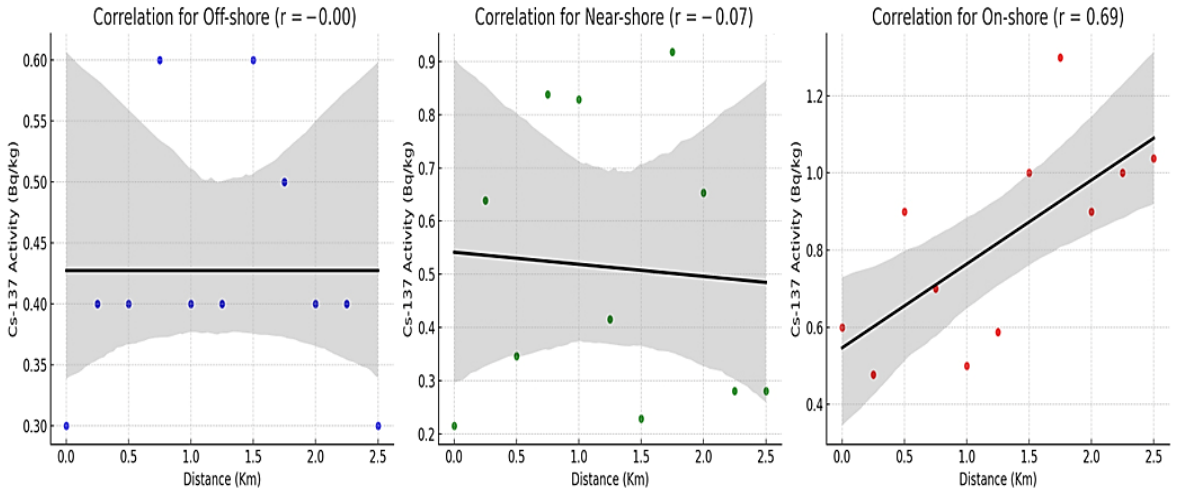

Figure 27. Correlation analysis between distance and Cs-137 activity along each shore (by author).

Cs-137 activity concentrations were measured at every 250 m along the entire coastal area at distances of on-shore, near-shore, and off-shore. In Figure 27, the spatial distribution of Cs-137 was observed to have variations across the coastline. The activity concentrations of Cs-137 in offshore areas were relatively low (~0.3 to 0.6 Bq/kg) with slight variation. The activity concentrations were more variable at the on-shore and near-shore areas, ranging between 0.2 and 1.3 Bq/kg. The variability could be attributed to factors such as sediment composition, tidal and oceanic currents, and anthropogenic disturbances like fishing, sand winning, and tourism, which could contribute to localized fluctuations in Cs-137 accumulation (Akuo-ko et al., 2025).

The radionuclide was almost uniformly dispersed in the off-shore area, showing a relatively narrow range of concentrations between 0.4 and 0.5 Bq/kg as presented in Figure 28. The on-shore or coastline and near-shore showed wider variations in concentration. The short-distance fluctuations in Cs-137 concentration, particularly for the near-shore, indicate that Cs-137 deposition is influenced by anthropogenic and natural processes rather than being uniformly distributed.

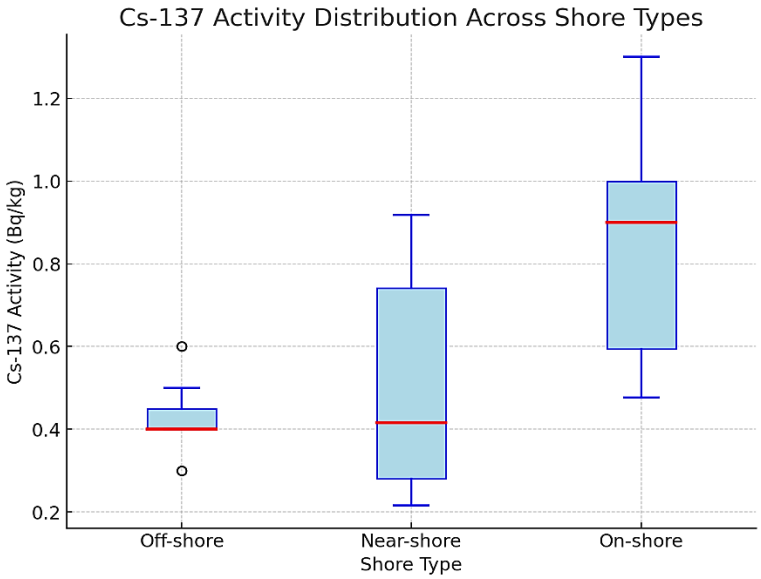

Figure 28. Relationship between distance and Cs-137 distribution in off-shore, near-shore, and on-shore areas (by author).

From the Cs-137 data, it was resolved that the high Cs-137 concentration (109.8 Bq/kg) measured during the initial investigation at Dixcove could be attributed to possible human error during sampling or calculation, or technical problems such as usage of contaminated sample holder, detector calibration problems, sediment characteristics, and measurement methods. Also, issues such as poor calibration for background noise or background subtraction approach, detector efficiency calibration, and minor errors in quantity evaluation could have significantly affected the estimation of the activity concentrations (Akuo-ko et al., 2025). However, the continuous change of Cs-137 levels in sediment is anticipated since the marine environment is the most dynamic aspect of the ecosystem. (Al-Mur & Gad, 2022). Therefore, the differences in Cs-137 activity concentration observed at Dixcove could be attributed to the abovementioned reasons.

4.3 Indoor radon levels in the Greater Accra region

4.3.1 Frequency distribution and normality of data

Indoor radon concentrations were measured in 95 residences in the Greater Accra region for a 90-day exposure period using the SSTND method. The frequency distribution of the measured indoor concentrations is presented in Figure 29.

The indoor radon levels determined for the individual residences ranged from 36.1 ± 2.7 to 92.0 ± 5.2 Bq/m^3. The measured indoor radon concentrations were less than 100 Bq/m^3. The average indoor radon concentration for the study area was 50.8 ± 3.4 Bq/m^3. The geometric mean and the geometric standard deviation values of the radon concentrations were estimated to be 50.0 Bq/m^3 and 1.2, respectively. The ages of the homes surveyed were recorded in the study. The ages varied from 1 to 100 years, with the mean age estimated at 19.1 years.

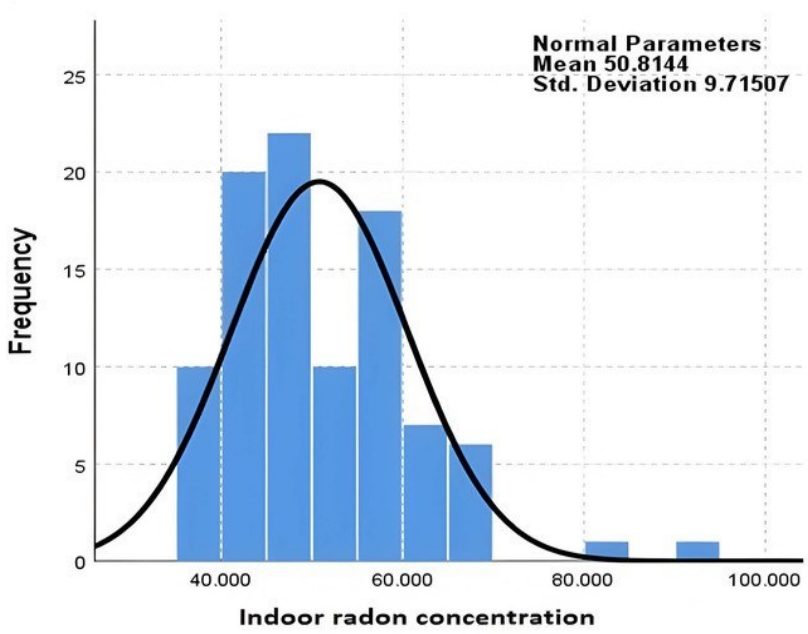

Figure 29. Frequency distribution of the indoor radon levels in Bq/m^3 for residences (by author).

The normality of the indoor radon data was tested with cumulative frequency distribution, normalizing Q-Q plots, and the Kolmogorov-Smirnov normality test. Figure 30 shows the indoor radon concentrations' normal distribution and Q-Q plot. Figure 31 also shows the normal distribution and Q-Q plot of the age of residences surveyed.

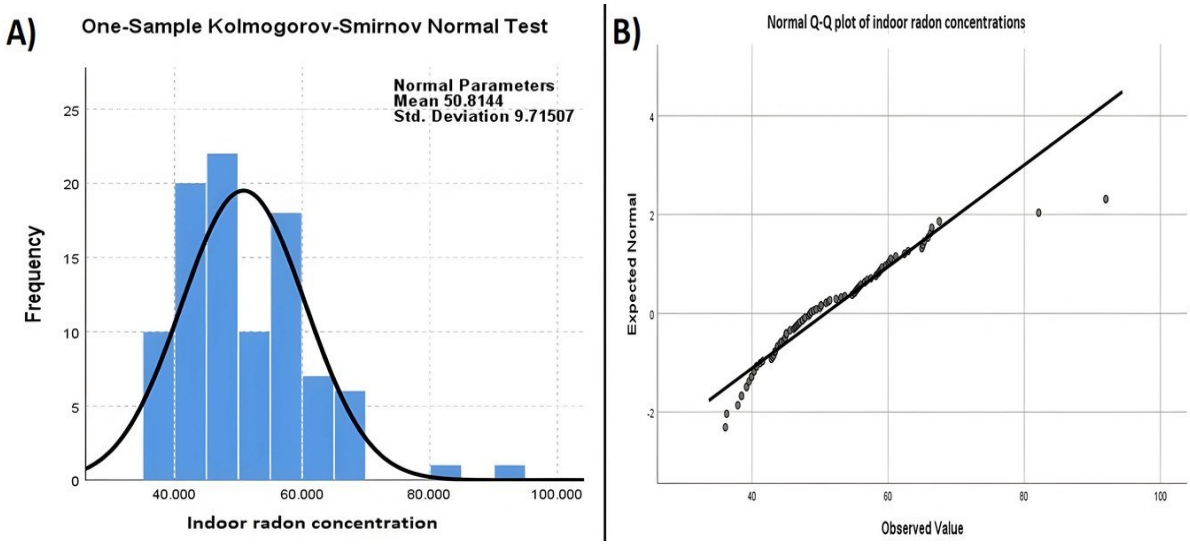

Figure 30. Normal distribution of indoor radon levels (A) and (B) normalizing Q-Q plot of indoor radon levels in Bq/m^3 (by author).

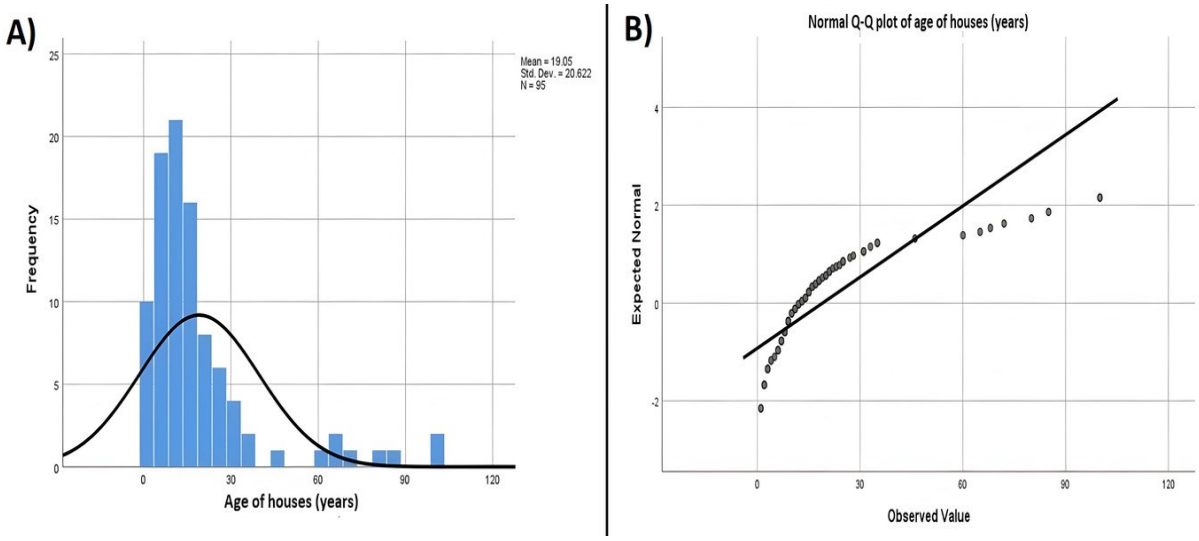

Figure 31. Normal distribution of the age of residences (A) and (B) normalizing Q-Q plot of the age of residences in years (by author).

Figures 30 and 31 indicate that the data are not normally distributed, especially as analyzed from the Q-Q plots. The Kolmogorov-Smirnov normality test also showed that the radon concentrations and the age of residences were not normally distributed. Their *p*- values were

below 0.05. The data's lack of a normal distribution could be attributed to the soil compositions, different types of building materials, and ventilation in the residences.

The radon data and age of residence were then normalized using a lognormal distribution. The evaluated geometric mean of indoor radon (50.0 Bq/m^3) and age of residences (12.4 y) were almost the same as their median values (48.5 Bq/m^3, 12.0 y), suggesting the need for a lognormal distribution. The lognormal distribution of radon and age data is presented in Figures 32 and 33. The log-transformed data were tested for normality with the Kolmogorov-Smirnov test. They proved to be normally transformed with *p*- values of 0.2 and 0.1 for the radon levels and age of residences, respectively.

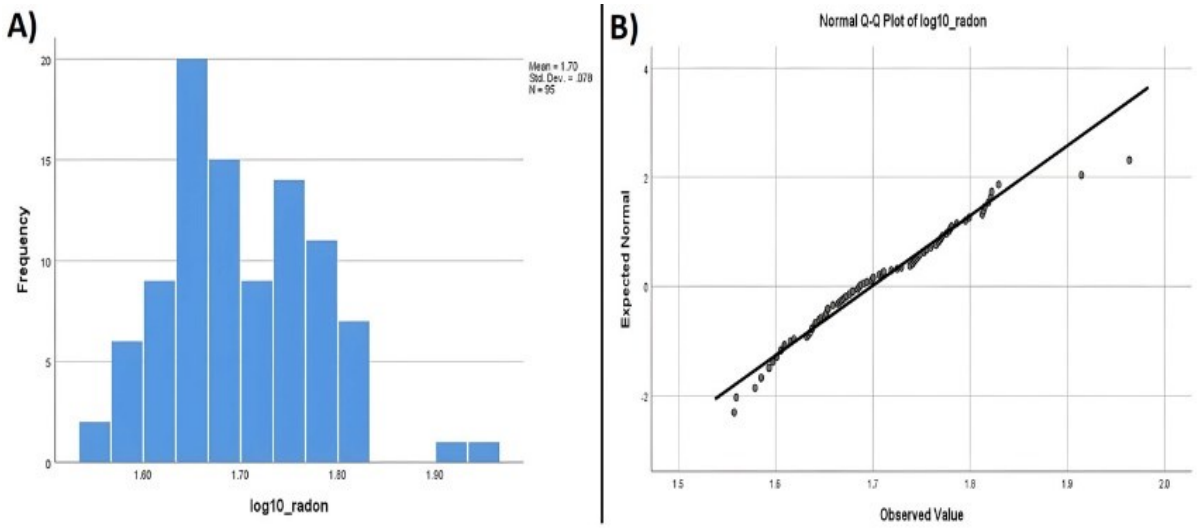

Figure 32. Lognormal distribution of indoor radon levels (A) and (B) Q-Q plot of lognormal indoor radon levels in Bq/m^3 (by author).

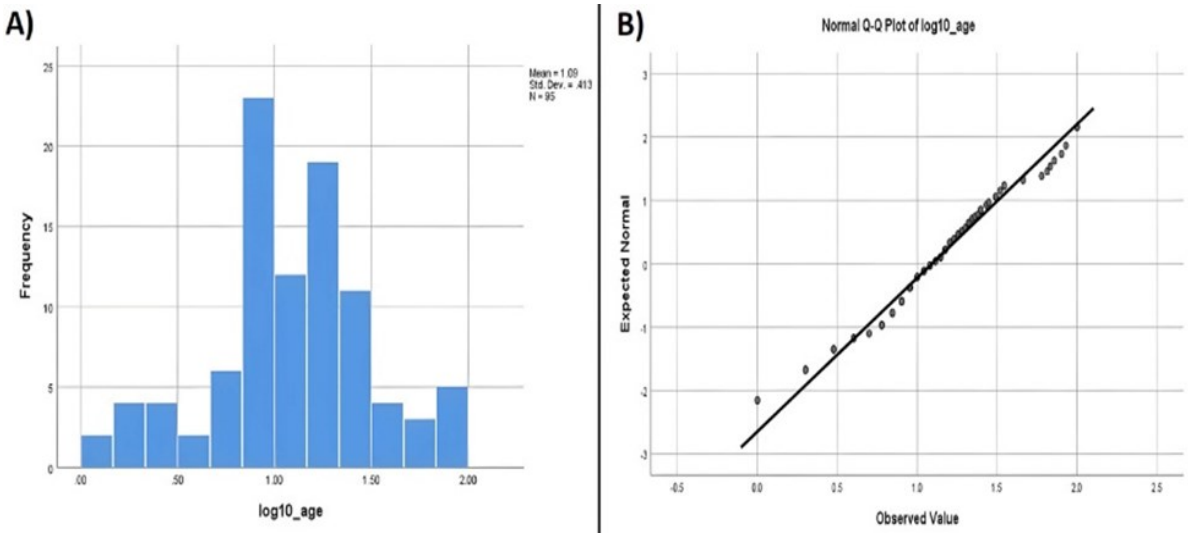

Figure 33. Lognormal distribution of age of residences (A) and (B) Q-Q plot of lognormal of age of residences in years (by author).

4.3.2 Indoor radon concentrations

(i) Comparison of data to international guideline levels

All the indoor radon concentrations measured in the study were below 100 Bq/m^3. The concentrations did not exceed the recommended level of 100 Bq/m^3 suggested by the World Health Organization (WHO) and 300 Bq/m^3 given by the International Commission on Radiological Protection (ICRP) (WHO, 2009; ICRP, 2010). The mean indoor radon concentration determined for this study, 50.8 ± 3.4 Bq/m^3, was above the worldwide indoor radon mean of 39 Bq/m^3 proposed by UNSCEAR. This signifies that the population of the study area is susceptible to internal exposure to indoor radon and its related health risks (UNSCEAR, 2014). The global geometric mean (GM) and geometric standard deviation (GSD) specified by UNSCEAR were compared to those obtained in this survey. The GM for this study was 13 Bq/m^3 more than the world value of 37 Bq/m^3, while the GSD (1.2) was less than the world value of 2.2 (UNSCEAR, 2000). The primary sources of radon in residences in this study were from soil geology and composition, the different types of materials used in building construction, air ventilation within residences, the lifestyle of occupants, and soil gas infiltration (Adelikhah et al., 2021; Otoo et al., 2018; Imani et al., 2021).

(ii) Indoor radon concentration and age of residences

The age of dwellings was also considered a factor in evaluating indoor radon exposure. Some old residences were identified to have high indoor radon levels, particularly in densely inhabited areas. For example, a 25-year-old house recorded a radon level of 82.1 ± 2.5 Bq/m^3. Such a concentration can be due to the cracks observed in the building walls and floors, aiding the infiltration of radon gas from the soil into the house. Again, some young residences also recorded high radon concentrations as seen in the case of a 9-year-old residence with the highest indoor radon level of 92.0 ± 5.2 Bq/m^3 and a 1-year-old house with a 55.1 ± 5.1 Bq/m^3 concentration. Such could be due to the geology of the area. Very old houses of 100 years recorded average concentrations of 44.8 ± 4.5 Bq/m^3 and 56.0 ± 4.0 Bq/m^3. These observations mean that there was no relationship between the indoor radon levels and the age of the surveyed residences.

(iii) The influence of geology on indoor radon concentration

The geology of an area influences the concentration of indoor radon. Previous studies have shown that the geology of the study area is composed of quartzite, granite, and gneiss rocks, which are primarily used for building construction in the region. These studies have shown a relationship between the radioactivity levels of the rocks and radon concentrations (Otoo et al., 2018; Csordás et al., 2014). The findings showed that the radioactivity of rocks and soils depended on the area's geology. High radioactivity levels of U-238 were determined in rocks and soils from places like Shai Hills, Weija, Dodowa, and James Town, especially in igneous and granite rocks (Yeboah et al., 2001). The results of this study corresponded to the findings of previous studies on radioactivity, especially since radon is a decay product of U-238. For example, low to medium radon levels were observed in residences in Shai Hills, corresponding to low activity concentrations estimated in the same area. In addition, rocks with significant radioactivity concentration and tectonic faults with elevated release can cause a significant rise in indoor radon levels in homes (Rakmetkazhy and Bulgakova, 2015), as observed in places like Weija and its surrounding towns.

(iv) The contribution of building materials to indoor radon levels

Elevated indoor radon levels in dwellings can also be attributed to the type of building materials used in construction (Kocsis et al., 2021). Human exposure to ionizing radiation from radionuclides, including radon, can be significant, particularly when the building materials constitute radiation doses above normal background levels. Materials such as concrete bricks, cement, and tiles are made from raw materials with considerable concentrations of the natural radionuclides U-238, Th-232, and K-40. Hence, radon and its daughter isotopes can concentrate in dwellings and lead to internal radiation exposures when inhaled (Kocsis et al., 2021; Otoo et al., 2018). Studies on radioactivity concentrations in building materials in the region revealed that they had radon levels between 17.4 ± 0.7 and 42.1 ± 2.8 Bq/m^3. The studies also showed that low radioactivity in building materials corresponded to low radon concentrations, demonstrating that, to some degree, indoor radon concentrations are influenced by radioactivity levels in building materials (Otoo et al., 2018; Csordás et al., 2014).

(v) Ventilation and indoor radon levels

As humans spend most of their time indoors, they become vulnerable to inhaling radon and its progenies. The situation becomes more of a concern when there is little or no ventilation, as frequent air flow into buildings reduces the radon concentration (Adelikhah et al., 2021). It has already been stated that building materials increase radon levels in both new and old residences and are the main entry path of radon into residences (Csordás et al., 2021; Adelikhah et al., 2022). Since building materials from the study area contain average radon levels, the relatively high radon levels measured in some residences can be attributed to inadequate ventilation. It was observed during the survey that some dwellings had either few or small windows, which limited aeration in the homes, especially in populated areas. Again, the lifestyle of residents is such that windows are closed during the night, in rainy seasons, when no one is at home, and the preference for air conditioners instead of fresh air during high temperatures contributes to high indoor radon in residences and the associated health risks. Therefore, radon levels in dwellings can be reduced when there is enough ventilation.

4.3.3 Induced radiation dose and health risk assessment

The inhalation of radon and its progenies is responsible for approximately half of humans' overall annual effective dose from natural ionizing radiation sources (Cosma et al., 2009). In the study, the average indoor radon concentrations were assumed to be the same as the annual average indoor radon concentrations. This was used to determine the radiation dose and health risk assessment of radon inhalation. The AED, ELCR, and LCC per year due to radon inhalation were evaluated.

(i) Annual effective dose (AED)

The estimated annual effective dose ranged between 0.9 and 2.3 mSv/y with a mean dose of 1.3 mSv/y. The mean annual effective dose corresponded to the mean annual indoor radon concentration of 50.8 Bq/m^3. The mean effective dose, 1.3 mSv/y, is below the ICRP's recommended level of 3.0 mSv/y (ICRP, 2010). Residences in the central and south-western part of the Greater Accra region had high effective doses varying between 1.4 and 2.3 mSv/y. The highest mean indoor radon concentration of 92.0 ± 5.2 Bq/m^3, corresponding to the highest effective dose of 2.3 mSv/y, was observed in these areas. This could be due to the densely populated nature of the area, the poor ventilation, and houses being constructed close to each other with limited spaces and windows for good aeration. In addition to this, several housing projects are taking place in the study area that could result in the disturbance of soils and rocks to release radon gas into the atmosphere, thereby increasing the risk of internal radiation exposure.

(ii) ELCR and LCC due to indoor radon

The ELCR and LCC parameters determined the assessment of the impact of indoor radon on lung cancer. The ELCR values were estimated to vary from 3.5 to 8.9, with an average of 4.9 for every 100,000 population. The LCC per 1,000,000 people ranged from 16.4 to 41.7, with an average of 23.1. Earlier studies indicated that there is an increased risk of lung cancer even at a low indoor radon level of 40 Bq/m^3 (Cosma et al., 2009). According to a fact sheet on Ghana reported by the WHO and Global Cancer Observatory, lung cancer ranked 8th among the top ten categories of cancers that affect the country's population, with a percentage of 45.1. In 2020, the country recorded a total of 535 new lung cancer cases and a death toll of 487 (Globacon, 2021). Consequently, approximately 5% of lung cancer deaths are estimated

annually in this study as a result of indoor radon exposure. This percentage falls within the WHO's estimate of 3-14% annually. The risk of lung cancer is proportional to radon levels in indoor environments, as stated by the WHO. Lung cancer cases rise by 16% for every 100 Bq/m^3 radon concentration (WHO, 2009; Adelikhah et al., 2021). Therefore, there is a relationship between indoor radon exposure and lung cancer risk.

4.3.4 Spatial distribution of indoor radon concentrations

The spatial distribution maps of indoor radon levels for the Greater Accra region were created using the interpolation methods Inverse Distance Weighting (IDW), Empirical Bayesian Kriging (EBK), and Ordinary Kriging (OK). The IDW and OK methods are based on the distance between two points, those of observation and those estimated in the interpolation (Adelikhah et al., 2021). The IDW also weighs the effect of the observed point on the estimated interpolation, only regarding the distance. The theory of this technique is that the characteristic value of an unsampled point is the weighted average of identified values in the zone (Chen and Liu, 2012). On the other hand, the OK technique is based on the relationship between the points and the creation of a preliminary function, i.e., variogram, which is repetitively updated. The OK computes the semivariogram identified from data points and utilizes the single semivariogram to make estimations at unknown points; however, in the case of the EBK method, it also recognizes the uncertainty. Thus, the spatial distribution maps of indoor radon levels for the dwellings surveyed were plotted over a 5 x 5 km^2 grid using the ArcGIS software as shown in Figure 34 A, B, and C. The maps categorized the study area so that the population would be aware of areas of increased risk of radon exposure and related lung conditions.

Out of the three interpolation maps, the IDW was the most accurate in describing a pictorial view of the measured indoor radon within the study area. The IDW also recorded the lowest Mean Absolute Error (MAE) and Average Standard Error (ASE) of 7.7 and 11.6, respectively. The OK and EBK could not appropriately describe the radon concentrations within the study area because the OK depends on normally distributed input data. On the other hand, the EBK needs additional data, such as soil gas, faults, and soil types, to generate suitable interpolation maps for this study (Coletti et al., 2021).

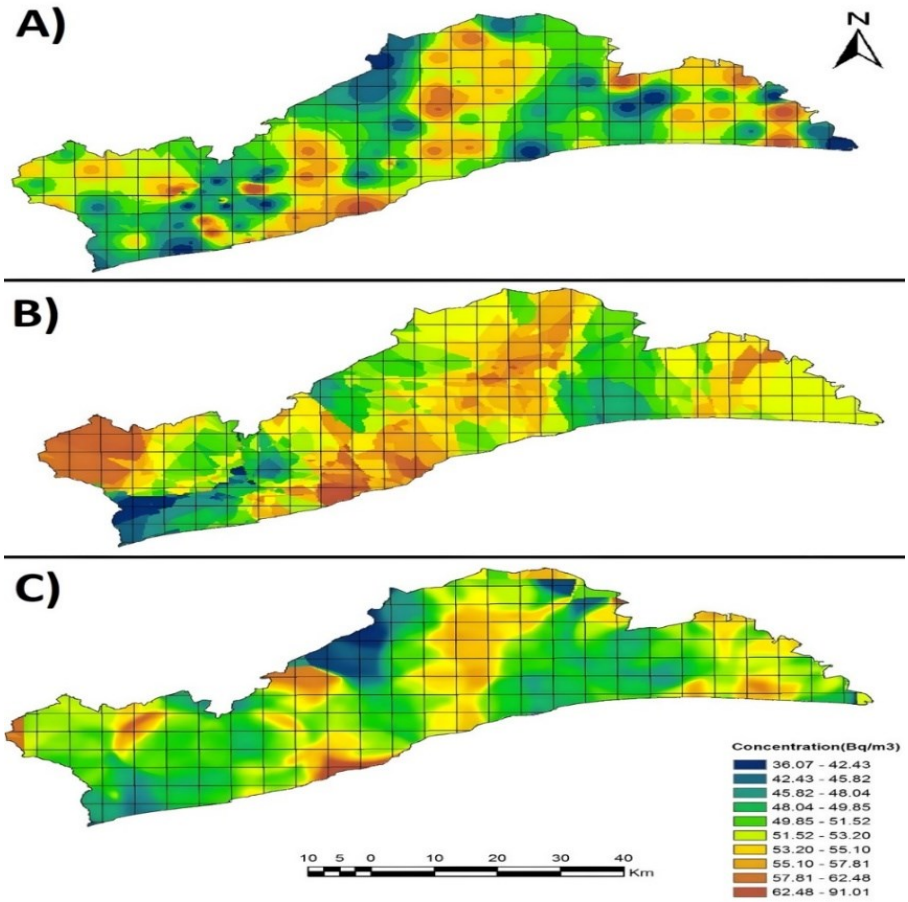

Figure 34. Projected indoor radon maps using (A) IDW, (B) OK, and (C) EBK interpolation techniques (by author).

The IDW map displayed that high indoor radon levels were recorded in populated and less populated areas, especially in dense areas like Madina, Adentan, Kaneshie, Ashiaman, Pokuase, Dome, Amasaman, Tema, James Town, Haatso, Kwabenya, and Legon Hills. Dawhenya, Osudoku, Dedukope, and Afienya were among the less populated towns with high indoor radon activity. Poor ventilation practices and old houses with smaller window sizes mainly characterize such areas. Thus, the spatial distribution map helped visually identify areas prone to high indoor radon levels and the related health implications.

4.4 Po-210 in cigarettes on the Ghanaian market

4.4.1 Po-210 activity concentration

The activity concentrations of Po-210 measured in both local and foreign cigarettes have been presented in Table 7.

Table 7. Activity concentration of Po-210 in cigarette samples and the estimated effective doses.

	Sample ID	Po-210 activity (mBq/cig)	E (mSv/y)	ELCR ($\times 10^{-3}$)
Local brands	CPI	30.1 ± 4.9	0.076	0.266
	CP2	30.7 ± 5.2	0.078	0.273
	CP3	29.9 ± 4.3	0.076	0.266
	CP4	27.3 ± 3.9	0.069	0.242
	CP5	29.3 ± 4.2	0.074	0.259
	CP6	23.1 ± 3.4	0.058	0.203
	CP7	27.6 ± 4.3	0.070	0.245
	CP8	24.7 ± 3.2	0.062	0.217
	CP9	30.9 ± 4.1	0.078	0.273
	CP10	16.4 ± 2.5	0.041	0.144
Imported brands	CP11	25.3 ± 4.5	0.064	0.224
	CP12	19.4 ± 3.8	0.049	0.172
	CP13	21.8 ± 4.6	0.055	0.193
	CP14	28.5 ± 4.7	0.072	0.252
	CP15	32.3 ± 5.2	0.082	0.287
	Average	26.5 ± 4.2	0.067	0.234
	Minimum	16.4 ± 2.5	0.041	0.144
	Maximum	32.3 ± 5.2	0.082	0.287
	Standard deviation	4.5	0.011	0.040

The activity concentrations of Po-210 in cigarettes ranged from 16.4 ± 2.5 to 32.3 ± 5.2 mBq/cig. The local cigarettes had activities between 16.4 ± 2.5 and 30.9 ± 4.1 mBq/cig, with an average of 30.9 ± 4.1 mBq/cig, while the foreign cigarette brands had activities between

19.4 ± 3.8 and 32.3 ± 5.2 mBq/cig, with an average of 25.5 ± 4.6 mBq/cig. The overall mean Po-210 activity concentration was determined as 26.5 ± 4.2 mBq/cig. Some cigarettes (CP1, CP2, CP9, and CP15) recorded high Po-210 activities above 30 mBq/cig. CP15 had the highest activity concentrations of 32.3 ± 5.2 mBq/cig, which was among the foreign cigarettes, and the lowest activity of 16.4 ± 2.5 mBq/cig was observed among the local cigarettes (CP10). The high Po-210 activities in the cigarettes could be attributed to the tobacco leaves used in the production of cigarettes, which may have been cultivated in soils with high Po-210 levels, and the type of fertilizers applied to the tobacco plants. Therefore, smoking local cigarettes can cause more Po-210 to be inhaled than foreign cigarettes if the same quantity of cigarettes is smoked in the same manner (Schayer et al., 2009).

From the data presented in Table 7, the mean activity concentration of Po-210 is slightly higher in local tobacco cigarettes than in foreign tobacco cigarettes. This suggests that, on average, local tobacco cigarettes might have a marginally higher level of Po-210. While the differences are not drastic, the higher average in local tobacco cigarettes could be of concern due to the health implications of Po-210 exposure. Figure 35 shows that the local samples are more clustered around their mean value, while foreign samples show more spread, consistent with the calculated standard deviations. The more significant variability in foreign tobacco cigarettes could suggest inconsistent manufacturing or material sourcing processes. However, it is important to note that these findings are based on the study's sample collection and may not necessarily represent all local and foreign tobacco cigarettes available on the Ghana market. Further analysis with a larger sample size and more brands could provide a more comprehensive understanding. Additionally, the health implications of these concentrations of Po-210 should be considered in the context of other risk factors and total exposure to different compounds and radiations.

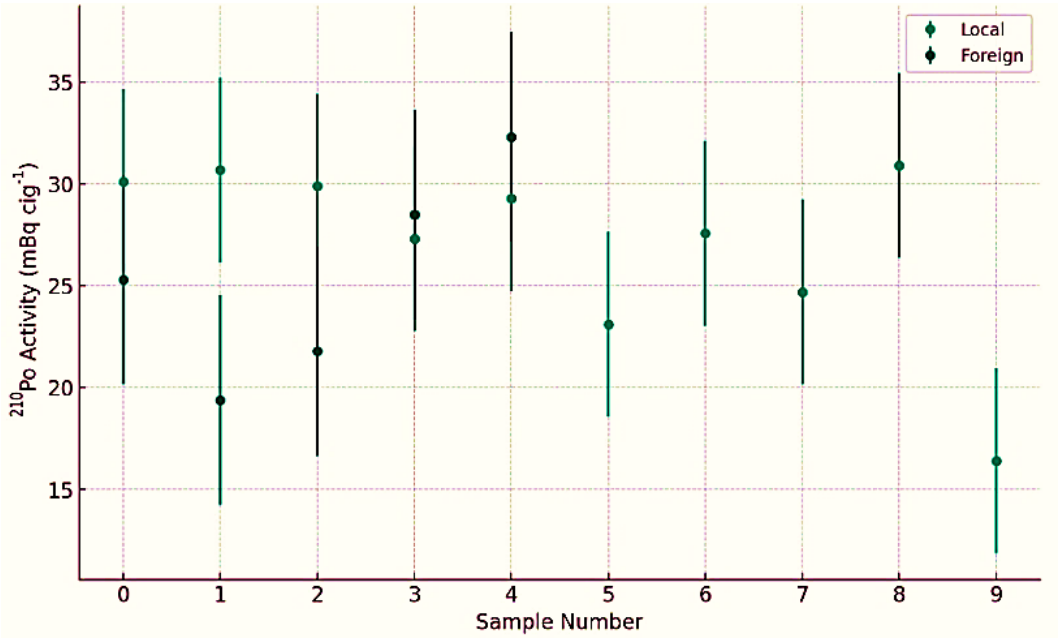

Figure 35. Visual representation of the variability and distribution of Po-210 activity concentration in both local and foreign tobacco cigarette samples (by author).

4.4.2 Estimation of induced dose due to Po-210 in cigarettes

The annual effective dose from inhaling Po-210 in cigarette smoke was determined from the activity concentrations of Po-210, which were computed and presented in Table 7. The determined committed annual effective doses were between 0.041 mSv/y and 0.082 mSv/y. The average effective dose of 0.067 mSv/y corresponded to the average activity concentration of 26.5 mBq/cig. The foreign cigarettes had a mean effective dose of 0.064 mSv/y, while the local cigarettes had an average of 0.068 mSv/y. The average effective dose was below the ICRP and UNSCEAR reference levels of 1- 20 mSv/y and 1.26 mSv/y, respectively (ICRP, 2007; UNSCEAR, 2000). Thus, the average and highest doses are below the world reference level of 1.26 mSv/y for the inhalation radionuclides from natural radiation sources (Boumala et al., 2019; UNSCEAR, 2008). Again, the effective doses determined in the study were similar to those estimated in other countries (Kovács et al., 2007; Schayer et al., 2009; Horvath et al., 2017; Kubalek et al., 2016).

The estimation of the effective dose for a smoker is dependent on several factors, predominantly the conversion factor per unit of intake and the amount of Po-210 concentration retained in the lungs after smoking (Kubalek et al., 2016; Boujelbane et al.,

2020; Sakoda et al., 2012). In this investigation, 50% was used as the quantity of smoke retained in the lungs, and a conversion factor of 3.3 μSv was used to calculate the effective dose (UNSCEAR, 2000; ICRP, 2012). The number of cigarettes smoked per day, the time and speed of smoking are the other factors influencing the estimation of effective radiation dose (Kubalek et al., 2016). In Ghana, it has been projected that six cigarettes are smoked averagely in a day which is less than the 20 cigarettes smoked per day in Hungary (Kovács et al., 2007; Nketiah-Amponsah et al., 2018) and hence the low effective doses evaluated in this investigation assuming the time and speed of smoking are the same.

Studies show that during smoking, large volumes of Po-210 are transferred from the cigarette into the cigarette smoke due to the high volatility and activity concentration of Po-210. Consequently, most of the Po-210 is inhaled, reaching the gastrointestinal tract (Kubalek et al., 2016; Boryło et al., 2013). The quantity of Po-210 inhaled is characteristic of a smoker, and it depends on the manner of smoking, that is, the frequency of puffs, volume, and duration (Ghanbar-Moghaddam & Fathiyand, 2020). Again, studies show that Po-210 activity concentrations have been detected in the blood of smokers, and the concentration is dependent on the number of cigarettes smoked in a day (Boryło et al., 2013). Thus, a smoker of 6 cigarettes will have less concentration of Po-210 detected in the blood than a smoker of a larger number of cigarettes per day. Po-210 concentration has also been detected in patients with lung cancer and significant concentrations in current and former smokers (Zagà et al., 2021). Therefore, smoking cigarettes is an important route of entry of Po-210 into the blood and lungs of smokers, resulting in cancerous diseases.

4.4.3 Estimation of ELCR and lung cancer deaths

The extra risk of developing cancer due to exposure to carcinogenic elements in cigarette smoke over a period was assessed with the ELCR (Table 7). The lung cancer risk from the inhalation of cigarette smoke was determined to range between 0.144×10^{-3} and 0.287×10^{-3}. The highest risk factor of 0.287×10^{-3} corresponded to the highest effective dose and Po-210 activity concentration of 0.082 mSv/y and 32.3 mBq/cig, respectively. The mean ELCR was estimated to be 0.234×10^{-3}, less than the world reference mean of 1.16×10^{-3} for tobacco samples (Shousha and Ahmad, 2016). The ELCR factors represented 14- 29 deaths for every 100,000 population. Cigarette smoking approximately doubles the risk of humans to diseases

and three times raises the risk of sudden deaths. The level of risk surges with the number of cigarettes smoked per day (Boryło et al., 2013). In 2020, 487 people died of lung cancer in Ghana (Stabile et al., 2017). This translates into 3-6% (mean ~ 5%) of lung cancer deaths per the ELCR factors evaluated in this study. Hence, the radioactive Po-210 in cigarettes contributes about 0.234% of lung cancer cases to the overall cancer cases in Ghana, representing a significant 1.67% of deaths due to radiation from smoking (Globacon, 2021).

Another contributing factor to the risks of lung cancer is the fact that cigarette filters do not effectively decrease the number of cancerous substances in cigarette smoke (Skwarzec et al., 2001). Only a small amount of nearly 1- 16.5% of Po-210 in cigarettes is absorbed, resulting in elevated concentrations of inhaled carcinogens, causing an increased risk of lung cancer. The importance of cigarette filters is to reduce the amount of nicotine, tar, and particles from cigarette smoke. Instead, they cause recurrent and stronger inhalation of the smoke and deeper dispersion of particles and smoke in the lungs. This makes its removal difficult, remaining comparatively longer (Karagueuzian et al., 2012; Persson and Holm, 2011; ICRP, 2012; Skwarzec et al., 2001). The inability of filters to efficiently decrease the number of inhaled carcinogens could account for relatively high effective doses recorded in some cigarette brands analyzed in this study.

The results of the radioactivity concentrations, the committed annual effective dose, and the cancer risks of Po-210 observed in this investigation indicate that natural radionuclides from natural sources, including tobacco leaves, can harm human health. The health risks associated with radioactive elements in cigarettes, particularly Po-210, and their cancer implications demand strengthened and sustainable efforts to control cigarette consumption in Ghana.

4.5 Natural radioactivity in soils and sediment from mining areas

4.5.1 Activity concentrations of Ra-226, Th-232 and K-40 in soils and sediment

Different soil and sediment samples from the Atiwa West mining areas were evaluated for the radioactivity levels of Ra-226, Th-232, and K-40. Table 8 presents the statistical data of the measured radionuclides in Bq/kg in soil and sediment samples, and Figures 36- 38 show the distribution of the radionuclides.

Table 8. Statistics of measured radionuclides from the different sampling areas.

		Ra-226 (Bq/kg)	Th-232 (Bq/kg)	K-40 (Bq/kg)
Mining sites	Mean	24.1 ± 2.3	33.5 ± 2.5	262 ± 25
	Minimum	12.9 ± 1.4	10.8 ± 1.2	48 ± 10
	Maximum	29.1 ± 1.8	44.0 ± 1.8	429 ± 36
	Standard deviation	3.5	8.8	115.1
	Geometric mean	23.8 ± 2.2	31.9 ± 2.4	225 ± 24
Sediment	Mean	18.8 ± 2.0	17.0 ± 1.7	167 ± 20
	Minimum	15.8 ± 1.7	14.3 ± 1.8	128 ± 20
	Maximum	22.4 ± 2.3	20.2 ± 1.6	223 ± 25
	Standard deviation	2.2	2.0	37.9
	Geometric mean	18.7 ± 2.0	16.9 ± 1.7	163 ± 18
Farms	Mean	21.1 ± 2.1	21.4 ± 2.2	136 ± 18
	Minimum	17.3 ± 1.7	15.8 ± 2.5	40 ± 10
	Maximum	28.8 ± 3.0	26.8 ± 3.0	269 ± 21
	Standard deviation	3.8	3.7	65.3
	Geometric mean	20.8 ± 2.0	21.1 ± 2.1	117 ± 17
Undisturbed lands	Mean	22.4 ± 2.1	31.7 ± 2.7	184 ± 21
	Minimum	16.2 ± 1.6	25.9 ± 2.4	41 ± 11
	Maximum	26.8 ± 1.7	38.8 ± 4.1	310 ± 27
	Standard deviation	3.2	3.9	87.8
	Geometric mean	22.2 ± 2.1	31.4 ± 2.6	159 ± 20.3

From Table 8, the radioactivity levels of Ra-226 ranged between 12.9 ± 1.4 to 29.1 ± 1.8 Bq/kg with a mean of 24.1 ± 2.3 Bq/kg in soils from mining sites, 18.8 ± 2.0 Bq/kg in sediments, 21.1 ± 2.1 Bq/kg in soils from farmlands and 22.4 ± 2.1 Bq/kg in soils from undisturbed lands. For Th-232, average activity concentrations were 33.5 ± 2.5 Bq/kg, 17.0 ± 1.7 Bq/kg, 21.4 ± 2.2 Bq/kg, and 31.7 ± 2.7 Bq/kg for mining sites, sediments, farmlands, and undisturbed lands, respectively. The activity concentrations of K-40 recorded averages

of 262 ± 25 Bq/kg for mining sites, 167 ± 20 Bq/kg for sediments, 136 ± 18 Bq/kg for farmlands, and 184 ± 21 Bq/kg for undisturbed lands. The overall mean activity concentrations of Ra-226, Th-232, and K-40 measured in soil and sediment samples were 22.1 ± 2.1 Bq/kg, 27.5 ± 2.3 Bq/kg, and 198 ± 22 Bq/kg, respectively. The average activity concentrations followed a descending order of K-40 > Th-232 > Ra-226. The average concentrations were less than the world averages of 35 Bq/kg for Ra-226, 30 Bq/kg for Th-232 (except for mining sites), and 400 Bq/kg for K-40 (UNSCEAR, 2000).

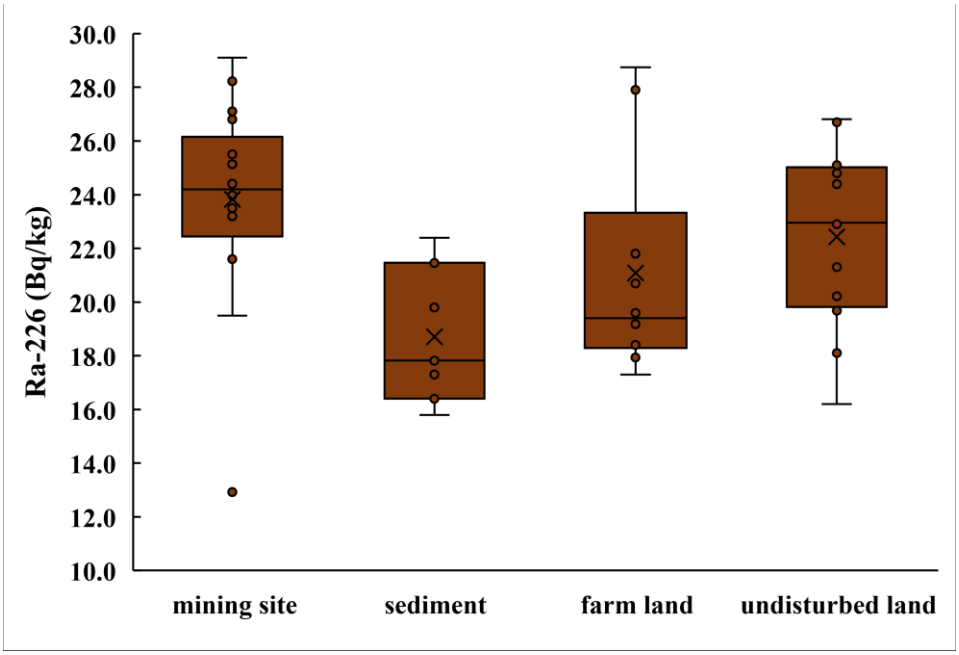

Figure 36. Distribution of Ra-226 activity concentration in soil and sediment (by author).

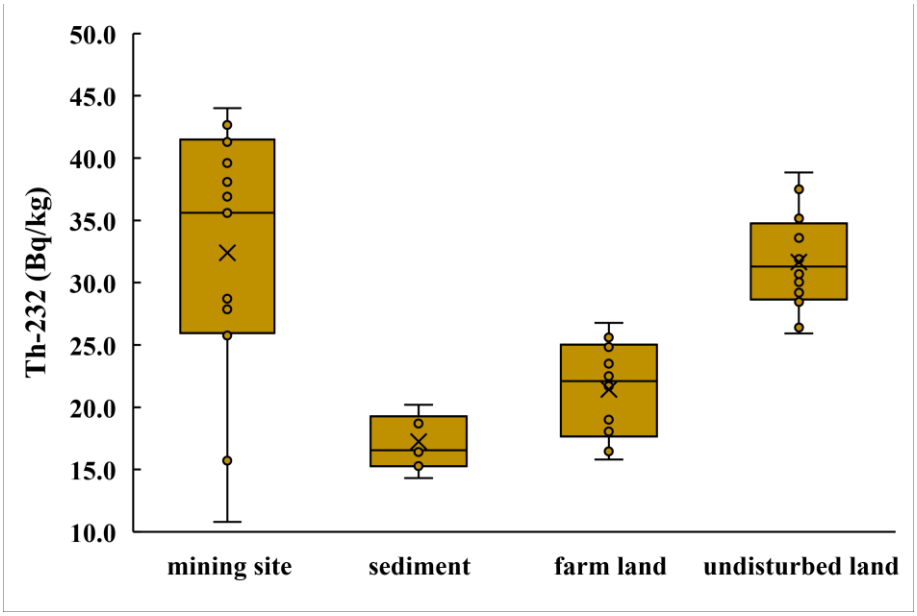

Figure 37. Distribution of Th-232 activity concentration in soil and sediment (by author).

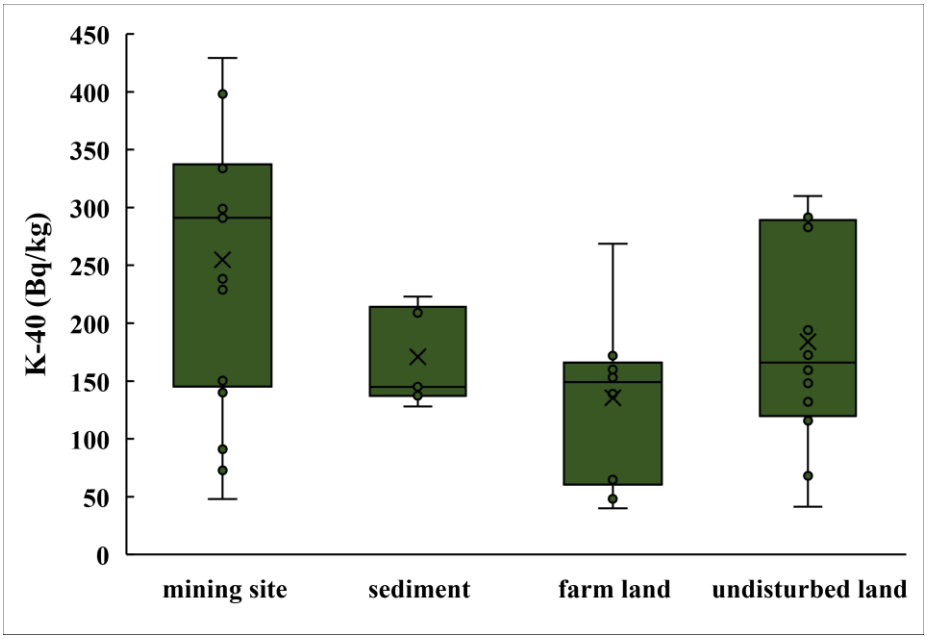

Figure 38. Distribution of K-40 activity concentration in soil and sediment (by author).

This study observed that most soil samples from farmlands and undisturbed areas showed decreasing Ra-226 and Th-232 activity concentrations with increasing distance from mining sites, proving that mining elevates background radioactivity levels. High Th-232 activity concentrations were also observed in soil samples from mining sites and undisturbed lands. Ra-226 and Th-232 levels in soils were higher than in sediments. High K-40 also recorded

high activity levels in mining sites, sediments, and undisturbed lands, while some farm areas had low K-40 concentrations. Generally, Th-232 levels were higher than Ra-226 levels and above the world average value of 30 Bq/kg in most sample locations (UNSCEAR, 2000). High Th-232 in soil and sediment increases radiological safety concerns as the increase in Th-232 activity levels elevates background radiation levels, which will cause soils from the area to be unfit as building material and for other purposes (Orosun et al., 2019). The variations in the measured natural radionuclides' activity concentrations depend on the study area's geological rock formations (Yachiso et al., 2022). The distribution of radionuclides in the area could be influenced by the geological mineralization, geographical discrepancies, chemical composition of rock formations, or meteorological conditions of the study area (Idriss et al., 2018; Dina et al., 2022).

4.5.2 Relationships among measured radionuclides in soils and sediment

Ra-226, Th-232, and K-40 activity concentrations were correlated and presented in Figures 39a, b, and c. The regression analysis showed a positive association between Ra-226 and Th-232 ($R^2 = 0.43$), Th-232 and K-40 ($R^2 = 0.46$) and Ra-226 and K-40 ($R^2 = 0.26$).

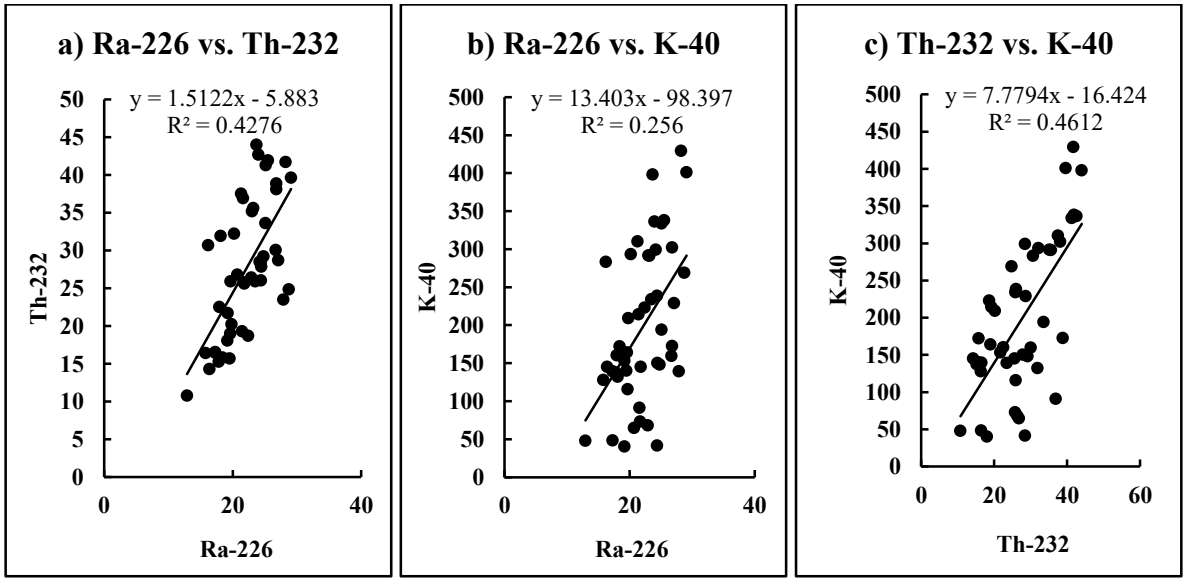

Figure 39. Activity correlation between (a) Ra-226 and Th-232, (b) Ra-226 and K-40 and (c) Th-232 and K-40 (by author).

Pearson correlation analysis estimates the strength of association between radionuclides and radiological parameters. The study showed Ra-226 and Th-232 had a good correlation coefficient of $R^2 = 0.65$, indicating the radionuclides decay together in nature (Sureshghandi et al., 2014; Akuo-ko et al., 2023a). Good correlations between radiological parameters and Ra-226 and Th-232 were observed since their estimation is related to the radionuclides.

4.5.3 Radiological risk assessment

Health hazards are associated with exposure to radiation from the radionuclides in soil and sediment from the different sampling locations. Figures 40 and 41 show the evaluated radiological parameters for the study. The Ra_{eq} activity concentrations ranged from 32.0 Bq/kg to 120.9 Bq/kg. The minimum and maximum activities were observed in mining site locations. The mean Ra_{eq} value of 76.7 Bq/kg was estimated. Ra_{eq}, which evaluates the internal and external gamma dose due to radon and its daughter isotopes, assesses the suitability of soils as building materials. Ra_{eq} values were below the UNSCEAR average of 370 Bq/kg (UNSCEAR, 2008; 2000) and thus the soils can be used for building purposes. The gamma dose rates were evaluated to be between 14.5 and 56.1 nGy/h, with an average of 35.1 nGy/h. All the investigated locations had gamma dose rates below the world average of 60.0 nGy/h. The AED, which estimates the radiation dose induced from radionuclides, recorded values from 17.8 µSv/y to 68.8 µSv/y with a mean value of 43.0 µSv/y. The estimated AED values were less than the guidance level of 70.0 µSv/y for public exposure (UNSCEAR, 2000). The AGDE values determined from the various locations were between 100.1 µSv/y and 396.3 µSv/y, with a mean of 245.3 µSv/y. The average AGDE value was below the world mean of 300.0 µSv/y (UNSCEAR, 2000). However, some locations (22%) recorded doses higher than 300.0 µSv/y. Such locations were the mining areas and some undisturbed lands near the mining areas.

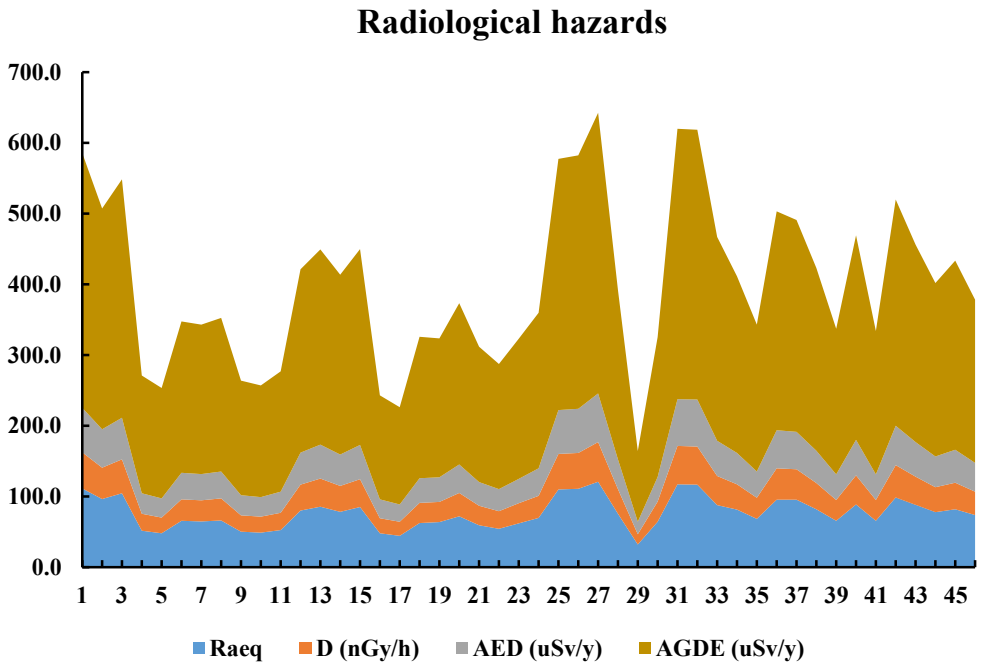

Figure 39. Ra_{eq}, D, AED, and AGDE due to radionuclides in soil and sediment (by auhor).

Consistent with the ICRP and UNSCEAR (ICRP, 1990; UNSCEAR, 2000), the external and internal exposure to natural radiation must be minimal to limit the radiation dose to 1.0 mSv/y. This means H_{ex} and H_{in} must be less than or equal to unity. In the study, both indices were found to have averages below unity, i.e., 0.3 and 0.2 for H_{in} and H_{ex}, respectively. The gamma index (I_{γ}), which considers the collective effect of natural radionuclides in a location, was estimated to range from 0.1 to 0.4 with an average of 0.3, less than the world average of 1.0 (Botwe et al., 2017). The present study similarly assessed the likelihood of cancer cases in the study area by computing the excess lifetime cancer risk. ELCR factors ranged from 0.06×10^{-3} to 0.24×10^{-3}. The computed average factor of 0.15×10^{-3} was less than the reference factor of 0.29×10^{-3} (UNSCEAR, 2000). Generally, the lowest radiological values were observed at a mining site that recorded the lowest activity concentrations for the measured radionuclides.

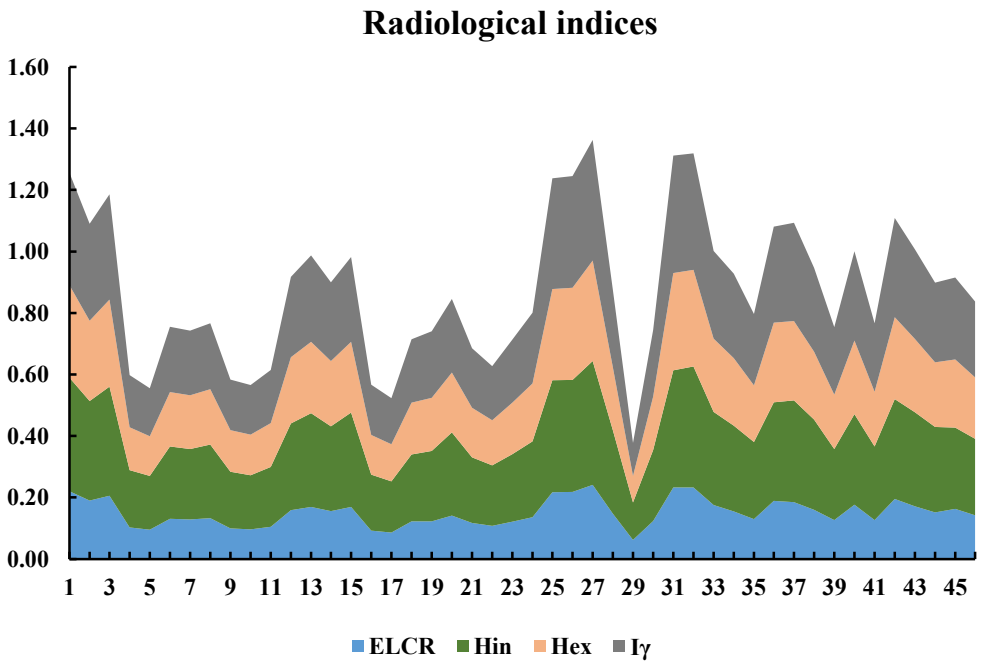

Figure 41. ELCR, H_{in}, H_{ex}, and I_{γ} due to radionuclides in soil and sediment (by author).

4.6 Natural radioactivity and radon exhalation rate in soils from mining areas

4.6.1 Distribution of radionuclides in soils

Radionuclides and radon exhalation rates were determined in soils from 22 locations within the study area. The radioactivity concentrations were examined in soils collected from mining sites, farming areas, and undisturbed areas of both residential and non-residential areas. Table 9 presents the statistics of the radionuclides' distribution, while Figure 42 shows the frequency distribution of the radionuclides.

Table 9. Statistics of radionuclide concentration and exhalation rates.

	Ra-226 (Bq/kg)	**Th-232 (Bq/kg)**	**K-40 (Bq/kg)**	**CRn (Bq/m^3)**	**$E_M \times 10^{-5}$ (Bq/kg/h)**	**$E_A \times 10^{-3}$ ($Bq/m^2/h$)**
Average	26.9 ± 1.7	57.5 ± 3.6	237.5 ± 17.6	560.0 ± 54	4.0 ± 0.4	1.2 ± 0.11
Minimum	18.0 ± 1.2	29.5 ± 2.8	78.8 ± 17.1	390.6 ± 38	2.8 ± 0.3	0.8 ± 0.09
Maximum	80.9 ± 1.4	103.3 ± 5.2	429.1 ± 23.4	907.5 ± 93	6.5 ± 0.7	2.0 ± 0.21
Geomean	25.4	54.6	209.7	548.5	3.9	1.2
Standard deviation	12.6	18.9	113.1	120.6	0.8	0.3

The activity concentrations of Th-232 and K-40 showed a normal distribution of data using the Kolmogorov-Smirnov normality test, with *p*-values > 0.05, whereas Ra-226 lacked a normal distribution, which could be attributed to the outlier activity concentration of 80.9 Bq/kg recorded in a farming area (SL08). The activity concentrations of Ra-226, Th-232 and K-40 were within the range of 18.0 ± 1.2- 80.9 ± 1.4 Bq/kg, 29.5 ± 2.8- 103.3 ± 5.2 Bq/kg and 78.8 ± 17.1- 429.1 ± 23.4 Bq/kg with mean activities of 26.9 ± 1.7 Bq/kg, 57.5 ± 3.6 Bq/kg and 237.5 ± 17.6 Bq/kg, respectively. Except for the outlier activity concentration identified for Ra-226, all others were below the worldwide mean of 35 Bq/kg. K-40 also had concentrations below the global mean of 400 Bq/kg except for three sampling locations (SL08, SL15, and SL18). On the other hand, Th-232 recorded concentrations above the worldwide mean of 30 Bq/kg in all locations except for SL18.

Rn-222 activity concentrations as presented in Table 9 and Figure 43 proved to be normally distributed using the Kolmogorov-Smirnov and Shapiro-Wilk normality tests, where *p*-values > 0.05. Rn-222 concentrations measured by CR-39 in the exhalation chambers ranged between 390.6 ± 38 and 907.5 ± 93 Bq/m^3 with a mean, geometric mean, and standard deviation of 560.0 ± 54.3 Bq/m3, 548.5, and 120.6, respectively. Rn-222 activity concentration in soils from mining areas ranged from 390.6 ± 38- 589.8 ± 54 Bq/m^3 (mean: 503.5 ± 46.9 Bq/m^3), for undisturbed areas the concentrations varied between 472.2 ± 45 and

707.3 ± 71 Bq/m^3 (602.8 ± 60 Bq/m^3) while farming areas had Rn-222 concentrations ranging from 415.8 ± 40- 907.5 ± 93 Bq/m^3 (632.8 ± 63 Bq/m^3).

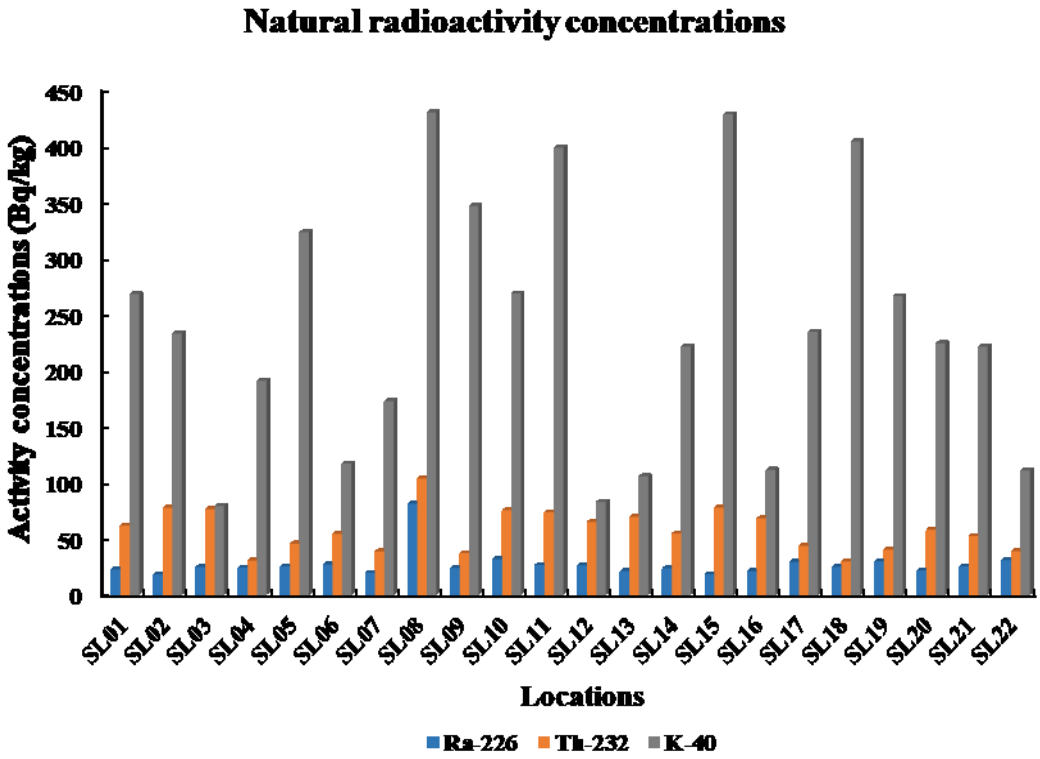

Figure 42. Distribution of radionuclides in soil samples (by author).

Generally, farming and undisturbed areas recorded elevated Rn-222 activity concentrations of ~410 Bq/m^3 and above, in contrast to mining areas, which recorded maximum concentrations of ~580 Bq/m^3 and below. This could be because soil is constantly disturbed at mining sites, causing the escape of Rn-222 gas from the soil. (Mazur et al., 2014; Liza et al., 2023; Singh et al., 2010; Mullerova et al., 2017). The exhaled Rn-222 will likely be inhaled by miners working without protective clothing, including nose masks. Therefore, miners are at risk of internal radiation exposure and consequential respiratory tract diseases.

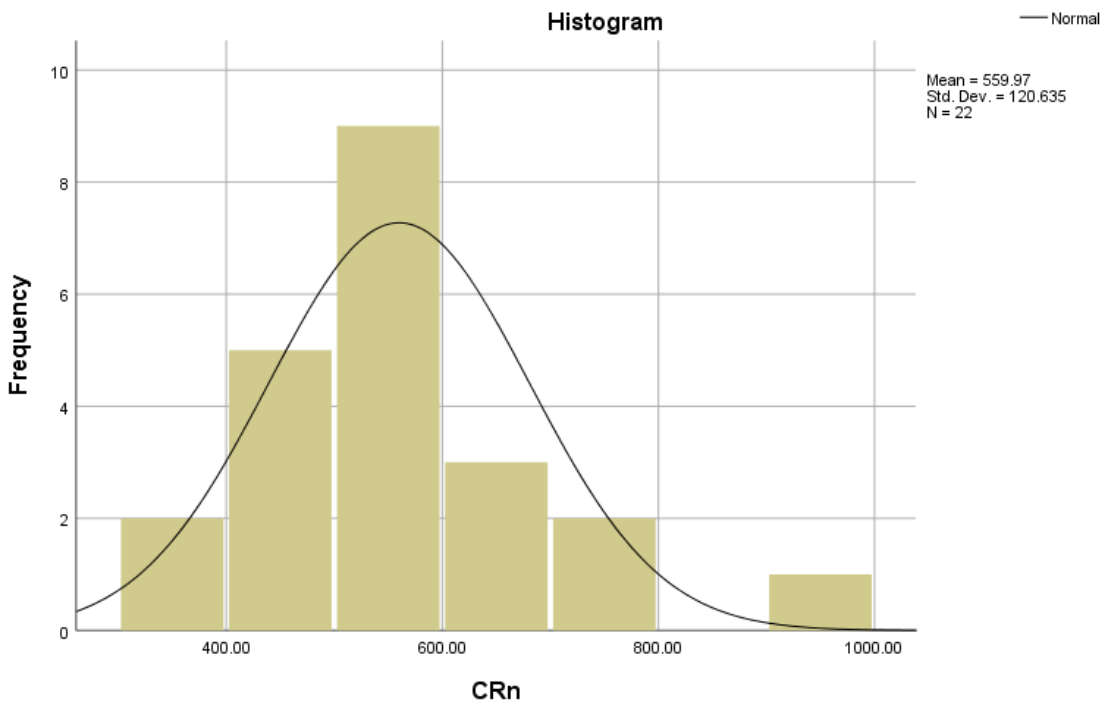

Figure 43. Frequency distribution of radon concentrations (CRn) in Bq/m^3 (by author).

4.6.2 Evaluation of radon exhalation rates

The Rn-222 area and mass exhalation rates of soil were measured using tightly closed vessels with CR-39 detectors, and the obtained data are presented in Table 10.

Table 10. Mean Ra-226 activity concentration and mass and area exhalation rates.

Location	Description of location	Ra-226 (Bq/kg)	CRn (Bq/m^3)	$E_M \times 10^{-5}$ (Bq/kg/h)	$E_A \times 10^{-3}$ (Bq/m^2/h)
SL01	Mining area	22.3 ± 1.8	497.4 ± 41	3.6 ± 0.3	1.1 ± 0.09
SL02	Mining area	18.0 ± 1.2	395.2 ± 32	2.8 ± 0.2	0.9 ± 0.07
SL03	Mining area	24.5 ± 1.4	544.2 ± 52	3.9 ± 0.4	1.2 ± 0.11
SL04	Mining area	24.1 ± 2.0	547.6 ± 50	3.9 ± 0.3	1.2 ± 0.08
SL05	Mining area	25.3 ± 1.8	563.4 ± 51	4.1 ± 0.4	1.2 ± 0.12
SL06	Farming area	26.8 ± 3.2	603.4 ± 62	4.3 ± 0.4	1.3 ± 0.13
SL07	Farming area	19.4 ± 2.4	415.8 ± 40	3.0 ± 0.3	0.9 ± 0.08
SL08	Farming area	80.9 ± 1.4	907.5 ± 93	6.5 ± 0.7	2.0 ± 0.21
SL09	Farming area	23.7 ± 2.6	525.0 ± 51	3.8 ± 0.4	1.1 ± 0.08

SL10	Farming area	31.5 ± 1.3	712.1 ± 71	5.1 ± 0.5	1.5 ± 0.11
SL11	Mining area	26.4 ± 1.4	589.8 ± 54	4.2 ± 0.4	1.3 ± 0.09
SL12	Mining area	26.0 ± 2.0	587.2 ± 55	4.2 ± 0.4	1.3 ± 0.11
SL13	Mining area	20.9 ± 1.2	455.8 ± 46	3.3 ± 0.3	1.0 ± 0.11
SL14	Mining area	23.4 ± 1.5	514.8 ± 51	3.7 ± 0.4	1.1 ± 0.10
SL15	Mining area	18.1 ± 1.6	390.6 ± 38	2.8 ± 0.3	0.8 ± 0.09
SL16	Mining area	20.7 ± 1.5	453.0 ± 46	3.3 ± 0.3	1.0 ± 0.09
SL17	Undisturbed area	28.9 ± 1.8	654.8 ± 66	4.7 ± 0.5	1.4 ± 0.12
SL18	Undisturbed area	24.7 ± 1.2	549.0 ± 58	3.9 ± 0.4	1.2 ± 0.08
SL19	Undisturbed area	29.6 ± 1.9	674.6 ± 64	4.9 ± 0.5	1.5 ± 0.12
SL20	Undisturbed area	21.5 ± 1.7	472.2 ± 45	3.4 ± 0.3	1.0 ± 0.08
SL21	Undisturbed area	25.1 ± 1.4	558.6 ± 58	4.0 ± 0.4	1.2 ± 0.14
SL22	Undisturbed area	30.8 ± 1.6	707.3 ± 71	5.1 ± 0.5	1.5 ± 0.14
Average		**26.9 ± 1.7**	**560.0 ± 54**	**4.0 ± 0.4**	**1.2 ± 0.11**

From Table 10, Rn-222 area exhalation rates were between $0.8 \pm 0.09 \times 10^{-3}$ and $2.0 \pm 0.21 \times 10^{-3}$ Bq/m^2/h, with an average of $1.2 \pm 0.11 \times 10^{-3}$ Bq/m^2/h. Rn-222 mass exhalation rates were between $2.8 \pm 0.3 \times 10^{-5}$ and $6.5 \pm 0.7 \times 10^{-5}$ Bq/kg/h, with a mean of $4.0 \pm 0.4 \times 10^{-5}$ Bq/kg/h. The maximum area and mass exhalation rates of $2.0 \pm 0.21 \times 10^{-3}$ Bq/m^2/h and $6.5 \pm 0.7 \times 10^{-5}$ Bq/kg/h corresponded to the outlier concentrations of Ra-226 and Rn-222 observed in a farming area (SL08). Farming areas recorded the highest mean area and mass exhalation rates of 1.4×10^{-3} Bq/m^2/h and 4.5×10^{-5} Bq/kg/h, respectively, compared to mining and undisturbed areas. Mining areas recorded the lowest mean exhalations, which could be due to the continuous mining activities allowing Rn-222 to escape from the soils. The data showed that area exhalation rates for some sampling locations (36%) were above the recommended level of 1.25×10^{-4} Bq/m^2/h by UNSCEAR. It suggests that radiological effects may be associated with using such soils as building materials (Otoo et al., 2022; UNSCEAR, 2000). The differences in area and mass exhalation rates for the sampled locations can be attributed to the fluctuating Ra-226 concentrations and the geological formations of the locations in the study area (Gulan et al., 2017; Singh et al., 2007; Abate & Amtatie, 2020) as well as the different soil types, soil particle sizes, soil porosity, and soil

surface crystallography (Otoo et al., 2022; Frutos-Puerto et al., 2020). The data presented showed that farming and undisturbed areas recorded higher exhalation rates than observed for mining areas. This could be due to the reason that human activities leading to soil disturbance and subsequently the escape of radon gas from soil pores are minimal in farming and undisturbed areas and as a result, radon gas is trapped in soils with limited means of escape into the environment (Liza et al., 2023; Singh et al., 2010) while the low exhalation rates in mining areas could be attributable to the escape of Rn-222 gas from soil pores through the constant mining activities. A linear relationship was reached between Ra-226, Rn-222, and the exhalation rates in the studied soil samples. The area and mass exhalation rates increased with high Ra-226 concentrations in soils, as it was realized that sampling areas with high Ra-226 concentrations had high radon exhalation rates.

4.6.3 Statistical analyses of the relationship between radionuclides and exhalation rates

(i) Regression analysis

The relationship between Rn-222, Ra-226, and the exhalation rates determined with regression analysis is presented in Figures 44 and 45 (a-d). Figure 44 shows a positive relationship between Ra-226 and Rn-222, with a coefficient value of 1. This is significant as it demonstrates that the concentration of Rn-222 is dependent on the concentration of Ra-226 occurring in the soil (Frutos-Puerto et al., 2020; Otoo et al., 2022; 2018). Ra-226 and Rn-222 showed strong relationships with the exhalation rates ($R^2 = 1$), indicating that the exhalation rates are determined from Rn-222, which also depends on Ra-226 concentrations. Thus, a linear relationship was observed between the radionuclides and the exhalation rates, and this agrees with the outcome of studies conducted in other regions of the world (Shoeib & Thabayneh, 2014; Otoo et al., 2018; Frutos-Puerto et al., 2020; Salahedin et al., 2022; Yousef et al., 2015).

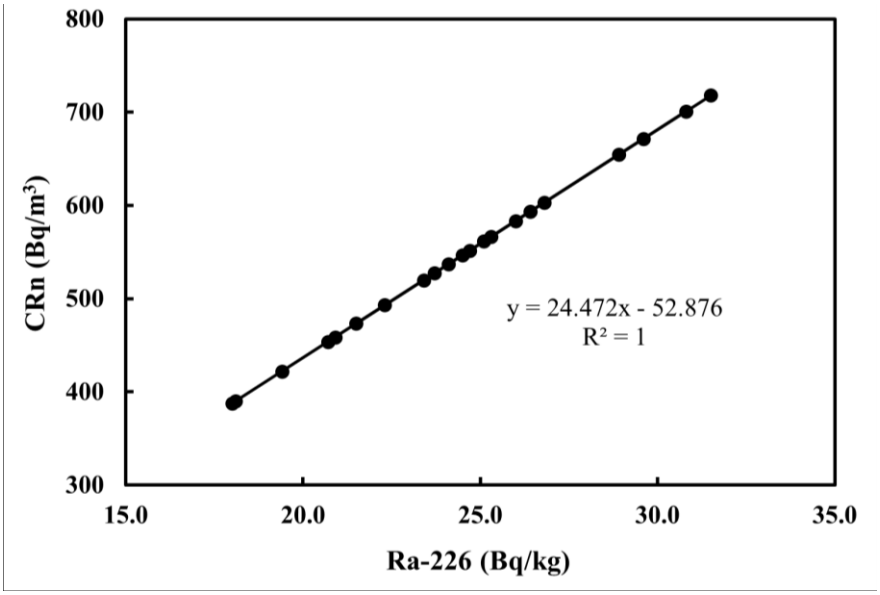

Figure 44. Linear regression of the activity concentrations of Ra-226 and Rn-222 (by author).

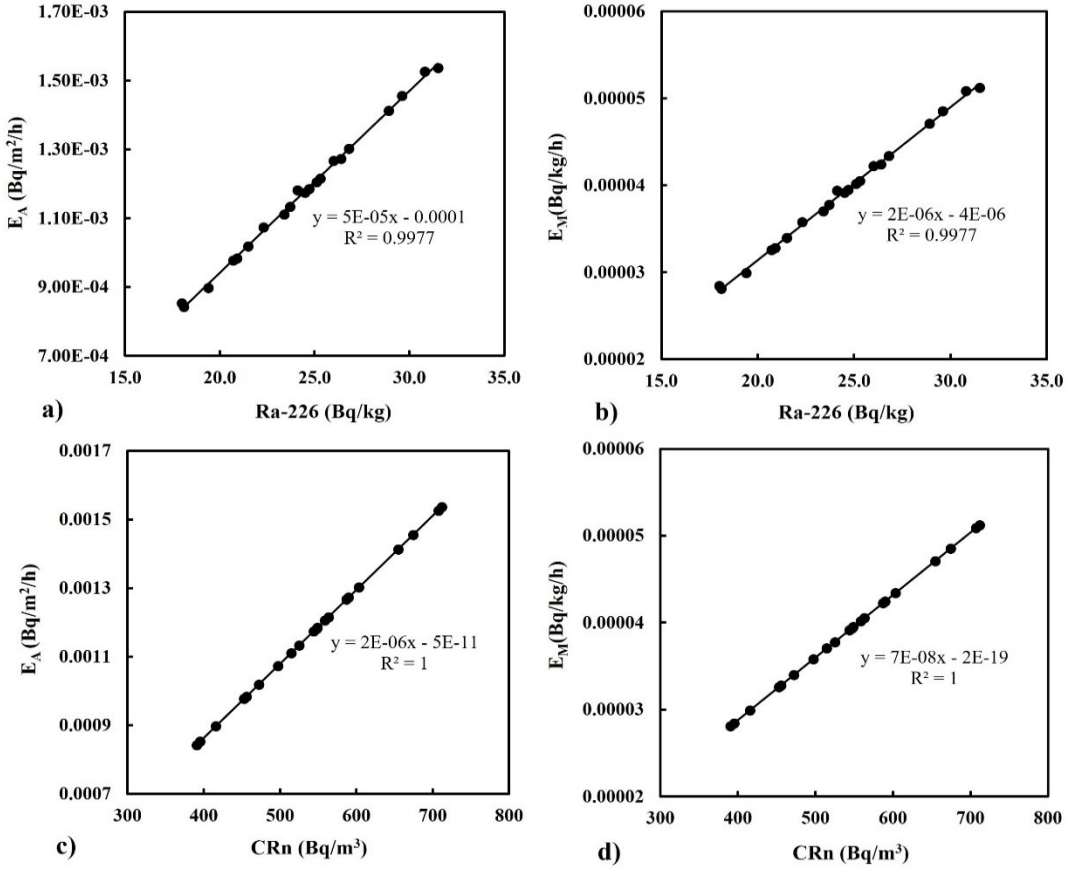

Figure 45. Linear regression between concentrations of Ra-226, Rn-222, and the exhalation rates (by author).

(ii) Pearson correlation

Table 11. Pearson correlation analysis between radionuclides, exhalation rates, and radiological parameters.

	Ra-226	**Th-232**	**K-40**	**Ra_{eq}**	**H_{ex}**	**H_{in}**	**D**	**CRn**	**E_M**	**E_A**
Ra-226	1									
Th-232	0.45	1								
K-40	0.34	0.13	1							
Ra_{eq}	0.74	0.90	0.44	1						
H_{ex}	0.74	0.90	0.44	1	1					
H_{in}	0.85	0.83	0.44	0.98	0.98	1				
D	0.75	0.88	0.49	0.99	0.99	0.98	1			
CRn	0.84	0.16	0.19	0.44	0.44	0.57	0.46	1		
E_M	0.84	0.16	0.19	0.44	0.44	0.57	0.46	1	1	
E_A	0.84	0.16	0.19	0.44	0.44	0.57	0.46	1	1	1

From Table 11, the Pearson correlation analysis showed positive relationships between the radionuclides, exhalation rates, and radiological parameters. Weak correlation coefficients were observed between Ra-226/ K-40 (0.34) and Ra-226/ Th-232 (0.45). In general, Ra-226 had a strong influence on the radiological parameters estimated in the soils whereas Th-232 had less influence on some of the parameters (CRn, E_M and E_A). K-40 minimally contributed to the radiation hazards estimated in this study. Ra-226 and CRn showed a strong positive correlation (0.84), indicating that Ra-226 is the primary source of Rn-222 levels in soils and its parent radionuclide. Thus, the emanation of Rn-222 from soils relies on the concentration of Ra-226 and its decay in the soil (Shahrokhi et al., 2023; Otoo et al., 2020; 2018). The same correlation coefficient (0.84) was observed between Ra-226 and the exhalation rates since their determination depends on Ra-226 and Rn-222 concentrations. H_{ex} and H_{in} also correlated well with Rn-222 (0.44 and 0.57, respectively), suggesting that radon gas partly contributes to the total radiation dose and cancer diseases related to radionuclides in an environment (Akuo-ko et al., 2023a; 2023b). Therefore, using soils from the study region for

building construction, brick works, and pottery could result in long-term inhalation of Rn-222 and its related health issues (UNSCEAR, 2000), though the exposure rates are low.

(iii) Cluster analysis

Cluster analysis graphically illustrated the extent of the relationship between the radionuclides, exhalation rates, and radiological parameters. The single linkage method with correlation coefficient distance between variables was used to perform the cluster analysis. In Figure 45, three main clusters were obtained in the dendrogram analysis. Cluster 1 is made up of CRn, $E_{M,}$ and E_A. This cluster explains the relationship between CRn and the exhalation rates, as high CRn concentrations result in high exhalation rates in soils. Ra-226 is connected to Cluster 1 because radon is a decay product of Ra-226 and largely influences CRn, $E_{M,}$ and E_A rates in soils (Mehta et al., 2019; Mullerova et al., 2017). Cluster 2 consisted of Th-232, Ra_{eq}, H_{ex}, H_{in}, and D. This Cluster is also connected to Ra-226. Thus, the determination of Ra_{eq}, H_{ex}, H_{in}, and D largely depended on the activity concentrations of Ra-226 and Th-232. Radiation hazards in the soils are primarily due to these radionuclides and thus correlate well with the radiological parameters. Cluster 3 consisted of only K-40. This is because, though K-40 is of a natural origin emitting gamma radiation, it did not have much influence on the other variables in the dendrogram, especially on the radiological parameters. The outcome of the cluster analysis agrees with that of the regression and Pearson correlation analyses.

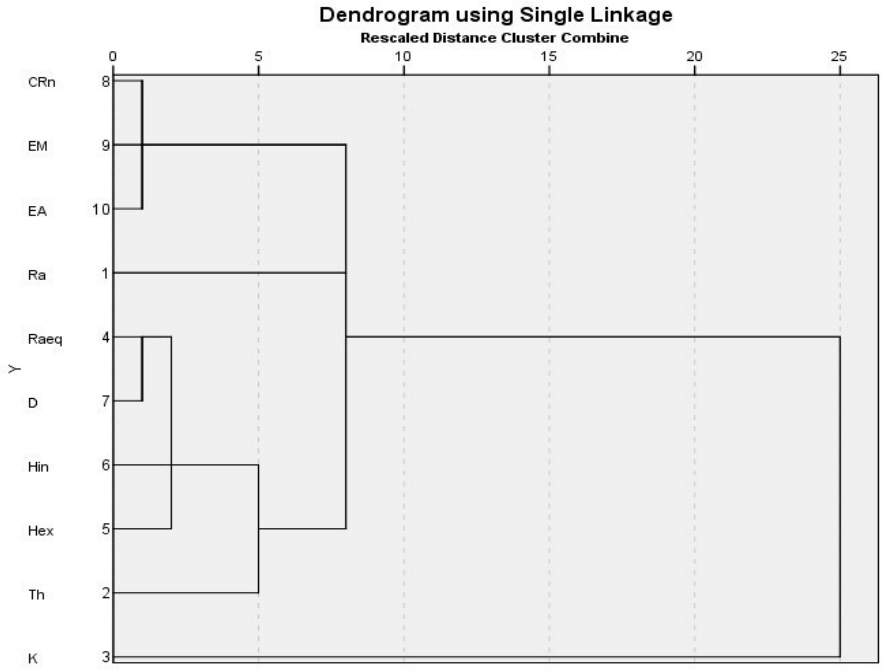

Figure 46. Dendrogram of radionuclides, exhalation rates, and radiological parameters (by author).

(iv) Principal Component Analysis (PCA)

PCA describes the patterns in variables and displays data to highlight similarities (Akuo-ko et al., 2023a). Thus, it assesses the interrelation between variables and describes them with reference to their common factors (Dina et al., 2022). This analysis used the Kaiser normalization method with varimax rotation to study the association between variables, and eigenvalues greater than 1 were considered. In Figure 47, the resultant PCA showed two factors having eigenvalues greater than 1, accounting for 88.81% of the total variance of the rotated matrix. As presented in Table 12, component 1 had 67.26% of the variance, loading heavily on Ra-226 and Th-232 and the radiological parameters. This is owed to the fact that Ra-226 and Th-232 are the primary sources of radioactivity in the soils of the study area and contribute relatively high radiation doses. However, Th-232 had more influence on the radiological parameters than Ra-226 since it is grouped with them. Also, the activity concentration of Th-232 measured in the soil samples were higher than Ra-226, hence the resultant graph. Component 2 had 21.55% of the variance loading on CRn, exhalation rates, and less on Ra-266. CRn, E_M and E_A are grouped because they are positively correlated. Ra-

226 was strongly correlated with Rn-222 levels and their exhalation rates in the investigated soils, and therefore their concentrations depended on the Ra-226 levels in the soils. K-40 had less influence on the variables. The outcome of the PCA is similar to the cluster, regression, and Pearson correlation analyses.

Table 12. Rotated component matrix

	Component 1	**Component 2**
Ra	0.920	0.260
Th	0.698	-0.608
K	0.446	-0.195
Ra_{eq}	0.916	-0.395
H_{ex}	0.928	-0.291
H_{in}	0.952	-0.225
D	0.925	-0.387
CRn	0.795	0.644
E_M	0.795	0.644
E_A	0.795	0.644
Variance explained (%)	**67.257**	**21.551**

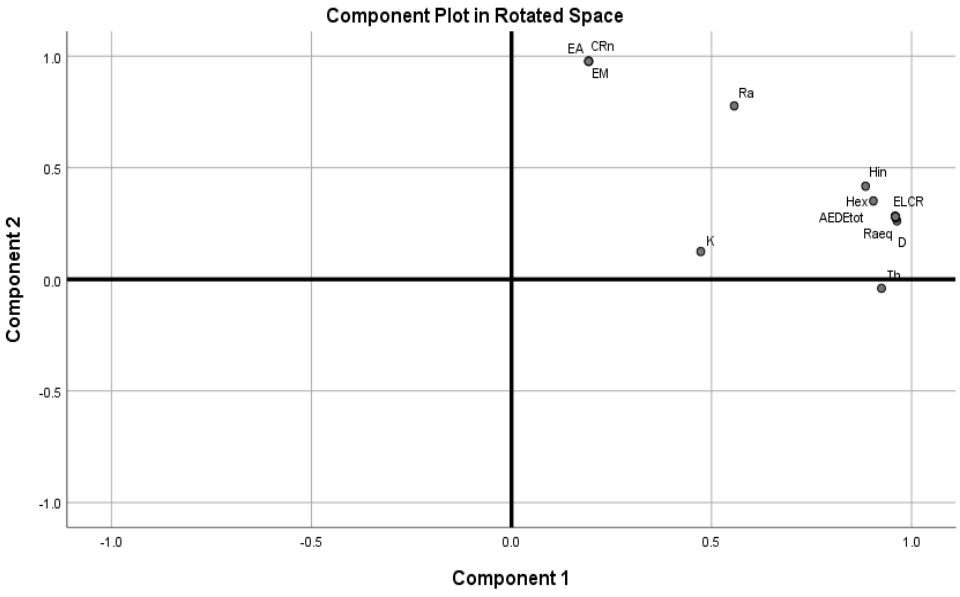

Figure 47. Rotated factor loadings of radionuclides, exhalation rates, and radiological hazards (by author).

4.6.4 Assessment of radiological hazards

Table 13. Radiological hazards of the investigated soil samples.

Location	**Ra_{eq} (Bq/kg)**	**H_{ex}**	**H_{in}**	**D (nGy/h)**	**$AEDE_{tot}$ (mSv/y)**	**ELCR × 10^{-3}**	**LCC × 10^{-6}**
SL01	130.7	0.4	0.4	58.5	0.36	1.26	6.5
SL02	146.3	0.4	0.4	64.6	0.40	1.39	7.1
SL03	139.4	0.4	0.4	60.6	0.37	1.30	6.7
SL04	82.1	0.2	0.3	37.4	0.23	0.80	4.1
SL05	114.9	0.3	0.4	52.5	0.32	1.13	5.8
SL06	112.9	0.3	0.4	49.8	0.31	1.07	5.5
SL07	87.6	0.2	0.3	39.3	0.24	0.84	4.3
SL08	261.7	0.7	0.9	117.7	0.72	2.53	13.0
SL09	103.2	0.3	0.3	47.7	0.29	1.02	5.3
SL10	159.5	0.4	0.5	71.1	0.44	1.53	7.9
SL11	162.0	0.4	0.5	73.1	0.45	1.57	8.1
SL12	124.7	0.3	0.4	54.5	0.33	1.17	6.0
SL13	128.0	0.3	0.4	55.8	0.34	1.20	6.2
SL14	118.0	0.3	0.4	52.8	0.32	1.13	5.8
SL15	161.6	0.4	0.5	72.9	0.45	1.56	8.0
SL16	126.2	0.3	0.4	55.1	0.34	1.18	6.1
SL17	108.8	0.3	0.4	49.3	0.30	1.06	5.4
SL18	97.9	0.3	0.3	46.1	0.28	0.99	5.1
SL19	107.3	0.3	0.4	48.9	0.30	1.05	5.4
SL20	121.2	0.3	0.4	54.1	0.33	1.16	6.0
SL21	116.6	0.3	0.4	52.3	0.32	1.12	5.8
SL22	94.6	0.3	0.3	42.2	0.26	0.91	4.7
Average	**127.5**	**0.3**	**0.4**	**57.1**	**0.35**	**1.23**	**6.3**
World	**370.0**	**1.0**	**1.0**	**60.0**	**1.0**	**0.29**	**170-230**

The Ra_{eq} concentrations ranged between 82.1 and 261.7 Bq/kg. The average Ra_{eq} was 127.5 Bq/kg, less than the reference average of 370 Bq/kg, equivalent to an effective dose of 1 mSv. The low Ra_{eq} values indicate that the inhabitants of the area are likely to receive a radiation dose below 1 mSv (UNSCEAR, 2000; Alazemi et al., 2016). The H_{ex} and H_{in} evaluate the hazards of natural gamma radiation on human health were found to range from 0.2 to 0.7 with a mean of 0.3 for H_{ex} and 0.3 to 0.9 with a mean of 0.4 for H_{in}. H_{ex} and H_{in} values less than 1 mean that natural gamma radiation in soils from the study area is less likely to result in respiratory complications such as cancer and asthma (Arafat et al., 2017; Ozmen et al., 2014). The absorbed gamma dose rates (D) in air were between 37.4 and 117.7 nGy/h. The average rate of 57.1 nGy/h was below the reference average of 60.0 nGy/h (UNSCEAR, 2000). Nonetheless, about 27% of individual locations had D values above the reference average, particularly in locations with high Th-232 levels. The health implications due to radiation exposure were assessed with the AEDE. The total AEDE ($AEDE_{tot}$) values were between 0.23 and 0.70 mSv/y. The mean value of 0.35 mSv/y was less than the reference level of 1 mSv/y (ICRP, 1990; UNSCEAR, 2000). The ELCR and LCC evaluated the probability of developing cancer due to radiation exposure in a lifetime. The ELCR factors ranged between 0.80×10^{-3} and 2.50×10^{-3} with a mean of 1.23×10^{-3}, which is above the reference factor of 0.29×10^{-3}. LCC due to exposure to indoor Rn-222 concentration was estimated per million population. The LCC was assessed to be between 4.1 and 13.0 with a mean of 6.3 per million population yearly. The LCC was lower than the world range of 170-230 per million populations (ICRP, 1993; Otoo et al., 2020).

4.7 Natural radioactivity in surface water and groundwater resources in mining areas

4.7.1 Activity concentration of radionuclides in water samples

Table 14 presents the descriptive statistics of the Ra-226, Ra-228, and K-40 concentrations in Bq/L measured in the water samples.

Table 14. Descriptive statistics of the measured radionuclides in Bq/L.

	Surface water			Groundwater		
	Ra-226	**Ra-228**	**K-40**	**Ra-226**	**Ra-228**	**K-40**
Minimum	0.52 ± 0.2	3.92 ± 1.0	10.90 ± 3.1	0.05 ± 0.03	0.29 ± 0.04	1.09 ± 0.10
Maximum	1.31 ± 0.2	5.12 ± 0.9	16.50 ± 3.2	0.13 ± 0.04	0.41 ± 0.06	1.65 ± 0.09
Average	1.02 ± 0.2	4.53 ± 0.9	13.97 ± 3.2	0.10 ± 0.04	0.36 ± 0.05	1.41 ± 0.10
Median	1.14	4.56	13.98	0.12	0.36	1.41
Geomean	0.97	4.52	13.86	0.10	0.35	1.40
Standard deviation	0.27	0.31	1.73	0.03	0.03	0.18

(i) Surface water

Table 14 and Figure 48 present the activity concentrations and descriptive statistics of radionuclides in surface water samples collected from the study area. The average activity concentration of Ra-226, Ra-228 and K-40 collected from surface water samples were 1.02 ± 0.2 Bq/L, 4.53 ± 0.9 Bq/L and 13.97 ± 3.2 Bq/L, respectively. It was realized from the results that the activity concentrations of Ra-228 were higher than Ra-226 in all the measurements. The results were consistent with the radioactivity levels measured in soil and sediments in the same study area, where Th-232 concentrations were higher than the Ra-226 concentrations. The mean activity concentrations of Ra-226 and Ra-228 were above WHO recommended levels of 1.0 Bq/L and 0.1 Bq/L, respectively (WHO, 2008; 2011; Avwiri et al., 2013). Ra-226 and Ra-228 concentrations in samples differed narrowly, signifying similarities in their bearing rock sources and potential contamination during the mining of such rocks (Alvarado et al., 2014).

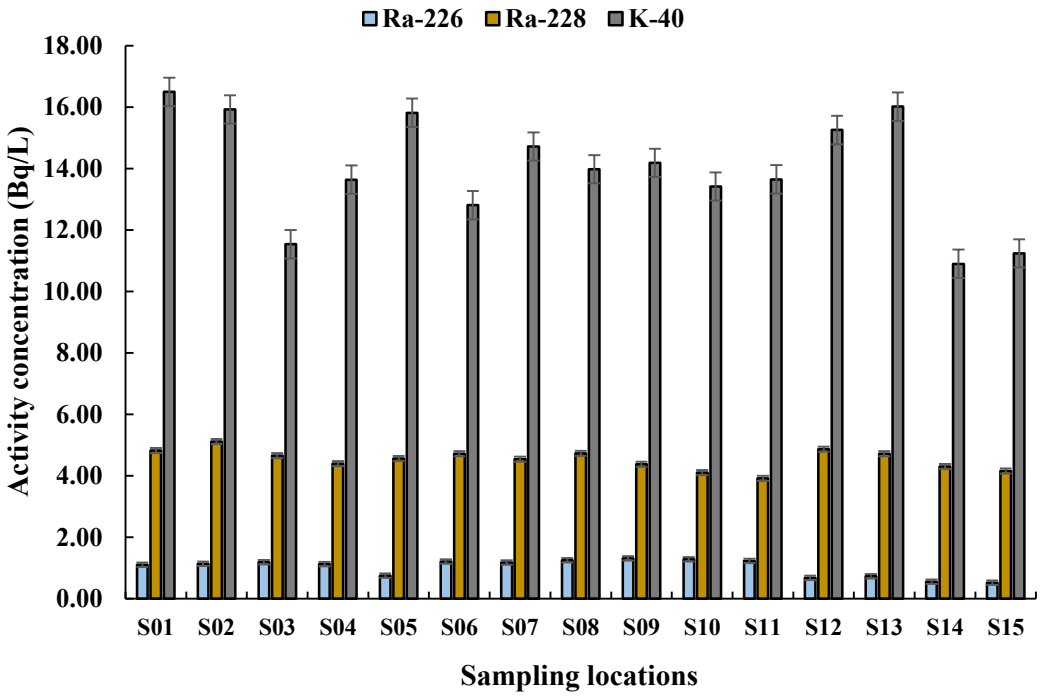

Figure 48. Activity concentrations measured in surface water samples (by author).

High radionuclide activities were recorded in mining sites and rivers and streams close to them. The highest Ra-228 concentration (S02) was observed at a gold ore washing area with its outlets into a river, and for Ra-226, the highest concentration (S09) was observed at a water source at a mining site. Low concentrations were observed in tailings from mining sites (S14 and S15). The records of radioactivity concentrations in surface water samples, especially in rivers and streams, could be attributed to the continuous artisanal mining in the study area. Mining operations, including the washing of ores in water bodies, and the washing down and leaching of radionuclides from mine tailings and wastes into water bodies, contribute to high radioactivity levels in water (Aliyu et al., 2015; Bello et al., 2020; Bansah et al., 2018; Avwiri et al., 2013). The continuous contamination of water resources within or close to mining sites has rendered such resources unfavorable for usage, especially when there is obvious contamination by the brownish colour of the surface water resources.

(ii) Groundwater

According to Table 14, the mean radioactivity levels determined in groundwater samples were 0.10 ± 0.04 Bq/L for Ra-226, 0.36 ± 0.05 Bq/L for Ra-228, and 1.41 ± 0.10 Bq/L for K-40. These concentrations are below the WHO and UNSCEAR guidelines for drinking water, except for Ra-228 (WHO, 2008; 2011; UNSCEAR, 2000). Similarly, activity concentrations of Ra-228 measured in the groundwater samples were higher than those of Ra-226. This confirms that the study area is enriched with thorium in its bedrocks and soils compared to uranium and radium. Therefore, high Ra-228 concentrations are due to the abundant Th-232 parent radionuclide in the aquifer rocks of the study area (Shabana & Kinsara, 2014). The differences in the activity concentrations of the Ra-226, Ra-228, and K-40 revealed that there are different sources of the radionuclides due to the different groundwater sources, depths, and the diverse transport mechanisms in their geological layers (Yehia et al., 2017). The concentrations of the measured radionuclides in groundwater samples are shown in Figure 49.

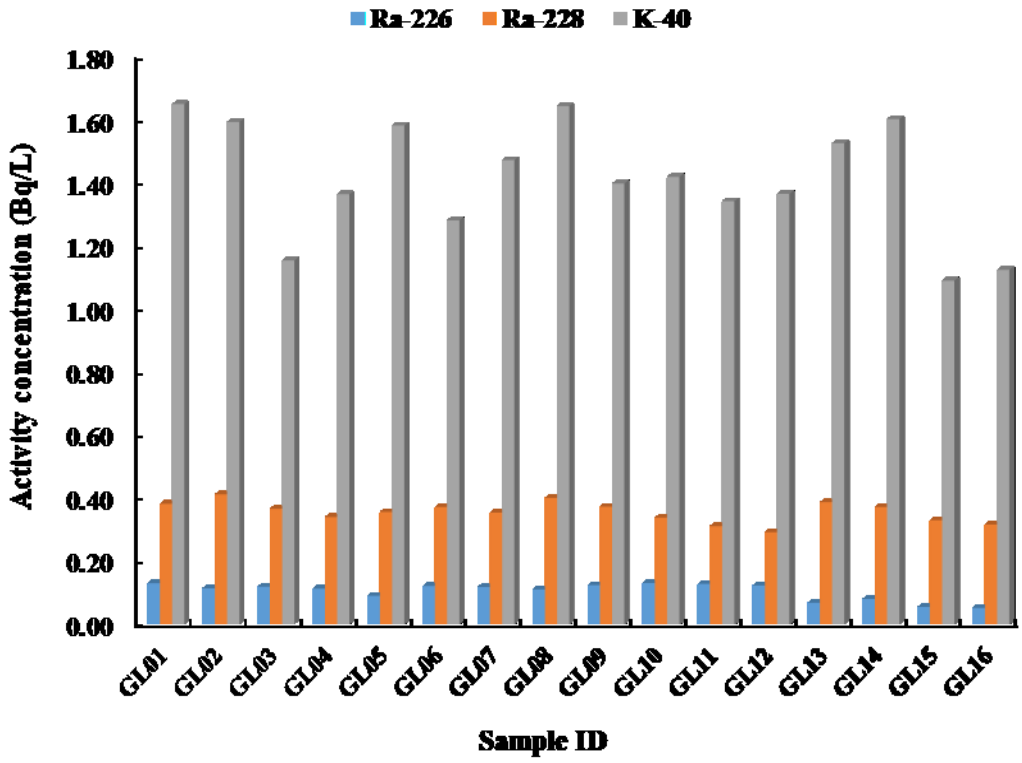

Figure 49. Activity concentrations measured in groundwater samples (by author).

The high Ra-228 levels measured in groundwater samples indicate that aquifer rocks have high concentrations of the radionuclide, as its concentration in groundwater is dependent on the minerals from which it was derived (Baeza et al., 2017; O¨rgu¨n et al., 2005). Again, Ra-228 levels are high because the radionuclide can diffuse out of sediments and aquifer rocks into the overlying waters (Hakam et al., 2001). Most sampling locations near mining sites recorded high Ra-226 and Ra-228 levels. This is as a result of the radionuclides leaching from mining sites into the bedrock while groundwater interacts with the geological formations of the area (Sherif & Sturchio, 2018; Alomari et al., 2020; Erőss et al., 2018; Zhong et al., 2020; Giri et al., 2011). The maximum and minimum Ra-226 concentrations were observed at GL10 and GL16, respectively, while for Ra-228, the maximum concentration was detected at GL02 and the lowest at GL12.

According to research, surface water and groundwater are not isolated components of the hydrologic system; instead, they interact in different climatic and physiographic landscapes, and the contamination or development of one primarily affects the other (Giri et al., 2011). Hence, the surface water pollution in the study region due to mining activities can be transferred to groundwater resources. Thus, in this study, both the surface water and groundwater are shown to be contaminated with radioactive elements. The existence of cracks within aquifers due to mining operations can increase the radionuclides leaching into groundwater resources as groundwater moves through the cracks containing radionuclides (Yidana et al., 2012; Giri et al., 2011).

4.7.2 Isotopic ratio of groundwater

In this study, isotopic ratios were computed to determine the origins and processes of the transportation of radium from aquifer rocks into groundwater. Radium isotope activities and their ratio (Ra-228/Ra-226) are often associated with the aquifer rocks' parent radionuclide abundances (Th-232, U-238). The relationship depends on the equilibrium state of the distinct parent-daughter pairs in the rocks, the time groundwater interacts with the rock, and the time of sampling water (Sherif & Sturchio, 2018). The estimated isotopic ratio ranged from 2.37 to 6.08, with an average of 3.70. The isotopic ratios exceeded the threshold of 1, signifying that high Ra-228 levels in water are of natural origin (Mathuthu et al., 2021; Kiro et al., 2015), and consequently, Ra-228 levels in aquifers underlying the groundwater of the

study region are high. The Volta Basin hydrogeological formation of Atiwa West is made up of aquifer rocks of primarily Precambrian to Paleozoic sandstones, shales, and conglomerates (Gordon et al., 2013; Gampson et al., 2017; Yidana et al., 2012; Gumma and Pavelic, 2012). According to Shabana and Kinsara (2014), Kiro et al. (2015), and Sherif and Sturchio (2018), sandstone aquifers showed isotopic ratios greater than 1 in groundwater samples, which is similar to the results obtained from groundwater from Atiwa West mining communities (Kiro et al., 2015; Sherif & Sturchio, 2018; Shabana & Kinsara, 2014).

4.7.3 Transfer factors of radionuclides in surface water

Radionuclides move through the environment by various routes, including the atmosphere and water resources, soil sub-compartment, and thereby contributing to human health risk (Asaduzzaman et al., 2014; Liu et al., 2021). The transfer of radionuclides from soil or sediment to water is an essential factor in evaluating internal radiation dose due to water consumption since there is a linear correlation between the two elements (Asaduzzaman et al., 2014). Transfer factors (TFs) of the ratio of radionuclide concentrations in water to that of soil/ sediment (using data from section 4.5.1) were determined for locations where soil and water were sampled. The determined TFs of Ra-226, Th-232/ Ra-228, and K-40 ranged between 0.02- 0.08, 0.10- 0.31, and 0.03- 0.11, respectively. The average TFs were 0.05 for Ra-226, 0.19 for Th-232/Ra-228, and 0.07 for K-40. The estimated TFs were high for mining sites, rivers, and streams. The TFs less than 1 show that radionuclide contamination in water is from an anthropogenic source, in this case, mining.

4.7.4 Estimation of committed effective dose (CED) and cancer risks

(i) Surface water

Radionuclides move from the respiratory tract to the gastrointestinal tract through ingestion and can be absorbed into the fluids of the human body from the small intestines. This necessitates the determination of radiation dose due to ingestion of radionuclides in water. The effective dose and cancer risk factors due to ingesting radionuclides in surface water from the study area are presented in Figure 50.

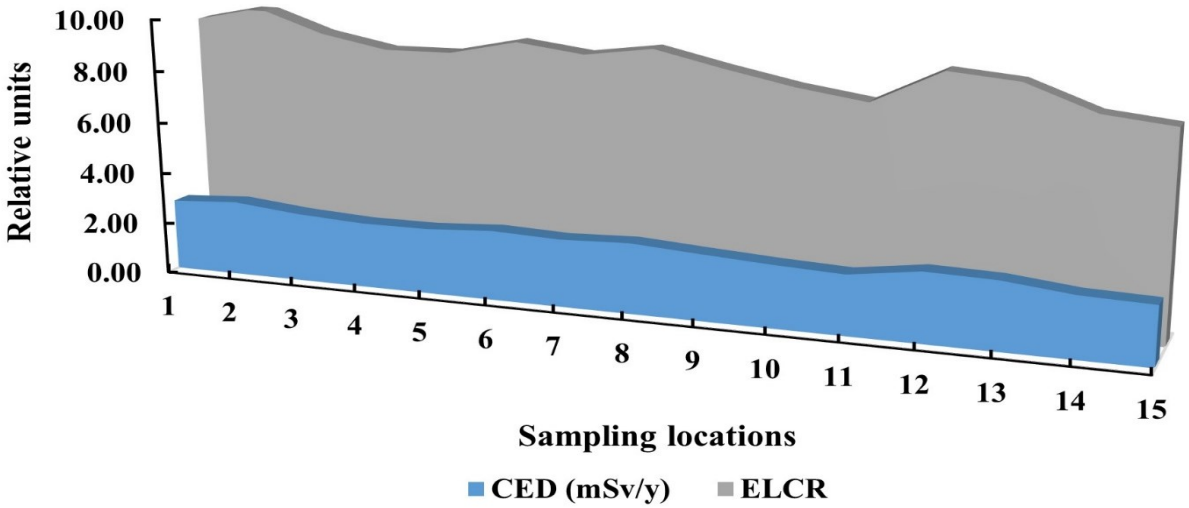

Figure 50. Committed Effective Dose (CED) and Excess Lifetime Cancer Risk (ELCR) (by author).

The evaluated CED varied between 2.25 mSv/y and 2.88 mSv/y, with an average CED of 2.55 mSv/y. The estimated effective doses were higher than the world reference values of 0.3 mSv/y given by UNSCEAR, and 0.1 mSv/y given by the WHO (UNSCEAR, 2000; WHO, 2008; ICRP, 1997). The ELCR factors were between 7.88×10^{-3} and 10.09×10^{-3}, with a mean of 8.94×10^{-3}, which is above the reference value of 0.29×10^{-3} (UNSCEAR, 2000). The maximum CED values (2.88 mSv/y and 2.73 mSv/y) and ELCR (10.09×10^{-3} and 9.55×10^{-3}) factors obtained for water samples from mining sites having direct washing outlets into a river, and thus the possibility of contaminating the river with radioactive elements from mining activities. Miners washing gold ores into rivers could account for the high CED and ELCR determined for such water resources. Also, farmers' dependence on such water resources and mine wastewater to irrigate their farms threatens human health. Hence, the likelihood of the populace developing cancer diseases in the long term is high.

(iii) Groundwater

Due to the obvious contamination of surface water resources by mining activities, residents of Atiwa West resort to groundwater as an alternative source of potable water. This is because surface water is the primary water source for treatment and supply to homes by the Ghana Water Company in the area. Inhabitants' reliance on groundwater makes it important to assess its quality for consumption and domestic use, as the presence of radionuclides in groundwater

is a significant component in determining groundwater quality (Sherif & Sturchio, 2018; Zhong et al., 2020). The estimation of the CED of groundwater was assessed based on the activity concentrations of Ra-226, Ra-228, and K-40 and their dose conversion factors. The CED was calculated for different age groups, namely infants (1-2 y), children (7-12 y), and adults (>17 y). Their annual consumption rates were also factored into the calculation (infants- 250 L, children- 350 L, adults- 730 L) (UNSCEAR, 2000).

The CED for infants varied between 0.46 and 0.63 mSv/y, with an average of 0.55 mSv/y. The children group had CED between 0.44 and 0.60 mSv/y and an average of 0.52 mSv/y, while the adult group had a range of 0.17 to 0.24 mSv/y and a mean of 0.21 mSv/y. The evaluated doses exceeded the WHO and ICRP reference levels of 0.1 mSv/y (WHO, 2008; ICRP, 1997). The CED estimated for the adult age group was less than the UNSCEAR reference level of 0.3 mSv/y for ingesting food and water, as shown in Figure 51. The high conversion factors of radionuclides for infants and children contributed to their high CED values. The ELCR factors were estimated for only the adult age group, and they were found to be between 0.89×10^{-3} and 1.22×10^{-3} with a mean of 1.06×10^{-3}. The ELCR factors were the upper bound reference level of 0.29×10^{-3} for the lifetime risk of stochastic effects. Since the CEDs were above 0.1 mSv/y, the ELCR was expected to be above its reference level. Therefore, the population, especially infants and children, is vulnerable to health implications, including cancers associated with the consumption of radionuclides in groundwater from the study area.

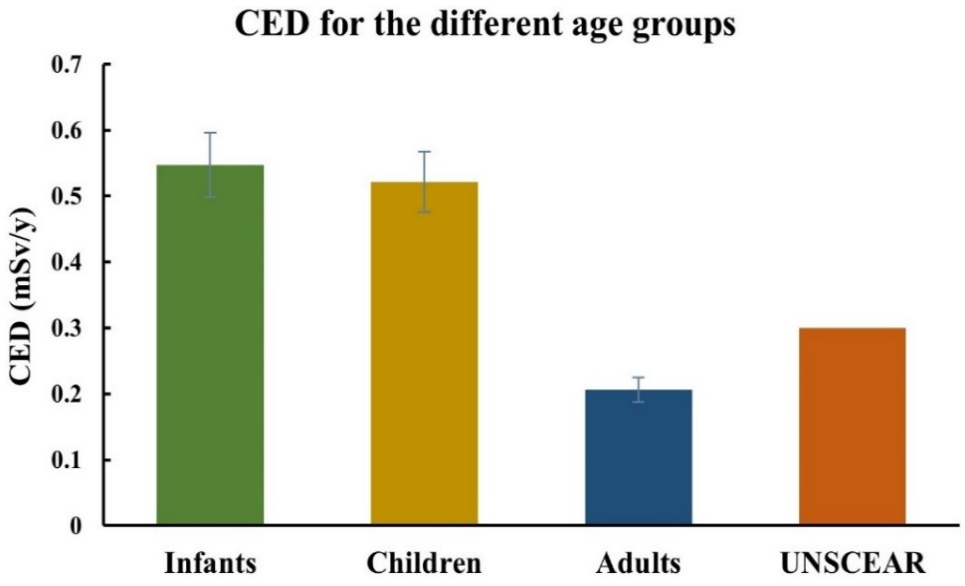

Figure 51. Comparison of CED for the different age groups (by author).

The consequential CED and ELCR from the radionuclide concentrations determined in water samples in the study could be attributed to several factors. Isotopic ratios revealed that aquifer rocks and soils underlying groundwater resources are composed of high concentrations of the thorium parent radionuclide. The indiscriminate and inexpert mining practices witnessed during the investigation aggravate the release of more radionuclides into water resources, causing pollution. This was evident by the evaluated transfer factors. Miners, the public, and neighboring environments, including surface and groundwater resources, are exposed to elevated radioactivity levels from mining activities and their subsequent radiation dose (Akuo-ko et al., 2024a; Mathuthu et al., 2021; Bello et al., 2019; Olise et al., 2016). The dependence of inhabitants, farmers, and animals on untreated water resources is detrimental to health. Therefore, determining the quality of water resources in terms of radioactivity levels, particularly in mining areas, is necessary to safeguard the health of adults, children, and infants.

CHAPTER FIVE

CONCLUSION AND RECOMMENDATIONS

5.1 Introduction

The radiological health risks posed by exposure to radiation were evaluated based on the radioactivity concentration of natural and anthropogenic radionuclides measured in the different environmental media. This chapter presents a general overview of the research's outcomes concerning the objectives outlined for this work. Thus, the chapter summarizes the findings, draws conclusions, and makes recommendations.

5.2 Summary of findings

The following is the summary of the findings realized in this research concerning the objectives set out for the study:

- Radioactivity concentrations measured in beach sediment along the entire coastline of Ghana were between 14 ± 4 and 134 ± 7 Bq/kg for Ra-226, 8 ± 1 and 77 ± 1 Bq/kg for Th-232, 207 ± 75 and 1273 ± 69 Bq/kg for K-40 and 1.1 ± 0.6 and 111.4 ± 0.3 Bq/kg for Cs-137. The average concentrations were 43 ± 6 Bq/kg, 22 ± 1 Bq/kg, 393 ± 74 Bq/kg, and 8.4 ± 0.5 Bq/kg for Ra-226, Th-232, K-40, and Cs-137, respectively. The assessed radiological parameters were below global averages except for AGDE. Spatial distribution maps revealed that the radionuclides Ra-226 and Th-232 occur in relative abundance along central and eastern coastlines compared to the western coast.
- Indoor radon measurements within residences of the Greater Accra region were found to range between 36.1 ± 2.7 and 92.0 ± 5.2 Bq/m^3, and the annual mean for the entire area was 50.8 ± 3.4 Bq/m^3. This corresponded to an annual effective dose of 0.9 and 2.3 mSv/y, with a mean of 1.3 mSv/y. The mean LCC estimated for the region was 23.1 people per million population.
- Po-210 activity levels measured in cigarettes on the Ghanaian market ranged between 16.4 ± 2.5 and 32.3 ± 5.2 mBq/cig, with a mean of 26.5 ± 4.2 mBq/cig. The committed annual effective doses due to inhalation of Po-210 in cigarette smoke were estimated to be between 0.041 mSv/y and 0.082 mSv/y, with a mean annual effective dose of

0.067 mSv/y for an adult Ghanaian smoker, which is lower than the reference values set by ICRP and UNSCEAR. The average ELCR was estimated as 0.234×10^{-3}, less than the world average of 1.16×10^{-3} for internal radiation exposure.

- Activity concentrations of radionuclides measured in soils from mining areas for radon exhalation studies ranged from 18.0 ± 1.2- 80.9 ± 1.4 Bq/kg (mean: 26.9 ± 1.7 Bq/kg) for Ra-226, 29.5 ± 2.8- 103.3 ± 5.2 Bq/kg (mean: 57.5 ± 3.6 Bq/kg) for Th-232, and 78.8 ± 17.1- 429.1 ± 23.4 Bq/kg (mean: 237.5 ± 17.6 Bq/kg) for K-40. Rn-222 concentrations 390.6 ± 38 to 907.5 ± 93 Bq/m^3 with an average value of 560.0 ± 54 Bq/m^3. The average mass and area exhalation rates were estimated to be $4.0 \pm 0.4 \times 10^{-5}$ Bq/kg/h and $1.2 \pm 0.11 \times 10^{-3}$ Bq/m^2/h, respectively. Some farming areas and undisturbed lands recorded high exhalation rates above the world average. Statistical analysis demonstrated a linear relation between Ra-226, Rn-222, and the exhalation rates.
- Radioactivity measurements determined in soils and sediment from Atiwa West district ranged from 12.9 ± 1.4- 29.1 ± 1.8 Bq/kg (mean: 22.1 ± 2.1 Bq/kg) for Ra-226, 10.8 ± 1.2- 44.0 ± 1.8 Bq/kg (mean: 27.5 ± 2.3 Bq/kg) for Th-232 and 40.0 ± 10- 429 ± 36 Bq/kg (mean: 198 ± 22 Bq/kg) for K-40. Activity concentrations of Th-232 were high in soils from mining sites and undisturbed lands. Ra-226 and Th-232 concentrations in soils from farms and undisturbed lands were high near mining sites. Sediment samples recorded lower Ra-226 and Th-232 levels than in soil samples.
- Activity concentrations of Ra-226, Ra-228 and K-40 in surface water samples were found to range between 0.52 ± 0.2 to 1.31 ± 0.2 Bq/L for Ra-226, 3.92 ± 1.0 to 5.12 ± 0.9 Bq/L for Ra-228 and 10.90 ± 3.1 to 16.50 ± 3.2 Bq/L for K-40. The average concentrations were 1.02 ± 0.2 Bq/L, 4.53 ± 0.9 Bq/L and 13.97 ± 3.2 Bq/L for Ra-226, Ra-228 and K-40, respectively. Activity concentration of Ra-228 in water samples is consistent with high Th-232 concentrations measured in soils and sediments from the study area. Thus, the study area is more abundant in thorium in soils and bedrocks than in radium. Estimated transfer factors indicated a possible radionuclide contamination of surface water resources from soil due to the mining activities in the study area.

- Radioactivity concentration in groundwater resources was determined to range from 0.05 ± 0.03- 0.13 ± 0.04 Bq/L, 0.29 ± 0.04- 0.41 ± 0.06 Bq/L, and 1.09 ± 0.10- 1.65 ± 0.09 Bq/L, respectively. The mean concentrations were below the world average values except for Ra-228, above 0.10 Bq/L. High Ra-228 levels in groundwater resources were attributed to the abundance of thorium in soils and aquifer rocks of the area. Groundwater resources near mining sites recorded high radioactivity concentrations, suggesting the likelihood of radionuclides leaching into groundwater.

5.3 Conclusions

The following conclusions were drawn from the study:

- Ra-226 concentrations measured in sediment samples along the Ghanaian coastline were higher than all the concentrations of Th-232.
- Th-232 and Ra-228 activity concentrations in soils, sediment, and water studied in mining areas were generally observed to be higher than Ra-226 concentrations in those samples.
- The different radionuclide distribution patterns and activity concentrations of Ra-226, Th-232, and K-40 in offshore and inland soils and sediment can be attributed to the various geological formations and characteristics in these parts of the country. Mineral deposits from weathering and erosion of igneous and metamorphic rocks are the main sources of high Ra-226 concentrations in beach sediments. Contrarily, the significantly high Th-232 in inland soil and water resources results from sedimentary rock formations. Though the low radiological values were estimated for beach sediment, signifying that they could be used as building materials, the relatively high AGDE values recorded at some locations suggest that such sediment may be used cautiously due to the radiation risk they pose to human health.
- Indoor radon levels measured in the greater Accra region were concluded to be due to soil composition, geology of the area, building materials used in construction, and the lifestyle of residents. Poor ventilation contributed to relatively high indoor radon levels, especially in densely populated areas. Indoor radon, which contributes to internal radiation exposure, accounts for 5% of lung cancer deaths each year. The IDW interpolation method appropriately predicted the indoor radon distribution for the study area.

- The Po-210 in cigarettes studied shows that cigarette smoking is accountable for approximately 3-6% of the total lung cancer deaths in Ghana. This study is considered a preliminary investigation of the effect of internal radiation exposure of natural radionuclides such as Po-210 in cigarette products consumed in Ghana, and as part of the investigation to determine the cause of lung cancer death cases in the country.
- The high radon exhalation rates observed in some sampling locations signify the possible radiological effects of using such soils as building materials. Though radiological risk evaluation showed parameters having values below world reference averages except for ELCR, there is a need to be cautious of the dangers posed by radioactivity in the environment.
- The mean activity concentrations of Ra-226, Th-232, and K-40 measured in soil and sediment samples from mining areas were observed to be less than the world average values. However, some individual locations had higher Th-232 and K-40 concentrations. All the evaluated radiological risk parameters were below world averages. Nevertheless, it was observed that a few sample locations recorded AGDE values higher than the recommended average. This suggests a possible radiological hazard posed by mining activities in the study area since mining is known to cause elevated radioactivity concentrations.
- The recorded mean Ra-226 and Ra-228 activity concentrations in surface water samples were above world reference values of 1.0 Bq/L and 0.1 Bq/L, respectively. The corresponding annual committed effective dose and lifetime cancer risks determined for the water samples were well above the recommended levels of 0.3 mSv/y and 0.29×10^{-3}, respectively. These indicate that the population is vulnerable to radiological dangers since miners wash gold ores directly in water bodies and sometimes direct the liquid wastes into the water bodies of the study area.
- Isotopic ratios evaluated in the study showed that aquifer rocks and soils beneath groundwater resources contained high concentrations of the thorium parent radionuclide. Thus, Ra-228 contributed a higher radiation dose than Ra-226 in the groundwater resources. The estimated annual committed effective doses compared to the recommended WHO and ICRP guidelines were above 0.1 mSv/y but lower than 0.3 mSv/y ingestion value for adults given by UNSCEAR. Consequently, the

inhabitants of the area, especially infants and children, are prone to health implications such as cancers related to the ingestion of radionuclides in groundwater from the investigated locations.

- In general, soils and sediments along coastal areas in Ghana are abundant in radium radionuclide, while soils and sediments in inland areas are abundant in the thorium radionuclide due to differences in the geological formations.

5.4 Recommendations

Based on the conclusions of this study, the following are recommended in view of the radionuclide distribution in the Ghanaian environment and its health implications:

- Continuous monitoring of radioactivity levels along the shorelines of Ghana is recommended, especially for the coastal area with high Cs-137 activity concentration. Such monitoring measurements should consider increasing the number of sampling locations in coastal areas, and more radionuclides must be measured. Other spectrometric techniques such as alpha beta spectrometry and liquid scintillation counters could be employed to measure the natural radionuclides in sediments along the coast.
- The most apparent remedy for areas with high indoor radon levels is to improve the ventilation of the residences, which will, in effect, allow radon gas to escape. Also, it is recommended that further indoor radon studies be carried out in other regions of Ghana, incorporating different measuring devices and procedures. Such investigations must also consider other aspects such as thoron levels, soil gas, soil permeability, soil and rock types, building materials used, faults, etc. This would aid in compiling a national radon map for the country and estimating concentrations and the number of radon-related lung cancer cases.
- Health risks associated with the radioactive substances in cigarettes and their consequential cancer implications, together with the societal and economic toll, call for reinforcement and sustained efforts in the regulation of cigarette consumption. Also, there is a need for public awareness of the detrimental effects of radioactive substances in cigarettes.

- Radon exhalation rates determined in soils from mining, farming, and undisturbed areas indicate that soils from Atiwa West mining areas pose less radiological risk. However, long-term exposure could result in cancers and respiratory diseases in cases of elevated concentrations. Therefore, in assessing and monitoring radioactivity levels and radiological risks in such areas, radon exhalation rates must also be considered to correctly evaluate the potential radiological risks of mining to miners and the public.
- Further investigations employing additional measurement techniques, such as Liquid Scintillation, to determine activity concentrations in soil and sediment and extending them to more areas would allow the appropriate regulatory agencies to implement measures to ensure that residents and miners are not exposed to the radionuclides beyond acceptable levels.
- Surface water resources within the study area must be continuously monitored and assessed for radionuclide contamination and health hazards to protect the population's well-being. Again, regulations are needed to protect water resources from being polluted with radionuclides by mining activities and to enforce strict adherence to such rules.
- The dependency of the populace on groundwater resources cannot be overlooked due to probable health problems in case of high radioactivity levels. Thus, determining the quality of groundwater resources in terms of radioactivity levels, especially in mining areas, is significant in protecting the health of inhabitants. Therefore, groundwater resources within the study area should be subjected to efficient treatment processes to remove radionuclides before consumption.

THESIS POINTS

I. Thesis

I investigated the use of natural materials as building materials as a means of exposure to ionizing radiation. I measured natural and artificial gamma emitting isotopes in soils and sediment in coastline and mining areas. Radioactivity concentrations measured in beach sediment along the entire coastline of Ghana were between 14 ± 4 and 134 ± 7 Bq/kg for Ra-226, 8 ± 1 and 77 ± 1 Bq/kg for Th-232, 207 ± 75 and 1273 ± 69 Bq/kg for K-40 and 1.1 ± 0.6 and 111.4 ± 0.3 Bq/kg for Cs-137. The average concentrations were 43 ± 6 Bq/kg, 22 ± 1 Bq/kg, 393 ± 74 Bq/kg, and 8.4 ± 0.5 Bq/kg for Ra-226, Th-232, K-40, and Cs-137, respectively.

Radioactivity measurements determined in soils and sediment from Atiwa West district (mining area) ranged from 12.9 ± 1.4- 29.1 ± 1.8 Bq/kg (mean: 22.1 ± 2.1 Bq/kg) for Ra-226, 10.8 ± 1.2- 44.0 ± 1.8 Bq/kg (mean: 27.5 ± 2.3 Bq/kg) for Th-232 and 40.0 ± 10- 429 ± 36 Bq/kg (mean: 198 ± 22 Bq/kg) for K-40. Although the low radiological values were estimated for studied materials, signifying that they could be used as building materials, the relatively high AGDE values recorded at some locations suggest that such sediment may be used cautiously due to the radiation risk they pose to human health.

II. Thesis

I investigated the lung cancer risk associated with indoor radon and Po-210 in cigarettes. The indoor radon measurements in the study area ranged between 36.1 ± 2.7 and 92.0 ± 5.2 Bq/m^3, with an estimated annual mean of 50.8 ± 3.4 Bq/m^3. All the measured dwellings recorded radon levels below the WHO reference level of 100 Bq/m^3. The annual effective doses were between 0.9 and 2.3 mSv/y, with a mean of 1.3 mSv/y. The average LCC evaluated for the region was 23.1 people per million population.

Po-210 activity concentrations measured in cigarettes ranged from 16.4 ± 2.5- 32.3 ± 5.2 mBq/cig (mean: 26.5 ± 4.2 mBq/cig). The committed annual effective doses due to inhalation of Po-210 in cigarette smoke were between 0.041 mSv/y and 0.082 mSv/y (mean: 0.067 mSv/y) which is below the reference values set by ICRP (0.1

mSv/y) and UNSCEAR (0.3 mSv/y). The average ELCR was estimated as 0.234×10^{-3}, below the world average of 1.16×10^{-3} for internal radiation exposure. This study is considered a preliminary investigation of the effect of internal radiation exposure of natural radionuclides such as Rn-222 levels in family houses and Po-210 in cigarette products consumed in Ghana.

III. Thesis

I studied the influence of mining activities on activity concentrations of radionuclides in water resources. The recorded activity concentrations of Ra-226 (0.52- 1.31 Bq/L; mean: 1.02 Bq/L) and Ra-228 (3.92- 5.12 Bq/L; mean: 4.53 Bq/L) in surface water samples were above world reference values of 1.0 Bq/L and 0.1 Bq/L, respectively. The resultant annual committed effective dose (2.25- 2.88 mSv/y; mean: 2.55 mSv/y) and lifetime cancer risks (7.88×10^{-3}- 10.09×10^{-3}; mean: 8.94×10^{-3}) determined for the water samples were above the recommended levels of 0.3 mSv/y and 0.29×10^{-3}, respectively. This means that the population is susceptible to radiological dangers due to miners washing gold ores directly in water bodies and sometimes direct the liquid wastes into the water bodies of the study area.

In the case of groundwater resources activity concentrations of Ra-226 (0.05- 0.13 Bq/L; mean: 0.10 Bq/L) was below the reference level as compared to Ra-228 (0.29- 0.41 Bq/L; mean: 0.36 Bq/L). The estimated mean effective doses for infants (0.55 mSv/y) and children (0.52 mSv/y) were above reference levels. Similarly, the ELCR factors were above 0.29×10^{-3}. The results showed that mining activities enhanced radionuclide concentrations in underground water.

LIST OF PUBLICATIONS INCLUDED

This thesis is based on the publications listed below, which are also referenced in the text by the names of the first authors:

1. Akuo-ko, E.O., Shahrokhi, A., Adelikhah, M., Amponsem, E., Samolej, K., Csordás, A., Kovács, T. (2025). Horizontal distribution of natural radionuclides and Cs-137 in sediment along Dixcove beach. Journal of Marine Science and Engineering, 13, 452. 10.3390/jmse13030452
2. Akuo-ko, E.O., Otoo, F., Glover, E.T., Amponsem, E., Tettey-Larbi, L., Csordás, A., Kovács, T., Shahrokhi, A. (2024a). A comprehensive radiological survey of groundwater resources in artisanal mining communities in the Eastern region of Ghana: water quality vs. mining activities. Water, 16, 62, 1-14. 10.3390/w16010062
3. Akuo-ko, E.O., Otoo, F., Glover, E.T., Amponsem, E., Shahrokhi, A., Csordás, A., Kovács, T. (2024b). Statistical assessment of natural radioactivity, radon activity, and associated radiological exposure due to artisanal mining in Atiwa West district of the Eastern region, Ghana. Heliyon, 10, e34705, 1-14. 10.1016/j.heliyon.2020.e34705
4. Akuo-ko, E. O., Adelikhah, M., Amponsem, E., Csordas, A. and Kovacs, T. (2023a). Radiological assessment in beach sediment of coastline, Ghana. Heliyon 9, 2023, 16690, 1-14. 10.1016/j.heliyon.2023.e16690
5. Akuo-ko, E.O., Adelikhah, M., Amponsem, E., Csordás, A., Kovács, T. (2023b). Investigations of indoor radon levels and its mapping in Greater Accra region, Ghana. Journal of Radioanalytical and Nuclear Chemistry, 333, 2975-2986. 10.1007/s10967-023-09165-z

REFERENCES

Abate, T. (2022). The activity concentrations of radionuclides Ra-226, Th-232 and K-40 of soil samples in the case of Metekel Zone, Ethiopia. EPJ Nuclear Science and Technology, 8(14), 1-7. 10.1051/epjn/2022011

Abate, T., Amtatie, D. (2020). Investigation of radium contents and radon exhalation rates in soil samples in Menge District, Ethiopia. Nuclear Science, 5(2), 16-21. 10.11648/j.ns.20200502.11

Abdel-Halim, A. A., Saleh, I.H. (2016). Radiological characterization of beach sediments along the Alexandria-Rosetta coasts of Egypt. Journal of Taibah University for Science 10, 212-220. 10.1016/j.jtusci.2015.02.016

Abdulkarim, M.S., Umar, S., Mohammed, A., Modelu, D. (2018). Determination of radionuclides in soil samples taken from Gura Topp (Jos) using sodium iodide thallium detector NaI(Ti). Nigerian Journal of Basic and Applied Science, 26(2), 30-34. 10.4314/njbas.v26i2.5

Abo-Elmagd, M. (2014). Radon exhalation rates corrected for leakage and back diffusion-Evaluation of radon chambers and radon sources with application to ceramic tile. Journal of Radiation Research and Applied Science, 7(7), 390-398. 10.1016/j.jrras.2014.07.001

Addo, M.A., Gbadago, J.K., Affum, H.A., Adom, T., Ahmed, K., Okley, G.M. (2008). Mineral profile of Ghanaian dried tobacco leaves and local snuff: A comparative study. Journal of Radioanalytical and Nuclear Chemistry, 277, 517-524. 10.1007/s10967-007-7054-x

Adelikhah, M., Imani, M., Hegedűs, M., Kovács, T. (2022). Modelling of indoor external and internal exposure due to different building materials containing NORMs in the vicinity of a HNBRA in Mahallat, Iran. Heliyon 8, 1-7. 10.1016/j.heliyon.2022.e08909

Adelikhah, M., Shahrokhi, A., Imani, M., Chalupnik, S., Kovács, T. (2021). Radiological assessment of indoor radon and thoron concentrations and indoor radon map of dwellings in Mashhad, Iran. International Journal of Environmental Research and Public Health, 18, 141. 10.3390/ijerph18010141

Ademola, A.K., Bello, A.K., Adejumobi, A.C. (2014). Determination of natural radioactivity and hazard in soil samples in and around gold mining area in Itagunmodi, south-western, Nigeria. Journal of Radiation Research and Applied Science, 7(3), 249-255. 10.1016/j.jrras.2014.06.001

Ademola, A.K., Obed, R.I. (2012). Gamma radioactivity levels and their corresponding external exposure of soil samples from tantalite mining areas in Oke-Ogun, South-Western Nigeria. Radioprotection, 47(2), 243-252. 10.1051/radiopro/2012003

Adukpo, O.K., Faanu, A., Lawluvi, H., Tettey-Larbi, L., Emi-Reynolds, G., Darko, E.O., Kansaana, C., Kpeglo, D.O., Awudu, A.R., Glover, E.T., Amoah, P.A., Efa, A.O., Agyemang, L.A., Agyeman, B.K., Kpordzro, R., Doe, A.I. (2015). Distribution and assessment of radionuclides in sediments, soil and water from the lower basin of river Pra in the Central and Western Regions of Ghana. Journal of Radioanalytical and Nuclear Chemistry, 303, 1679-1685. 10.1007/s10967-014-3637-5

Agbalagba, E.O., Avwiri, G.O., Chad-Umoreh, Y.E. (2012). g-Spectroscopy measurement of natural radioactivity and assessment of radiation hazard indices in soil samples from oil fields environment of Delta State, Nigeria. Journal of Environmental Radioactivity, 109, 64-70. 10.1016/j.jenvrad.2011.10.012

Alabi-Doku, B.N., Chen, S., Alhassan, E.H., Abdullateef, Y., Rahman, M.M. (2018). Fisheries resources of Ghana: Present status and future direction. International Journal of Fisheries and Aquatic Research, 3(4), 35-41.

Alazemi, N., Bajoga, A.D., Bradley, D.A., Regan, P.H., Shams, H. (2016). Soil radioactivity levels, radiological maps and risk assessment for the state of Kuwait. Chemosphere, 154, 55-62. 10.1016/j.chemosphere.2016.03.057

Al-Mur, B.A., Gad, A. (2022). Radiation hazard from natural radioactivity in the marine sediment of Jeddah coast, Red Sea, Saudi Arabia. Journal of Marine Science and Engineering, 2022, 10, 1145. 10.3390/jmse10081145

Alomari, A.H., Saleh, M.A., Hashima, S., Alsayaheen, A., Abdeldin, I., Abukashabeh, A. (2020). U-238 and Th-232 isotopes in groundwater of Jordan: Geological influence, water

chemistry, and health impact. Radiation Physics and Chemistry, 2020, 170, 108660. 10.1016/j.radphyschem.2019.108660

Alvarado, J.A.C., Balsiger, B., Rollin, S., Jakob, A., Burger, M. (2014). Radioactive and chemical contamination of the water resources in the former uranium mining and milling sites of Mailuu Suu (Kyrgyzstan). Journal of Environmental Radioactivity, 138, 1-10. 10.1016/j.jenvrad.2014.07.018

Akuo-ko, E.O., Shahrokhi, A., Adelikhah, M.; Amponsem, E., Samolej, K., Csordás, A., Kovács, T. (2025). Horizontal distribution of natural radionuclides and Cs-137 in sediment along Dixcove beach. Journal of Marine Science and Engineering, 13, 452. https://doi.org/10.3390/jmse13030452

Akuo-ko, E.O., Otoo, F., Glover, E.T., Amponsem, E., Tettey-Larbi, L., Csordás, A., Kovács, T., Shahrokhi, A. (2024a). A comprehensive radiological survey of groundwater resources in artisanal mining communities in the Eastern region of Ghana: water quality vs. mining activities. Water, 16, 62, 1-14. 10.3390/w16010062

Akuo-ko, E.O., Otoo, F., Glover, E.T., Amponsem, E., Shahrokhi, A., Csordás, A., Kovács, T. (2024b). Statistical assessment of natural radioactivity, radon activity, and associated radiological exposure due to artisanal mining in Atiwa West district of the Eastern region, Ghana. Heliyon, 10, e34705, 1-14. 10.1016/j.heliyon.2020.e34705

Akuo-ko, E. O., Adelikhah, M., Amponsem, E., Csordas, A. and Kovacs, T. (2023a). Radiological assessment in beach sediment of coastline, Ghana. Heliyon 9, 2023, 16690, 1-14. 10.1016/j.heliyon.2023.e16690

Akuo-ko, E.O., Adelikhah, M., Amponsem, E., Csordás, A., Kovács, T. (2023b). Investigations of indoor radon levels and its mapping in Greater Accra region, Ghana. Journal of Radioanalytical and Nuclear Chemistry, 333, 2975-2986. 10.1007/s10967-023-09165-z

Akpanowo, M.A., Umaru, I., Iyakwari, S. (2019). Assessment of radiological risk from the soils of artisanal mining areas of Anka, North-West Nigeria. African Journal of Environmental Science and Technololgy, 13(8), 303-309. 10.5897/AJEST2019.2691

Akweetelela, A., Kgabi, N., Zivuku, M., Mashauri, D. (2020). Environmental radioactivity of groundwater and sediments in the Kuiseb and Okavango-Omatako basins in Namibia. Physics, Chemistry and Earth, 120, 102911, 1-7. 10.1016/j.pce.2020.102911

Alamy, (2024). https://www.alamy.com/stock-photo-illustration-showing-the-wide-range-of-adverse-health-effects-that-103991834.html. Retrieved on June 28, 2024.

Alazemi, N., Bajoga, A.D., Bradley, D.A, Regan, P.H., Shams, H. (2016). Soil radioactivity levels, radiological maps and risk assessment for the state of Kuwait. Chemosphere, 154, 55-62. 10.1016/j.chemosphere.2016.03.057.

Aliyu, A.S., Ibrahim, U., Akpa, C.T., Garba, N.N., Ramli, A.T. (2015). Health and ecological hazards due to natural radioactivity in soil from mining areas of Nasarawa State, Nigeria, Isotopes in Environment and Health Studies, 51(3), 448-468. 10.1080/10256016.2015.1026339

Alomari, A.H., Saleh, M.A., Hashima, S., Alsayaheen, A., Abdeldin, I., Abukashabeh, A. (2020). U-238 and Th-232 isotopes in groundwater of Jordan: Geological influence, water chemistry, and health impact. Radiation Physics and Chemistry, 2020, 170, 108660. 10.1016/j.radphyschem.2019.108660

Amekudzie, A., Emi-Reynolds, G., Faanu, A., Darko, E.O., Awudu, A. R., Adukpo, O., Quaye, L.A.N., Kpordzro, R., Agyemang, B., Ibrahim, B. (2011). Natural radioactivity concentrations and dose assessment in shore sediments along the coast of Greater Accra, Ghana. World Applied Sciences Journal, 13(11), 2338-2343.

Amponsah, A., Nasare, L.I., Tom-Dery, D., Baatuuwie, B.N. (2022). Land cover changes of Atiwa Range Forest Reserve, a biodiversity hotspot in Ghana. Trees, Forests and People, 9, 100301, ISSN 2666-7193. 10.1016/j.tfp.2022.100301

Anyimah-Ackah, E., Ofosu, I.W., Lutterodt, H.E., Darko, G., Kpeglo, D.O. (2021). Excess lifetime cancer risk and committed effective dose associated with dietary exposure to radioactivity of natural origin from mining areas. Journal of Consumer Protection Food Safety, 16(3), 219-225. 10.1007/s00003-021-01332

Arafat, A.A., Salama, M.H.M, El-Sayed, S.A., Elfeel, A.A. (2017). Distribution of natural radionuclides and assessment of the associated hazards in the environment of Marsa Alam-Shalateen area, Red Sea coast, Egypt. Journal of Radiation Research and Applied Science, 10(3), 219-232. 10.1016/j.jrras.2016.11.006

Asaduzzaman, Kh., Khandaker, M.U., Amin, Y.M., Bradley, D.A., Mahat, R.H., Nor, R. M. (2014). Soil-to-root vegetable transfer factors for Ra-226, Th-232, K-40, and Y-88 in Malaysia. Journal of Environmental Radioactivity, 135, 120-127. 10.1016/j.jenvrad.2014.04.009

Atibu, E.K., Arpagaus, P., Mulaji, C.K., Mpiana, P.T., Poté, J., Loizeau, J.-L., Carvalho, F.P. (2022). High environmental radioactivity in artisanal and small-scale gold mining in Eastern Democratic Republic of the Congo. Minerals, 12, 1278. 10.3390/min12101278

Avwiri, G.O., Osimobi, J.C., Agbalagba, E.O. (2013). Evaluation of natural occurring radionuclide variation with lithology depth profile of Udi and Ezeagu local government areas of Enugu State, Nigeria. International Journal of Engineering and Applied Science, 4(3) 1-10.

Baeza, A., Salas, A., Guillen, J., Munoz-Serrano, A., Ontalba-Salamanca, M.A., Jimenez-Ramos, M.C. (2017). Removal of naturally occurring radionuclides from drinking water using a filter specifically designed for Drinking Water Treatment Plants. Chemosphere, 167, 107-113. 10.1016/j.chemosphere.2016.09.148

Bala, P., Kumar, V., Mehra, R. (2017). Measurement of radon exhalation rate in various building materials and soil samples. Journal of Earth Systems and Science, 126(2), 1-8. 10.1007/s12040-017-0797-z.

Baltrenas, P., Grubliauskas, R., Danila, V. (2020). Seasonal variation of indoor radon concentration levels in different premises of a university building. Sustainability 12, 6174. 10.3390/su12156174

Bakar, A.S.A., Hamzah, Z., Saat, A. (2017). Distribution of 137Cs in surface soil of Fraser's Hill, Pahang, Malaysia. AIP Conference Proceeding, 1799, 030010. 10.1063/1.4972920.

Bansah, K.J., Dumakor-Dupey, N.K., Kansake, B.A., Assan, E., Bekui, P. (2018). Socioeconomic and environmental assessment of informal artisanal and small-scale mining in Ghana. Journal of Cleaner Production, 202, 465-475. 10.1016/j.jclepro.2018.08.150

Barba-Lobo, A., Gázquez, M.J., Bolívar, J.P. (2022). A practical procedure to determine natural radionuclides in solid materials from mining. Minerals, 12(5), 611. 10.3390/min12050611

Bello, S., Nasiru, R., Garba, N.N., Adeyemo, D. J. (2020). Annual effective dose associated with radon, gross alpha and gross beta radioactivity in drinking water from gold mining areas of Shanono and Bagwai, Kano state, Nigeria. Microchemical Journal, 154(104551), 1-7. 10.1016/j.microc.2019.104551

Bello, S., Nasiru, R., Garba, N. N., Adeyemo, D. J. (2019). Evaluation of the activity concentration of K-40, Ra-226 and Th-232 in soil and associated radiological parameters of Shanono and Bagwai artisanal gold mining areas, Kano State, Nigeria. Applied Science and Environmental Management, 23(9), 1655-1659. 10.4314/jasem.v23i9.8

Beogo, C.E., Cisse, O.I., Zougmore, F. (2022). Assessment of radiological hazards from soil samples in the Northeastern area of Burkina Faso. SN Applied Science, 4(73), 1-10. 10.1007/s42452-022-04960-x

Boryło, A., Skwarzec, B., Czyk, G.R., Siebert, J. (2013). Polonium Po-210 activities in human blood of patients with ischaemic heart disease from Gdan´Sk in Poland. Journal of Radioanalytical and Nuclear Chemistry, 298, 1685-1691. 10.1007/S10967-013-2670-0

Botwe, B.O., Schirone, A., Delbono, I., Barsanti, M., Delfanti, R., Kelderman, P., Nyarko, E., Lens, P.N.L. (2017). Radioactivity concentrations and their radiological significance in sediments of the Tema Harbour, Greater Accra, Ghana. Journal of Radiation Research and Applied Science, 10, 63-71. 10.1016/j.jrras.2016.12.002

Boujelbane, F., Samaali, M., Rahali, S., Dridi, W., Abdelli, W., Oueslati, M., Takriti, S. (2020). The activities of Po-210 and Pb-210 in cigarette smoked in Tunisia. Radiation, Environment and Biophysics, 1-6. 10.1007/S00411-020-00853-Y

Boumala, D., Belafrites, A., Tedjani, A., Mavon, Ch., Groetz, J.-E. (2019). Annual effective dose and excess life time cancer risk assessment from tobacco plants. Perspective Science, 12, 1-4. 10.1016/j.pisc.2019.100394

Chandrasekaran, A., Rajalakshmi, A., Ravisankar, R., Vijayagopal, P., Venkatraman, B. (2015). Measurements of natural gamma radiations and effects of physico-chemical properties in soils of Yelagiri hills, Tamilnadu India with statistical approach. Procedia Earth Planetary Science, 11, 531-538. 10.1016/j.proeps.2015.06.055

Chaparro, M.A.E., Suresh, G., Ramasamy, V., Sundarrajan, M. (2017). Magnetic assessment and pollution status of beach sediments from Kerala coast (southwestern India). Marine Pollution Bulletin 117, 171-177. 10.1016/j.marpolbul.2017.01.044

Chen, F.-W., Liu, C.-W. (2012). Estimation of the spatial rainfall distribution using inverse distance weighting (IDW) in the middle of Taiwan. Paddy Water Environment, 10, 209-222. 10.1007/s10333-012-0319-1

Coletti, C., Ciotoli, G., Benà, E., Brattich, E., Cinelli, G., Galgaro, A., Massironi, M., Mazzoli, C., Mostacci, D., Mozzi, P., Ruggiero, L., Sciarra, A., Tositti, L., Sassi, R. (2021). The Empirical Bayesian Regression Kriging (EBRK) to map the Geogenic Radon Potential (GRP). A case of study from the Euganean Hills (Italy). EGU General Assembly 2021, online, 19-30 Apr 2021, EGU21-10304. Accessed 04 May 2022. 10.5194/egusphere-egu21-10304

Coletti, C., Brattich, E., Cinelli, G., Cultrone, G., Maritan, L., Mazzoli, C., Mostacci, D., Tositti, L., Sassi, R. (2020). Radionuclide concentration and radon exhalation in new mix design of bricks produced reusing NORM by-products: The influence of mineralogy and texture, Construction and Building Materials, 260, 119820. 10.1016/j.conbuildmat.2020.119820.

Cosma, C., Szacsvai, K., Dinu, A., Ciorba, D., Dicu, T., Suciu, L. (2009). Preliminary integrated indoor radon measurements in Transylvania (Romania). Isotopes Environment Health Studies, 45, 259-268. 10.1080/10256010902871895

Csondor, K., Bajak, P., Surbeck, H., Izsak, B., Horvath, A., Vargha, M., Eross, A. (2020). Transient nature of riverbank filtered drinking water supply systems - A new challenge of

natural radioactivity assessment. Journal of Environmental Radioactivity, 211, 106072. 10.1016/j.jenvrad.2019.106072

Csordás, A., Szabó, K.Z., Sas, Z., Kocsis, E., Kovács, T. (2021). Indoor radon levels in Hungarian kindergartens. Journal of Radioanalytical and Nuclear Chemistry, 328, 1375-1382. 10.1007/s10967-020-07501-1

Csordás, A., Tóth-Bodrogi, E., Kovács, T. (2020). Configuration of the parameters for scanner-based track detector evaluation system. Nukleonika, 65, 133-137. 10.2478/nuka-2020-0021

Csordás, A., Fábián, F., Shahrokhi, A., Somlai, J., Kovács, T. (2014). Calibration of CR-39-based thoron progeny device. Radiation Protection Dosimetry, 160, 169-172. 10.1093/rpd/ncu072

Cuculovic, A., Stanojković, J., Nedić, O., Popović-Djordjević, J. (2024). Radioactivity and food safety in Serbia: Chernobyl accident and 4 decades later. Food Safety and Health. 2, 410-413. 10.1002/fsh3.12058

Daily Guide Network. (2021). https://dailyguidenetwork.com/beaches-bounce-back-as-revelers-troop-to-mark-new-year/. Retrieved on November 20, 2024.

Desideri, D., Assunta, M., Feduzi, M.L., Roselli, C. (2007). Po-210 and Pb-210 inhalation by cigarette smoking in Italy. Health Physics, 92, 58-63. 10.1097/01.HP.0000236597.72973.3c

Doku, D., Raisamo, S., Wiium, N. (2012). The role of tobacco promoting and restraining factors in smoking intentions among Ghanaian youth. Public Health, 12, 1-10. http://www.biomedcentral.com/1471-2458/12/662

Doyi, I., Oppon, O.C., Glover, E.T., Gbeddy, G., Kokroko, W. (2013). Assessment of occupational radiation exposure in underground artisanal gold mines in Tongo, Upper East Region of Ghana. Journal Environmental Radioactivity, 126, 77-82. 10.1016/j.jenvrad.2013.07.0007

Dina, N.T., Das, S.C., Kabir, M.Z., Rasul, Md.G., Deeba, F., Rajib, M., Islam, Md.S., Hayder, Md.A., Ali, Md.I. (2022). Natural radioactivity and its radiological implications from soils

and rocks in Jaintiapur area, North-east Bangladesh. Journal of Radioanalytical and Nuclear Chemistry, 331, 4457-4468. 10.1007/s10967-022-08562-0.

Dizman, S., Gorür, F.K., Keser, R., Gorür, O. (2019). The assessment of radioactivity and radiological hazards in soils of Bolu province, Turkey. Environment Forensics, 20(3), 211-218. 10.1080/15275922.2019.1629129.

Erőss, A., Csondor, K., Izsák, B., Vargha, M., Horváth, A, Pándics, T. (2018). Uranium in groundwater- The importance of hydraulic regime and groundwater flow system's understanding. Journal of Environmental Radioactivity, 195, 90-96. 10.1016/j.jenvrad.2018.10.002

European Euratom Council Directive 2013/59/Euratom Directives. (2013) Official Journal of the European Union, 1-73.

Faanu, A., Tettey-Larbi, L., Akuo-ko, E.O., Gyekye, P.K., Kpeglo, D.O., Lawluvi, H., Kansaana, C., Adjei-Kyereme, S., Efa, A.O., Toth-Bodrogi, E., Kov´acs, T., Shahrokhi, A. (2024). Radiological landscape of natural resources and mining: Unveiling the environmental impact of naturally occurring radioactive materials in Ghana's mining areas. Heliyon, 10, e24959, 1-19. 10.1016/j.heliyon.2024.e24959

Faanu, A., Adukpo, O.K., Tettey-Larbi, L., Lawluvi, H., Kpeglo, D.O., Darko, E.O., Emi-Reynolds, Awudu, G., R.A., Kansaana, C.P., Amoah, A., Efa, A.O., Ibrahim, A.D., Agyeman, B., Kpodzro, R., Agyeman, L. (2016). Natural radioactivity levels in soils, rocks, and water at a mining concession of Perseus gold mine and surrounding towns in Central Region of Ghana. SpringerPlus 5, 98. 10.1186/s40064-016-1716-5

Faanu, A., Lawluvi, H., Kpeglo, D.O., Darko, E.O., Emi-Reynolds, G., Awudu, A.R., Adukpo, O.K., Kansaana, C., Ali, I.D., Agyeman, B., Agyeman, L., Kpodzro, R. (2014). Assessment of natural and anthropogenic radioactivity levels in soils, rocks and water in the vicinity of Chirano Gold Mine in Ghana. Radiation Protection Dosimetry, 158(1) 87-99. 10.1093/rpd/nct197

Faanu, A., Kpeglo, D.O., Sackey, M., Darko, E.O., Emi-Reynolds, G., Lawluvi, H., Awudu, R., Adukpo, O.K., Kansaana, C., Ali, I.D., Agyeman, B., Agyeman, L., Kpodzro, R. (2013).

Natural and artificial radioactivity distribution in soil, rock and water of the Central Ashanti Gold Mine, Ghana. Environmental Earth Science, 70, 1593-1604. 10.1007/s12665-013-2244-z

Faanu, A., Darko, E.O., Ephraim, J.H. (2011). Determination of natural radioactivity and hazard in soil and rock samples in a mining area in Ghana. West African Journal Applied Ecology, 19, 79-92.

Faheem, M., Matiullah, M. (2008). Radon exhalation and its dependence on moisture content from samples of soil and building materials. Radiation Measurement, 43(8), 1458-1462. 10.1016/j.radmeas.2008.02.023

FAO/IAEA. (2017). Use of Cs-137 for soil erosion assessment. Fulajtar, E., Mabit, L., Renschler, C.S., Lee Zhi Yi, A., Food and Agriculture Organization of the United Nations, Rome, Italy. 1-64.

Fang, S.-C. (2019). Study on C-14 dating analysis of deep groundwater resources on islands. Journal of Environmental Radioactivity, 208-209, 105994. 10.1016/j.jenvrad.2019.105994

Focus, E., Rwiza, M.J., Mohammed, N.K., Banzi, F.P. (2021). The influence of gold mining on radioactivity of mining sites soil in Tanzania. EQA- International Journal of Environmental Quality, 46, 46-59. 10.6092/issn.2281-4485/13288

Fresh Water Systems, (2021). https://www.freshwatersystems.com/blogs/blog/what-is-groundwater-contamination-and-how-do-you-treat-it. Retrieved on June 10, 2023.

Frutos-Puerto, S., Pinilla-Gil, E., Andrade, E., Reis, M., Madruga, M.J., Rodriguez, C.M. (2020). Radon and thoron exhalation rate, emanation factor and radioactivity risks of building materials of Iberian Peninsula. PeerJ, 8, e10331. 10.7717/peerj.10331.

Galhardi, J.A., García-Tenorio, R., Bonotto, D.M., Frances, I.D. & Motta, J.G. (2017). Natural radionuclides in plants, soils and sediments affected by U-rich coal mining activities in Brazil. Journal of Environmental Radioactivity, 177, 37-47. 10.1016/j.jenvrad.2017.06.001

Gampson, E.K., Nartey, V.K., Golow, A.A., Akiti, T.T., Sarfo, M.A., Salifu, M., Aidoo, F., Fuseini, A.R. (2017). Physical and isotopic characteristics in peri-urban landscapes: a case study at the lower Volta River Basin, Ghana. Applied Water Science, 7, 729-744. 10.1007/s13201-0.15-0286-y

Gezera, F., Turhan, S., Kurnaz, A., Ufuktepe, Y. (2019). Radiometric characterization of zeolite minerals used in many industries and assessment of radiological risks. Applied Radiation Isotopes, 152, 57-63. 10.1016/j.apradiso.2019.06.036.

Ghanbar-Moghaddam, B., Fathivand, A. (2020). Study of Polonium-210 in Persian cigarette and tobacco crops. Radiation Protection Dosimetry, 119, 335-340. 10.1093/Rpd/Ncaa130

Giri, S., Jha, V.N., Singh, G., Tripathi, R.M. (2013). Estimation of annual effective dose due to ingestion of natural radionuclides in foodstuff s and water at a proposed uranium mining site in India. International Journal of Radiation Biology, 89(12), 1071-1078. 10.3109/09553002.2013.817707

Giri, S., Singh, G., Jha, V.N. (2011). Evaluation of radionuclides in groundwater around proposed uranium mining sites in Bagjata and Banduhurang, Jharkhand (India). Radiation protection, 46(1), 39-57. 10.1051/radiopro/2010056

Global Cancer Observatory. (2021). Ghana. World Health Organization. International Agency for Research on Cancer. Accessed on 17 March 2022. https://gco.iarc.fr/today

Gordon, C., Nukpezah, D., Tweneboah-Lawson, E., Ofori, B.D., Yirenya-Tawiah, D., Pabi, O., Ayivor, J.S., Koranteng, S., Darko, D., Mensah, A.M. (2013). West Africa – Water resources vulnerability using a multidimensional approach: Case study of Volta Basin. Climate vulnerability: Understanding and addressing threats to essential resources. Elsevier Inc., Academic Press, 283-309.

Gulan, L., Stajic, J.M., Bochicchio, F., Carpentieri, C., Milic, G., Nikezic, D., Zunic, Z.S. (2017). Is high indoor radon concentration correlated with specific activity of radium in nearby soil? A study in Kosovo and Metohija. Environmental Science and Pollution Research, 24, 19561-19568. 10.1007/s11356-017-9538-8

Gusain, G.S., Prasad, G., Prasad, Y., Ramola, R.C. (2009). Comparison of indoor radon level with radon exhalation rate from soil in Garhwal Himalaya. Radiation Measurement, 44(9-10), 1032-1035. 10.1016/j.radmeas.2009.10.033

Hakam, O.K., Choukri, A., Reyss, J.L., Lferde, M. (2001). Determination and comparison of uranium and radium isotopes activities and activity ratios in samples from some natural water sources in Morocco. Journal of Environmental Radioactivity, 57, 175-189.

Hamideen, M.S., Sharaf, J. (2012). Natural radioactivity investigations in soil samples obtained from phosphate hills in the Russaifa region, Jordan. Radiation Physics and Chemistry, 81, 1559-1562. 10.1016/j.radphyschem.2012.03.023

Horvath, M., Shahrokhi, A., Bator, P., Toth-Bodrogi, E., Kovacs, T. (2017). Determination of Po-210 content in cigarette smoke using a smoking machine: a case study of Iranian cigarettes. Journal of Environmental Radioactivity, 174, 66-70. 10.1016/j.jenvrad.2017.01.023

Huang, Y., Lu, X., Ding, X., Feng, T. (2015). Natural radioactivity level in beach sand along the coast of Xiamen Island, China. Marine Pollution Bulletin, 91, 357-361. 10.1016/j.marpolbul.2014.11.046

Hub Pages. (2017). https://discover.hubpages.com/health/The-Radioactive-Polonium-In-Cigarettes-Smoke. Retrieved on July 24, 2024.

IAEA. (2019). Design and conduct of indoor radon surveys. IAEA safety reports series; ISSN 1020–6450, no. 98. Classification: UDC 546.29:303.6 | STI/PUB/1848: 1-128.

IAEA. (1996). International basic safety standards for protection against ionizing radiation and safety of radiation sources. International Atomic Energy Agency, safety series 115.

ICRP. (2012). Compendium of dose coefficients based on ICRP 60. ICRP Publication 119 Ann 41.

ICRP. (2010). Lung Cancer Risk from radon and Progeny and Statement on Radon; Annals of the ICRP: New York, NY, USA.

ICRP. (2007). The 2007 recommendation of the International Commission on Radiological Protection. ICRP Publication 103, Oxford.

ICRP. (1997). Protection from potential exposures- Application to selected radiation sources. ICRP, 76, Ann ICRP 27(2).

ICRP. (1993). Protection against Radon-222 at home and works. ICRP, Publication.

ICRP. (1990). Recommendations of the International Commission on Radiological Protection. Volume 21.

Idriss, H., Salih, I., Alaamer, A.S., AL-Rajhi, M.A., Osman, A., Adreani, T.A., Abdelgalil, M.Y., Ali, N.Y. (2018). Health risk profile for terrestrial radionuclides in soil around artisanal gold mining area at Alsopag, Sudan. Acta Geophysica, 66(20), 673-681. 10.1007/s11600-018-0166-6. 2018

Idriss, H., Salih, I., Alaamer, A.S., Saleh, A., Abdelgali, M.Y. (2016). Environmental-impact assessment of natural radioactivity around a traditional mining area in Al-Ibedia, Sudan. Archives of Environmental Contamination and Toxicology, 70, 783-792. 10.1007/s00244-016-0271-y

Imani, M., Adelikhah, M., Shahrokhi, A., Azimpour, G., Yadollahi, A., Kocsis, E., Kovács, T. (2021). Natural radioactivity and radiological risks of common building materials used in Semnan Province dwellings, Iran. Environmental Science and Pollution Research, 28, 41492-41503. 10.1007/s11356-021-13469-6

Inayatullah, S.S., Madihah, B.M. (2016). Detection of natural radioactive materials in the soil of bauxite mining areas of Kuantan, Pahang, Malaysia. International Journal of Mathematics and Physical Sciences Research, 4(1), 74-76.

Innocent, A.J., Onimisi, M. Y., Jonah, S.A. (2013). Evaluation of naturally occurring radionuclide materials in soil samples collected from some mining sites in Zamfara State, Nigeria. British Journal of Applied Science and Technology, 3(4), 684-692. 10.9734/BJAST/2013/3244

IUCN. (2020). Atewa fate back in the public domain. Flowing water or bauxite breakdown? IUCN, 1-12.

Isinkaye, M.O., Emelue, H.U. (2015). Natural radioactivity measurements and evaluation of radiological hazards in sediment of Oguta Lake, South-East Nigeria. Journal of Radiation Research and Applied Sciences 8, 459-469. 10.1016/j.jrras.2015.05.001

Iwaoka, K., Enriquez, EB., Yajima, K., Hosoda, M., Tokonami, S., Yonehara, H., Garcia, T.Y., Kanda, R. (2019). Po-210 as a source of natural radioactivity in cigarettes distributed in the Philippines. Perspective Science, 12, 1-4. 10.1016/j.pisc.2019.100400

Jagercikova, M., Cornu, S., Le Bas, C., Evrard, O. (2015). Vertical Distributions of Cs-137 in Soils: A Meta-Analysis. Journal of Soils and Sediments, 15, 81-95. 10.1007/s11368-014-0982-5.

Jha, S.K., Patra, A.C., Verma, G.P., Iyer, I.S., Aswal, D.K. (2024). Natural radiation and environment. In: Aswal, D.K. (eds) Handbook on Radiation Environment, Volume 1. Springer, Singapore. 10.1007/978-981-97-2795-7_2

Joel, E.S., Maxwell, O., Adewoyin, O.O., Olawole, O.C., Arijaje, T.E., Embong, Z., Saeed, M.A. (2019). Investigation of natural environmental radioactivity concentration in soil of coastaline area of Ado-Odo/Ota Nigeria and its radiological implications. Scientific Reports, 9(4219), 1-8. 10.1038/s41598-019-40884-0

Joseph, S.S.S. (2023). Introduction. In: Environmental Radon. Environmental Science and Engineering. Springer, Singapore. 10.1007/978-981-99-2672-5_1.

Jwanbot, D.I., Izam, M.M., Nyam, G.G., John, H.N. (2013). Radionuclides analysis of some soils and food crops in Barkin Ladi LGA, Plateau State-Nigeria. Journal of Environment and Earth Science, 3(3), 79-87.

Karagueuzian, H.S., White, C., Sayre, J., Norman, A. (2012). Cigarette smoke radioactivity and lung cancer risk. Review. Nicotine and Tobacco Research, 14, 79-90. 10.1093/Ntr/Ntr145

Kaur, M., Tripathi, P., Choudary, I., Mehra, R., Kumar, A. (2017). Assessment of annual effective dose due to inhalation and ingestion of radon in water samples from some regions of Punjab, India. International Journal of Pure and Applied Physics, 13(2), 193-200.

Khandaker, M.U., Nasir, N.L.M., Asaduzzaman, Kh., Olatunji, M.A., Amin, Y.M., Kassim, H.A., Bradley, D.A., Jojo, P.J., Alrefaed, T. (2016). Evaluation of radionuclides transfer from soil-to-edible flora and estimation of radiological dose to the Malaysian populace. Chemosphere, 154, 528-536. 10.1016/j.chemosphere.2016.03.121

Kiro, Y., Weinstein, Y., Starinsky, A., Yechieli, Y. (2015). Application of radon and radium isotopes to groundwater flow dynamics: An example from the Dead Sea. Chemistry and Geology, 411, 155-171. 10.1016/j.chemgeo.2015.06.014

Kitamura, A., Yamaguchi, M., Kurikami, H., Yui, M., Onishi, Y. (2014). Predicting sediment and cesium-137 discharge from catchments in eastern Fukushima. Anthropocene 5, 22-31. 10.1016/j.ancene.2014.07.001

Klubi, E., Abril, J.M., Mantero, J., García-Tenorio, R., Nyarko, E. (2020). Environmental radioactivity and trace metals in surficial sediments from estuarine systems in Ghana (Equatorial Africa), impacted by artisanal gold-mining. Journal of Environmental Radioactivity, 218,106260, 1-10. 10.1016/j.jenvrad.2020.106260

Kocsis, E., Tóth-Bodrogi, E., Peka, A., Adelikhah, M., Kovács, T. (2021). Radiological impact assessment of different building material additives. Journal of Radioanalytical and Nuclear Chemistry, 330, 1517-1526. 10.1007/s10967-021-07897-4

Kovács, T., Somlai, J., Nagy, K., Szeiler, G. (2007). Po-210 and Pb-210 concentration of cigarettes traded in Hungary and their estimated dose contribution due to smoking. Radiation Measurement, 42, 1737-1741. 10.1016/j.radmeas.2007.07.006

Kpordzro, R. (2018). Assessment of factors affecting indoor radon -222 concentration in Dome and its environs - Greater Accra region of Ghana. School of Nuclear and Allied Sciences, University of Ghana, 1-106.

Kubalek, D., Sersa, G., Strok, M., Benedik, L., Jeran, Z. (2016). Radioactivity of cigarettes and the importance of Po-210 and thorium isotopes for radiation dose assessment due to

smoking. Journal of Environmental Radioactivity, 155-156, 97-104. 10.1016/j.jenvrad.2016.02.015

Kucukomeroglu, B., Karadeniz, A., Damla, N., Yesilkanat, C. M., Cevik, U. (2016). Radiological maps in beach sands along some coastal regions of Turkey. Marine Pollution Bulletin 112, 255-264. 10.1016/j.marpolbul.2016.08.007

Kubo, A., Tanabe, A., Suzuki, G., Ito, Y., Ishimaru, T., Kasamatsu-Takasawa, N., Tsumune, D., Mizuno, T., Watanabe, Y. W., Arakawa, H., Kanda, J. (2018). Radioactive cesium concentrations in coastal suspended matter after the Fukushima nuclear accident. Marine Pollution Bulletin 131, 341-346. 10.1016/j.marpolbul.2018.04.042

Kumar, A., Narang, S. (2014). Estimation of radon exhalation rate and radium content in soil samples of Pathankot District, Punjab using LR-115 plastic detector. International Journal of Education and Applied Research, 4, 23-25.

Ladan, S.C., Mustapha, I.M., Hassan, A. Aliyu, M.S., Tukur, S.R. (2022). Assessment of radioactivity concentration level in soil samples of some gold mining areas of Shiroro, Niger State, Nigeria. Journal of Radiation and Nuclear Applications, 7(2), 1-6. 10.18576/jrna/070201

Laith, A., Najam, Shaher, A., Younis, Fouzey, H.K. (2015). Natural radioactivity in soil samples in Nineveh Province and the associated radiation hazards. International Journal of Physics, 3(3), 126-132. 10.12691/ijp-3-3-6

Lee, H., Lee, J., Yoon, S., Lee, C. (2021). Rn-222 exhalation rates from some granite and marble used in Korea: Preliminary study. Atmosphere, 12(8), 1057. 10.3390/atmos12081057.

Leuangtakoun, S., Phan, G. T. T., Duong, T. C., Le, N., Khong, N. K., Singsoupho, S., Tran, H. and Bui, V. L.L. (2020). Natural radioactivity measurement and radiological hazard evaluation in surface soils in a gold mining area and surrounding regions in Bolikhamxay province, Laos. Journal of Radioanalytical and Nuclear Chemistry, 326, 997-1007. 10.01007/s10967-020-07408-x

Leuangtakoun, S., Hong, B.T., Loat, B.V., Cuong, P.V. (2018). Determination of natural radioactivity in soil samples around gold mining area in Khamkeut district, Bolikhamxay

Province, Laos using gammarRay spectrometer with NaI (Tl) detector. VNU Journal of Science: Mathematics-Physics, 34(3), 12-21. 10.25073/2588-1124/vnvumap.4270

Li, P., Sun, Q., Geng, J., Yan, X., Tang, L. (2022). Radon exhalation from temperature treated loess. Science of Total Environment, 832, 154925, 1-13. 10.1016/j.scitotenv.2022.154925.

Liu, X., Lin, W. (2018). Natural radioactivity in the beach sand and soil along the coastline of Guangxi Province, China. Marine Pollution Bulletin 135, 446-450. 10.1016/j.marpolbul.2018.07.057

Liu, Y., Zhou, W., Gao, B., Zheng, Z., Chen, G., Wei, Q., He, Y. (2021). Determination of radionuclide concentration and radiological hazard in soil and water near the uranium tailings reservoir in China. Environmental Pollution and Bioavailability, 33(1), 174-183. 10.1080/26395940.2021.1951123

Liza, R., Pereyra, P., Rau, J., Guzman, M., Sajo-Bohus, L., Palacios, D. (2023). Assessment of natural radioactivity and radon exhalation in Peruvian gold mine tailings to produce a geopolymer cement. Atmosphere, 14(3), 588. 10.3390/atmos14030588

Loffredo, F., Opoku-Ntim, I., Kitson-Mills, D., Quarto, M. (2022). Gini method application: Indoor radon survey in Kpong, Ghana. Atmosphere 13(8), 1179. 10.3390/atmos13081179

Łokas, E., Zwoliński, Z., Rachlewicz, G., Gąsiorek, M., Wilkosz, G., Samolej, K. (2017) Distribution of anthropogenic and naturally occurring radionuclides in soils and lakes of Central Spitsbergen (Arctic). Journal of Radioanalytical Nuclear Chemistry, 311, 707-717. 10.1007/s10967-016-5085-x.

Mann, N., Kumar, S., Kumar, A., Chauhan, R.P., Garg, A.K. (2014). Measurement of radon exhalation rates in soil samples from Western Haryana. Journal of Applied Physics, 5(2), 56-59.

Mathuthu, M., Uushona, V., Indongo, V. (2021). Radiological safety of groundwater around a uranium mine in Namibia. Physics, Chemistry and Earth, 122, 102915. 10.1016/j.pce.2020.102915

Martins da Silva, N.V., Rodrigues, P.C.H., Faria, L.E., Rocha, Z., Correa, J.N. (2022). Comparative analysis of radon gas concentration in caves developed in carbonatic, quartzitic

and ferruginous lithologies. Journal of Environmental Radioactivity, 249, 106891, 1-11. 10.1016/j.jenvrad.2022.106891

Mazur, J., Kozak, K. (2014). Complementary system for long term measurements of radon exhalation rate from soil. Review of Scientific Instruments, 85(2), 022104, 1-7. 10.1063/1.4865156

Mehta, V., Kaur, R., Singh, S.P., Shikha, D. (2019). Measurement of radon concentration, its exhalation rates in some soil samples of Punjab. AIP Conference Proceedings, 2142, 120012, 1-5. 10.1063/1.5122508

Mihci, M., Buyuksarac, A., Aydemir, A., Celebi, N. (2010). Indoor and outdoor radon concentration measurements in Sivas, Turkey, in comparison with geological setting. Journal of Environmental Radioactivity, 101, 952-957. 10.1016/j.jenvrad.2010.06.013

Misdaq, M.A., Chaouqi, A., Ouguidi, J., Touti, R., Mortassim, A. (2015). Radon and Thoron measured in petrol and gas-oil exhaust fumes by using CR-39 and LR-115. Nuclear Track Detectors. Health Physics, 108, 592-596. 10.1097/HP.0000000000000285

Modibo, O.B., Tamakuma, Y., Suzuki, T., Yamada, R., Zhuo, W., Kranrod, C., Iwaoka, K., Akata, N., Hosoda, M., Tokonami, S. (2021). Long-term measurements of radon and thoron exhalation rates from the ground using the vertical distributions of their activity concentrations. International Journal of Environmental Research and Public Health, 18 (4) 1489. 10.3390/ijerph18041489

MOFEP. (2019). Programme-based budget estimates for 2019, Atiwa West District Assembly. Ministry of Finance, Composite budget for 2019-2022. Accessed July 23, 2023. https://mofep.gov.gh/sites/default/files/composite-budget/2019/ER/Atiwa-West.pdf

Mouri, G., Golosov, V., Shiiba, M., Hori, T. (2014). Assessment of the caesium-137 flux adsorbed to suspended sediment in a reservoir in the contaminated Fukushima region in Japan. Environmental Pollution 187, 31-41. 10.1016/j.envpol.2013.12.018

Mullerova, M.M., Holy, K., Blahus˘iak, P., Bulko, M. (2017). Study of radon exhalation from the soil. Journal of Radioanalytical and Nuclear Chemistry, 315, 237-241. 10.1007/s10967-017-5657-4

Munoz, E., Frutos, B., Olaya, M., Sanchez, J. (2017). A finite element model development for simulation of the impact of slab thickness, joints, and membranes on indoor radon concentration. Journal of Environmental Radioactivity, 177, 280-289. 10.1016/j.jenvrad.2017.07.006

Najam, L. A., Younis, S. A. (2015). Assessment of natural radioactivity level in soil samples for selected regions in Nineveh Province (IRAQ). International Journal of Novel Research in Physics Chemistry & Mathematics, 2(2), 1-9.

NDPC. (2019). National Development Planning Commission (NDPC) 2019 annual progress report on the implementation of the District Medium Term Development Plan 2018-2021 of the agenda for jobs: Creating prosperity and equal opportunity for all, 2018-2021, Atiwa West District Assembly, January 2020. Retrieved July 23, 2023, on https://ndpc.gov.gh/media/ER_Atiwa_West_APR_2019.pdf

Nguelem, E.J.M., Ndontchueng, M.M., Motapon, O. (2016). Determination of Ra-226, Th-232, K-40, U-235 and U-238 activity concentration and public dose assessment in soil samples from bauxite core deposits in Western Cameroon. SpringerPlus, 5(1253), 1-12. 10.1186/s40064-016-2895-9

Nguyen, T-N., Tran, Q-T., Nguyen,V-P., Le, N-S., Phan, S-H., Le, X-T., Vuong, T-T-H., Nguyen, V-P., Nguyen, D-T., Tran, D-K., Nguyen, M-D., Phan, Q-T., Vo, T-M-T., Duong, V-T., Le, N-C. (2020). Activity Concentrations of Sr-90 and Cs-137 in Seawater and Sediment in the Gulf of Tonkin, Vietnam. Journal of Chemistry, 1-8. 10.1155/2020/8752606

Nketiah-Amponsah, E., Afful-Mensah, G., Ampaw, S. (2018). Determinants of cigarette smoking and smoking intensity among adult males in Ghana. BMC Public Health, 18, 1-10. 10.1186/s12889-018-5872-0

Nsiah-Akoto, I., Andam, A.B., Akiti, T.T., Fletcher, J.J. (2019). Study of radium and radon exhalation rate in soil samples, Offinso Municipality. AIP Conference Proceedings, 2109, 100003-5. 10.1063/1.5110138

Nsiah-Akoto, I., Fletcher, J.J., Oppon, O.C., Andam, A.B. (2011). Indoor radon levels and the associated effective dose rate determination at Dome in the Greater Accra region of Ghana. Research Journal of Environment and Earth Science, 3, 124-130.

Nyarko, E., Botwe, B.O., Ansong, J.E., Delfanti, R., Barsanti, M., Schirone, A., Delbono, I. (2011). Determination of Pb-210, Ra-226 and Cs-137 in beach sands along the coastline of Ghana. African Journal of Environmental Pollution Health 9(2), 17-23.

Nuccetelli, C., Rusconi, R., Forte, M. (2012). Radioactivity in drinking water: regulations, monitoring results and radiation protection issues. Ann Ist Super Sanità, 48(4), 362-373. 10.4415/ANN_12_04_04

Nyhan, M.M., Coull, B.A., Blomberg, A.J., Vieira, C.L.J., Garshick, E., Aba, A., Vokonas, P., Gold, D.R., Schwartz, J., Koutrakis, P. (2018). Associations between ambient particle radioactivity and blood pressure: The NAS (Normative Aging Study). Journal of American Heart Association, 7, e008245. 10.1161/JAHA.117.008245

Odumo, O.B., Mustapha, A.O., Patel, J.P., Angeyo, H.K. (2011). Radiological survey and assessment of associated activity concentration of the naturally occurring radioactive materials (NORM) in the Migori artisanal gold mining belt of southern Nyanza, Kenya. Applied Radiation and Isotopes, 69(6), 912-916. 10.1016/j.apradiso.2011.02.016

Öge, T.O., Özdemir, F.B., Öge, M. (2021). Assessment of environmental radioactivity in soil samples from Bartın Province, Turkey. Journal of Radioanalytical and Nuclear Chemistry, 328, 149-162. 10.1007/s10967-021-07629-8

OHG. (2025). https://www.ourhomelandghana.com/general/tallow-ghana-announces-maintenance-works-on-jubilee/. Retrieved on March 30, 2025.

Oliveira de Souza, S., Freire, F.D., Kozlowska, B., Walencik-Lata, A., Dias, M., Veiga, A.J.P. (2015). Radionuclides in waters and soil near the Lagoa real uranium mine. International Nuclear Atlantic Conference - INAC 2015, São Paulo, SP, Brazil, October 4-9, 2015, Associação Brasileira De Energia.

Olise, F.S., Akinnagbe, D.M., Olasogba, O.S. (2016). Radionuclides and radon levels in soil and ground water from solid minerals-hosted area, south-western Nigeria. Cogent Environmental Science, 2, 1142344. 10.1080/23311843.2016.1142344

Olise, F.S., Owoade, O.K., Olaniyi, H.B., Obiajunwa, E.I. (2010). A complimentary tool in the determination of activity concentrations of naturally occurring radionuclides. Journal of Environmental Radioactivity, 101, 910-914. 10.1016/j.jenvrad.2010.06.006

O¨rgu¨n, Y., Altınsoy, N., Gu¨ltekin, A.H., Karahan, G. (2005). C-elebi, N. Natural radioactivity levels in granitic plutons and groundwaters in Southeast part of Eskisehir, Turkey. Applied Radiation Isotopes, 63, 267-275. 10.1016/j.apradiso.2005.03.008

Orosun, M., Usikalu, M., Oyewumi, K. (2020). Radiological hazards assessment of laterite mining field in ilorin, North-central Nigeria. International Journal of Radiation Research, 18(4), 895-906. 10.18869/acadpub.ijrr.18.4.895

Orosun, M.M., Usikalu, M.R., Oyewumi, K.J., Adagunodo, T.A. (2019). Natural radionuclides and radiological risk assessment of granite mining field in Asa, North-central Nigeria. MethodsX, 6, 2504-2514. 10.1016/j.mex.2019.10.032

Otoo, F., Darko, E.O., Garavaglia, M. (2022). Correlation analysis of natural radionuclides, radon exposure, soil particles, and moisture from quarry towns in Greater Accra Region, Ghana. Water Air Soil Pollution, 233(8), 1-16. 10.1007/s11270-022-05791-7

Otoo, F., Darko, E.O., Garavaglia, M., Adukpo, O.K., Amoako, K., Tandoh, J.B., Inkoom, S., Nunoo, S., Adu, S. (2021). Assessment of natural radioactivity and radon exhalation rate associated with rock properties used for construction in greater Accra region, Ghana. Journal of Radioanalytical and Nuclear Chemistry, 328, 911-923. 10.1007/s10967-021-07709-9

Otoo, F., Arhin, I., Darko, E.O. (2020). Studies of radon levels, radium concentration, and estimated effective dose in dwellings and soils in gold mining towns in Abirem of Eastern Region of Ghana. Radiation Protection Dosimetry, 191(3), 1-14. 10.1093/rpd/ncaa129

Otoo, F., Darko, E.O., Garavaglia, M., Giovani, C., Pividore, S., Andam, A.B., Amoako, J.K., Adukpo, O.K., Tandoh, J.B., Inkoom, S. (2018a). Seasonal indoor radon studies in buildings of Accra Metropolis of Greater Accra region of Ghana. Radioprotection, 53, 199-206. 10.1051/radiopro/2018023

Otoo, F., Darko, E.O., Garavaglia. M., Giovani, C., Pividore, S., Andam. A.B., Amoako, J.K., Adukpo, O.K., Tandoh, J.B., Inkoom, S. (2018b). Public exposure to natural radioactivity

and radon exhalation rate in construction materials used within Greater Accra Region of Ghana. Scientific African, 1, 1-12. 10.1016/j.sciaf.2018.e00009

Owusu-Dabo, E., Lewis, S., McNeill, A., Anderson, S., Gilmore, A., Britton, J. (2009). Smoking in Ghana: A review of tobacco industry activity. Tobacco Control 18, 206-211. 10.1136/Tc.2009.030601

Özmen, F.S., Cesur, A., Boztosun, I., Yavuz, M. (2014). Distribution of natural and anthropogenic radionuclides in beach sand samples from Mediterranean Coast of Turkey. Radiation Physics and Chemistry, 103, 37-44. 10.1016/j.radphyschem.2014.05.034

Pantelić, G., Čeliković, I., Živanović, M., Vukanac, I., Nikolić, J.K., Cinelli, G., Gruber, V. (2018). Literature review of indoor radon surveys in Europe, Publications Office of the European Union, Luxembourg, ISBN 978-92-79-97643-8 (online), JRC114370: 1-104. 10.2760/977726

Patel, K., Rogan, J., Cuba, N., Bebbington, A. (2016). Evaluating conflict surrounding mineral extraction in Ghana: Assessing the spatial interactions of large and small-scale mining. Extraction Industry Society 3, 450-463. 10.1016/j.exis.2016.01.006

Persson, B.R.R., Holm, E. (2011). Polonium-210 and Lead-210 in the terrestrial environment: A historical review. Journal of Environmental Radioactivity, 102, 420-429. 10.1016/J.Jenvrad.2011.01.005

Pintilie-Nicolov, V., Georgescu, P.L., Iticescu, C., Moraru, D.L., Pintilie, A.G. (2021). The assessment of the annual effective dose due to ingestion of radionuclides from drinking water consumption: calculation methods. Journal of Radioanalytical and Nuclear Chemistry, 327, 49-58. 10.1007/s10967-020-07438-5

Quansah, E. K. (2014). Preliminary studies on impacts of ocean acidification on diversity of fish species landed by artisanal and semi-industrial fisheries and coastal community livelihoods in Ghana. Master's Thesis. University of Ghana, 1-111.

Qureshi, A.A., Tariq, S., Din, K.U., Manzoor, S., Calligaris, C., Waheed, A. (2014). Evaluation of excessive lifetime cancer risk due to natural radioactivity in the rivers,

sediments of Northern Pakistan. Journal of Radiation Research and Applied Science, 7(4), 438-447. 10.1016/j.jrras.2014.07.008

Radon solutions. (2022). https://radonsolutionsllc.net/. Retrieved on December 3, 2024.

Rakmetkazhy, I.B., Bulgakova, O. (2015). The health effects of radon and uranium on the population of Kazakhstan. Genes and Environment, 37, 1-10. 10.1186/s41021-015-0019-3

Ramadhany, M.F., Wijaya, G.S., Muharini, A. (2022). Assessment of natural radioactivity concentration and radiological risk in Tanjung Enim's coal mine, South Sumatra Indonesia. Research Square, 1-11. 10.21203/rs.3.rs-1469889/v3

Saad, A.F., Abdallah, R.M., Hussein, N.A. (2013). Radon exhalation from Libyan soil samples measured with the SSNTD technique. Applied Radiation Isotopes, 72, 163-168. 10.1016/j.apradiso.2012.11.006

Saad, A.F., Al-Awami, H.H., Hussein, N.A. (2014). Radon exhalation from building materials used in Libya. Radiation Physics and Chemistry, 101, 15-19. 10.1016/j.radphyschem.2014.03.030

Saat, A., Isak, N.M., Hamzah, Z., Wood, A.K. (2014). Study of radionuclides linkages between fish, water and sediment in former tin mining lake in Kampung Gajah, Perak, Malaysia. Malaysian Journal of Analytical Science, 18(1), 170-177.

Sahoo, B.K., Sapra, B.K., Gaware, J.J., Kanse, S.D., Mayya, Y.S. (2011). A model to predict radon exhalation from walls to indoor air based on the exhalation from building material samples. Science of Total Environment, 409(13), 2835-2641. 10.1016/j.scitotenv.2011.03.031

Sakoda, A., Fukao, K., Kawabe, A., Kataoka, T., Hanamoto, K., Yamaoka, K. (2012). Radioactivity of Pb-210 in Japanese cigarettes and radiation dose from smoking inhalation. Radiation Protection Dosimetry, 150, 109-113. 10.1093/rpd/ncr364

Sakoda, A., Ishimori, Y., Yamaoka, K. (2011). A comprehensive review of radon emanation measurements for mineral, rock, soil, mill tailing and fly ash. Applied Radiation and Isotopes, 69, 10, 1422-1435. 10.1016/j.apradiso.2011.06.009

Salaheldin, G., Elhaddad, M., Sidique, E. (2022). Radon concentration and exhalation rate for granitic rocks, Central Eastern Desert, Egypt. Arabian Journal of Geosciences, 15, 12-21. 10.1007/s12517-022-09693-0

Schayer, S., Nowak, B., Wang, B., Qu, Q., Cohen, B. (2009). Po-210 and Pb-210 activity in Chinese cigarettes. Health Physics, 96, 543-549. 10.1016/J.Pisc.2019.100400

Shabana, E.I., Kinsara, A.A. (2014). Radioactivity in the groundwater of a high background radiation area. Journal of Environmental Radioactivity, 137, 181-189. 10.1016/j.jenvrad.2014.07.013

Shahrokhi, A., Tettey-Larbi, L., Akuo-ko, E.O., Tóth-Bodrogi, E., Kovács, T. (2023). The new conception of radiological sustainability possibilities by reutilization of residues products and building materials. Sustainability, 15(13), 10647, 1-13. 10.3390/su151310647.

Shahrokhi, A., Adelikhah, M., Chalupnik, S., Kovács, T. (2021). Multivariate statistical approach on distribution of natural and anthropogenic radionuclides and associated radiation indices along the north-western coastline of Aegean Sea, Greece. Marine Pollution Bulletin, 163, 112009. 10.1016/j.marpolbul.2021.112009

Shahrokhi, A., Adelikhah, M., Chalupnik, S., Kocsis, E., Toth-Bodrogi, E., Kovács, T. (2020). Radioactivity of building materials in Mahallat, Iran–an area exposed to a high level of natural background radiation–attenuation of external radiation doses. Material Construction, 70, 1-13. 10.3989/mc.2020.03820

Shayeb, M. A., Baloch, M. A. (2020). Distribution of natural radioactivity in soil and date palm-pits using high purity germanium radiation detectors and LB-alpha/beta gasflow counter in Saudi Arabia. Nuclear Engineering and Technology, 52(6), 1282-1288. 10.1016/j.net.2019.12.009

Sherif, M.I., Sturchio, N.C. (2018). Radionuclide geochemistry of groundwater in the Eastern Desert, Egypt. Applied Geochemistry, 93, 69-80. 10.1016/j.apgeochem.2018.04.004

Shoeib, M.Y., Thabayneh, K.M. (2014). Assessment of natural radiation exposure and radon exhalation rate in various samples of Egyptian building materials. Journal of Radiation Research and Applied Sciences, 7(2), 174-181. 10.1016/j.jrras.2014.01.004

Shousha, H.A., Ahmad, F. (2016). Lifetime cancer risk of gamma radioactivity results from smoking. Radiation Cancers Review 3(1), 1-9. 10.18488/journal.95/2016.3.1/95.1.1.9

Shuaibu, H.K., Khandaker, M.U., Alrefae, T., Bradley, D.A. (2017). Assessment of natural radioactivity and gamma-ray dose in monazite rich black Sand Beach of Penang Island, Malaysia. Marine Pollution Bulletin 119, 423-428. 10.1016/j.marpolbul.2017.03.026

Singh, A., Owusu-Dabo, E., Dobbie, F., Mdege, N., McNeil, A., Britton, J., Bauld, L. (2020). A situational analysis of tobacco control in Ghana: Progress, opportunities and challenges. Journal of Global Health Reports, 4, 1-8. 10.29392/001c.12260

Singh, P.B., Pandit, B., Bhardwaj, V.N., Singh, P., Kumar, R. (2010). Study of radium and radon exhalation rate in some solid samples using solid state nuclear track detectors. Indian Journal of Pure and Applied Physics, 48(7), 493-495.

Singh, S., Sharma, D.K., Dhar, S., Kumar, A., Kumar, A. (2007). Uranium, radium and radon measurements in the environs of Nurpur area, Himachal Himalayas, India. Environmental Monitoring and Assessment, 128, 301-309.

Skwarzec, B., Ulatowski, J., Struminska, D.I., Boryło, A. (2001). Inhalation of Po-210 and Pb-210 from cigarette smoking in Poland. Journal of Environmental Radioactivity, 57, 221-230. 10.1016/s0265-931x(01)00018-2

Snapir, B., Simms, D.M. Waine, T.W. (2017). Mapping the expansion of galamsey gold mines in the cocoa growing area of Ghana using optical remote sensing. International Journal of Applied Earth Observation Geoinformation 58, 225-233. 10.1016/j.jag.2017.02.009

Sivakumar, S., Chandrasekaran, A., Ravisankar, R., Ravikumar, S.M., Jebakumar, J.P.P., Vijayagopal, P., Vijayalakshmi, I., Jose, M.T. (2014). Measurement of natural radioactivity and evaluation of radiation hazards in coastal sediments of east coast of Tamilnadu using statistical approach. Journal of Taibah University of Science, 8(4), 375-384. 10.1016/j.jtusci.2014.03.004.

Soniya, S.R., Abraham, S., Khandaker, M.U., Jojo, P.J. (2021). Investigation of diffusive transport of radon through bricks. Radiation Physics and Chemistry, 178, 108955, 1-6. 10.1016/j.radphyschem.2020.108955

Souffit, D.G., Saïdou, Modibo, B.O., Lepoire, D., Tokonami, S. (2022). Risk assessment of exposure to natural radiation in soil using RESRAD-ONSITE and RESRAD-BIOTA in the cobalt-nickel bearing areas of Lomié in Eastern Cameroon. Radiation, 2(2), 177-192. 10.3390/radiation2020013

Stabile, L., Buonanno, G., Ficco, G., Scungio, M. (2017). Smokers' lung cancer risk related to the cigarette-generated mainstream particles. Journal of Aerosol Science, 107, 41-54. 10.1016/j.jaerosci.2017.02.005

Suresh, S., Rangaswamy, D.R., Srinivasa, E., Sannappa, J. (2020). Measurement of radon concentration in drinking water and natural radioactivity in soil and their radiological hazards. Journal of Radiation Research and Applied Science, 13(1), 12-26. 10.1080/16878507.2019.1693175

Sureshgandhi, M., Ravisankar, R., Rajalakshmi, A., Sivakumar, S., Chandrasekaran, A., Anand, D.P. (2014). Measurements of natural gamma radiation in beach sediments of north-east coast of Tamilnadu, India by gamma ray spectrometry with multivariate statistical approach. Journal of Radiation Research and Applied Science, 7(1), 7-17. 10.1016/j.jrras.2013.11.001

Taroni, M. (2017). Re: What is the main source of natural background radiation? https://www.researchgate.net/post/What_is_the_main_source_of_natural_background_radiation/5979a965cbd5c21ecb372f93/citation/download. Retrieved on August 7, 2024.

Tsabaris, C., Kapsimalis, V., Eleftheriou, G., Laubenstein, M., Kaberi, H., Plastino, W. (2012). Determination of 137Cs activities in surface sediments and derived sediment accumulation rates in Thessaloniki Gulf, Greece. Environmental Earth Sciences, 66, 1431–1441. 10.1007/s12665-012-1530-5.

Takata, H., Kusakabe, M., Inatomi, N., Hasegawa, K., Ikenoue, T.; Watanabe, Y., Watabe, T., Suzuki, C., Misonoo, J., Mori-zono, S. (2017). Long-Term distribution of radioactive cesium in the coastal seawater and sediments of Japan. Rep. Mar. Ecol. Res. Inst., 22, 17–25.

Taqi, A.H., Shaker, A M., Battawy, A.A. (2018). Natural radioactivity assessment in soil samples from Kirkuk city of Iraq using HPGe detector. International Journal of Radiation Research, 16(4), 455-463. 10.18869/acadpub.ijrr.16.4.455

Thornton, B., Ohnishi, S., Ura, T., Odano, N., Sasaki, S., Fujita, T., Watanabe, T., Nakata, K., Ono, T., Ambe, D. (2103). Distribution of local Cs-137 anomalies on the seafloor near the Fukushima Dai-ichi Nuclear Power Plant. Marine Pollution Bulletin, 74, 344-350. 10.1016/j.marpolbul.2013.06.031.

Turhan, S., O¨zcıtak, E., Taskın, H., Varinlioglu, A. (2013). Determination of natural radioactivity by gross alpha and beta measurements in ground water samples. Water Research, 47(9), 3103-3108. 10.1016/j.watres.2013.03.030

UNSCEAR. (2014). Report to assembly with scientific annexes. New York: UNSCEAR.

UNSCEAR. (2008). Report, Sources and Effects of Ionizing Radiation. Volume I, Annex B, Exposures of the Public and Workers from Various Sources of Radiation.

UNSCEAR. (2000). Source and effects of ionizing radiation. UNSCEAR 2000 Report to the General Assembly, with Scientific Annex.

Vaupotic, J., Gregoric, A., Kobal, I., Zvab, P., Kozak, K., Mazur, J., Kochowska, E., Grzadziel, D. (2010). Radon concentration in soil gas and radon exhalation rate at the Ravne Fault in NW Slovenia. Natural Hazards and Earth System Science, 10, 895-899.

Wang, O., Song, J., Li, X., Yuan, H., Li, N., Cao, L. (2015). Environmental radionuclides in a coastal wetland of the Southern Laizhou Bay, China. Marine Pollution Bulletin, 97(1-2), 506-511. 10.1016/j.marpolbul.2015.05.035

West Africa. (2024). https://saylordotorg.github.io/text_world-regional-geography-people-places-and-globalization/s10-03-west-africa.html. Retrieved on November 30, 2024.

WHO. (2011). Guidelines for drinking water quality. World Health Organization, 4th Ed. 1-541.

WHO. (2009). Handbook on indoor radon: a public health perspective, ISBN 978 92 4 154767 3.

WHO. (2008). Guidelines for Drinking Water Quality. World Health Organization vol. 1, third ed.

Yachiso, G., Chaubey, A.K., Turi, B. (2022). Measurements of natural radioactivity levels in soil samples and hazards in Lega Dembi gold mining, East Guji, Oromia, Ethiopia. Research Square, 1-18. 10.21203/rs.3.rs-1854146/v1

Yamada, S., Kitamura, A., Kurikami, H., Yamaguchi, M., Malins, A. and Machida, M (2015). Sediment and 137Cs transport and accumulation in the Ogaki Dam of eastern Fukushima. Environmental Research Letters, 10, 014013, 1-9. 10.1088/1748-9326/10/1/014013

Yankson, P.W.K., Gough, K.V. (2019). Gold in Ghana: The effects of changes in large-scale mining on artisanal and small-scale mining (ASM). Extraction Industry Society, 6, 120-128. 10.1016/j.exis.2018.09.009

Yasumiishi, M., Nishimura, T., Aldstadt, J., Bennett, S. J., Bittner., T. (2021). Assessing the effect of topography on Cs-137 concentrations within forested soils due to the Fukushima Daiichi Nuclear Power Plant accident. Japan Earth Surface Dynamics, 9, 861-893. 10.5194/esurf-9-861-2021

Yeboah, J., Boadu, M., Darko, E.O. (2001). Natural radioactivity in soils and rocks within the Greater Accra Region of Ghana. Journal of Radioanalytical and Nuclear Chemistry, 249, 629-632. 10.1023/A:1013262702436

Yehia, M., Baghdady, A., Howari, F.M., Awad, S., Gad, A. (2017). Natural radioactivity and groundwater quality assessment in the northern area of the Western Desert of Egypt. Journal of Hydrology and Regional Studies, 12, 331-344. 10.1016/j.ejrh.2017.06.002

Yidana, S.M., Banoeng-Yakubo, B., Aliou, A-S., Akabzaa, T.M. (2012). Groundwater quality in some Voltaian and Birimian aquifers in northern Ghana- application of mulitvariate statistical methods and geographic information systems. Hydrology Science, 57(6), 1168-1183. 10.1080/02626667.2012.693612

Yordanova, I.I., Banov, M.D., Misheva, L.G., Staneva, D.N., Bineva, T. K. (2015). Natural radioactivity in virgin soils and soils from some areas with closed uranium mining facilities in Bulgaria. Open Chemistry, 13, 600-605. 10.1515/chem-2015-0065

Yousef, H., El-Farrash, A.H., Ela, A.A., Merza, Q. (2015). Measurement of radon exhalation in some building materials using nuclear track detectors. World Journal of Nuclear Science and Technology, 5(3), 141-148. 10.4236/wjnst.2015.53014

Zagà, V., Cattaruzza, M.S., Martucci, P., Pacifici, R., Trisolini, R., Bartolomei, P., Giacobbe, R., Patelli, M., Paioli, D., Esposito, M., Fabbri, V., Gallus, S., Gorini, G. (2021). The "Polonium in vivo" study: Polonium-210 in bronchial lavages of patients with suspected lung cancer. Biomedicine, 9, 1-11. 10.3390/biomedicines9010004

Zaga, V., Lygidakis, C., Chaouachi, K., Gattavecchia, E. (2011). Polonium and lung cancer. Journal of Onco1ogy, 1-11. 10.1155/2011/860103

Zakaly, M.H., Uosif, M.A.M., Issa, S.A.M., Tekin, H.O., Madkour, H., Tammam, M., El-Taher, A., Alharshan, G.A., Mostafa, M.Y.A. (2021). An extended assessment of natural radioactivity in the sediments of the mid-region of the Egyptian Red Sea coast Hesham. Marine Pollution Bulletin 171, 112658. 10.1016/j.marpolbul.2021.112658

Zaini, H., Siti, A., Abdul, R., Ahmad, S. (2011). Measurement of Ra-226, Ra-228 and K-40 in soil in district of Kuala Krai using gamma spectrometry. The Malaysian Journal of Analytical Sciences, 15(2), 159-166.

Zhong, Q., Wang, X., Wang, Q., Zhang, F., Li, L., Wang, Y., Du, J. (2020). Rn-222, Pb-210 and Po-210 in coastal zone groundwater: Activities, geochemical behaviors, consideration of seawater intrusion effect, and the potential radiation human-health risk. Applied Radiation Isotopes, 166, 109386. 10.1016/j.apradiso.2020.109386

Zhao, L., Liu, D., Wang, J., Du, J., Hou, X., Jiang, Y. (2018). Spatial and vertical distribution of radiocesium in seawater of the East China Sea. Marine Pollution Bulletin 128, 361-368. 10.1016/j.marpolbul.2018.01.047

Zubair, M., Shafiqullah. (2020). Measurement of natural radioactivity in several sandy-loamy soil samples from Sijua, Dhanbad, India. Heliyon 6(3), e03430, 1-8. 10.1016/j.heliyon.2020.e03430

Zubair, M., Khan, M.S., Verma, D. (2012). Measurement of radium concentration and radon exhalation rates of soil samples collected from some areas of Bulandshahr district, Uttar

Pradesh, India using plastic track detectors. Iranian Journal of Radiation Research, 10(2), 83-87.